

BIOCHEMICAL ANALYSIS OF HUMAN BASE EXCISION REPAIR

By

CLINT W. ABNER

A DISSERTATION PRESENTED TO THE GRADUATE SCHOOL OF THE
UNIVERSITY OF FLORIDA IN PARTIAL FULFILLMENT OF THE
REQUIREMENTS FOR THE DEGREE OF DOCTOR OF PHILOSOPHY

UNIVERSITY OF FLORIDA

2002

This dissertation is dedicated to my wife, Danielle, and to my son, Clint Jr., for all of their love and support.

ACKNOWLEDGMENTS

I would like to thank my advisor, Dr. Linda Bloom. Dr. Bloom has been an inspiration to me and a source of encouragement throughout graduate school. She has provided me with the tools that I need to further my career as a scientist. I would also like to thank the other members of my committee--Dr. Ben Dunn, Dr. Susan Frost, Dr. Art Edision, and Dr. Nick Muzyczka. I especially want to thank the other members of my lab for the many thought provoking conversations that we shared. I wish to express my deep gratitude to the many members of the Dunn and Cain labs for allowing me to become their friend.

I especially want to thank my family and friends for all of their love and support throughout these difficult years. Special thanks are in order for my mom, dad, John Parnell, Kathy Parnell, Meagan Parnell, Jack Moss, Dorothy Moss, Lance Pierce, and Hobson Elrod—they believed in me from the very start.

I wish to thank my wife, Danielle, and son, Clint Jr. Danielle has been my greatest supporter ever since our eyes met. She has given me more than I will ever be able to give back. I love her. I want to thank my son Clint Jr. for always loving me and for teaching me how to be a daddy. If I had just one wish—only one demand—I hope he's not like me. I hope he understands.

Finally, I want to thank God for loving me and for allowing me to do his work in science.

TABLE OF CONTENTS

	<u>Page</u>
ACKNOWLEDGMENTS.....	iii
LIST OF TABLES.....	vi
LIST OF FIGURES.....	vii
ABBREVIATIONS.....	ix
ABSTRACT.....	xii
 CHAPTER	
1 BACKGROUND AND SIGNIFICANCE.....	1
Chemical Instability of DNA.....	1
Other Types of DNA Base Damage.....	3
Limiting Genomic Instability.....	8
Nucleotide Excision Repair.....	10
Base Excision Repair.....	14
Characteristics of DNA Glycosylases.....	17
Human Alkyladenine DNA Glycosylase (hAAG).....	18
hAAG Substrate Specificity.....	24
Human Apurinic/Apyrimidinic Endonuclease (APE1).....	28
Stimulation of DNA Glycosylase Activity by APE1.....	31
Human Polymerase Beta and DNA Ligase.....	32
Genetic Studies of BER Proteins.....	34
Summary.....	37
 2 EXPERIMENTAL PROCEDURES	
Purification of Human Alkyladenine DNA Glycosylase (hAAG).....	39
Oligonucleotide Synthesis and Purification.....	42
³² P DNA hAAG Excision Assay.....	44
³² P DNA Electrophoretic Mobility Shift Assay (EMSA).....	45
Yeast Two-Hybrid Analysis.....	46
Yeast Colony PCR Analysis of Putative Clones.....	51
Western Blot Analysis.....	54
Protein Phosphorylation Assays.....	56

3	BASE EXCISION AND DNA BINDING ACTIVITIES OF HUMAN ALKYLADENINE DNA GLYCOSYLASE (hAAG).....	58
	Introduction.....	58
	Results.....	59
	Discussion.....	72
4	HUMAN AP ENDONUCLEASE 1 (APE1) STIMULATES TURNOVER OF HUMAN ALKYLADENINE DNA GLYCOSYLASE (hAAG).....	82
	Introduction.....	82
	Results.....	85
	Discussion.....	95
5	IDENTIFICATION OF NOVEL PROTEIN INTERACTIONS WITH hAAG USING YEAST TWO-HYBRID ANALYSIS TO SCREEN A LIVER cDNA LIBRARY.....	99
	Introduction.....	99
	Results.....	106
	Discussion.....	120
6	PROTEIN PHOSPHORYLATION OF hAAG BY PROTEIN KINASE-C AND CASEIN KINASE II.....	125
	Introduction.....	125
	Results.....	129
	Discussion.....	129
7	CONCLUSIONS AND FUTURE DIRECTIONS.....	132
	LIST OF REFERENCES.....	137
	BIOGRAPHICAL SKETCH.....	148

LIST OF TABLES

<u>Table</u>		<u>Page</u>
1-1	Oxidative lesions generated by γ radiation.....	7
1-2	A list of several known DNA alkylating agents.....	9
2-1	PCR cocktail.....	52
2-2	PCR cycle.....	52
5-1	A list of possible hAAG interacting proteins.....	118
5-2	Mapping the interaction on hAAG of MT-2A binding.....	121

LIST OF FIGURES

<u>Figure</u>	<u>Page</u>
1-1 Structure of pyrimidine dimers.....	4
1-2 Model for GG-NER and TCR-NER.....	13
1-3 Representation of the base excision repair pathway.....	15
1-4 Schematic diagram of the hAAG-DNA contacts.....	21
1-5 Electron density map of the flipped out pyrrolidine abasic nucleotide.....	22
1-6 hAAG substrate bases.....	25
1-7 Crystal structure of APE1.....	30
3-1 Structures for some of the damaged DNA base pairs tested as substrates for hAAG.....	60
3-2 hAAG excision assays.....	62
3-3 Single-turnover kinetics of excision of ϵ A and Hx when paired opposite thymine.....	64
3-4 Excision of ϵ A and Hx opposite cytosine and uracil.....	66
3-5 hAAG Δ 79 binding to damaged DNA.....	69
3-6 Binding of hAAG Δ 79E125Q to DNA containing ϵ A and Hx base pairs.....	70
3-7 Binding of hAAG Δ 79 to DNA containing abasic sites.....	73
4-1 Plots showing hAAG-FL and hAAG Δ 79 excision.....	87
4-2 Single turnover excision assays.....	88
4-3 APE1 stimulates hAAG-FL turnover.....	90
4-4 Single turnover excision assays in the presence of APE1.....	93

5-1	The yeast two hybrid principle.....	101
5-2	The pGBKT7 and pACT2 vectors.....	107
5-3	Phenotypic analysis of AH109.....	109
5-4	Comparative growth rates of AH109 and AH109 transformants.....	110
5-5	Transcriptional activation control experiments.....	112
5-6	hAAG and APE1 do not activate yeast reporter genes.....	114
5-7	Typical yeast colony PCR.....	115
5-8	Representation of hAAG deletion constructs.....	119
6-1	hAAG protein sequence.....	128
6-2	CK-II and PK-C phosphorylation of hAAG.....	130

ABBREVIATIONS

ϵ A, *I,N*⁶-ethenoadenine

7-MeG, 7-methylguanine

8-oxoG, 8-oxo-guanine

A, adenine

Ade, adenine

APE1, human apurinic/apyrimidinic endonuclease

BER, base excision repair

C, cytosine

CK-II, casein kinase II

CS, Cockayne's syndrome

DE52, diethylaminoethyl cellulose

DMSO, dimethyl sulfoxide

DNA, deoxyribonucleic acid

dRP, 5'-deoxyribose-5-phosphate

DTT, dithiothreitol

EDTA, ethylenediamine tetraacetic acid

EMSA, electrophoretic mobility shift assay

FEN1, flap endonuclease 1

G, guanine

HA, hemagglutinin

hAAG, human alkyladenine DNA glycosylase

His, histidine

HNPCC, hereditary nonpolyposis colorectal cancer

Hx, hypoxanthine

IPTG, isopropyl β -D-thiogalactopyranoside

Kan, kanamycin

Leu, leucine

MMR, mismatch repair

MT-2A, human metallothionein 2A

NER, nucleotide excision repair

O⁶-MeG, O⁶-methylguanine

PCNA, proliferating cell nuclear antigen

PEG, polyethylene glycol

PK-C, protein kinase C

PMSF, phenylmethylsulfonyl fluoride

Pol β , human DNA polymerase beta

RNA, ribonucleic acid

SAM, S-adenosylmethionine

SD, synthetic dropout

T, thymine

TBS, tris buffered saline

Trp, tryptophan

TTD, trichothiodystrophy

U, uracil

UDG, uracil DNA glycosylase

v/v, volume/volume

w/v, weight/volume

XP, xeroderman pigmentosum

YPD, yeast extract, peptone, dextrose

Abstract of Dissertation Presented to the Graduate School
of the University of Florida in Partial Fulfillment of the
Requirements for the Degree of Doctor of Philosophy

BIOCHEMICAL ANALYSIS OF HUMAN BASE EXCISION REPAIR

By

Clint W. Abner

May 2002

Chairperson: Linda B. Bloom

Major Department: Biochemistry and Molecular Biology

Contained in DNA is the genetic information required for survival of all cells. This information is encoded in the bases of DNA. These bases are chemically reactive and because of this are constantly undergoing modification (i.e., damage). DNA damage can arise by either endogenous or exogenous means and occurs at a high enough frequency that cells cannot survive unless the damage is repaired.

The human alkyladenine DNA glycosylase (hAAG) has broad substrate specificity, excising a structurally diverse group of damaged purines from DNA. To more clearly define the structural and mechanistic bases for substrate specificity of human alkyladenine DNA glycosylase, kinetics of excision and DNA binding activities were measured for several different damaged and undamaged purines within identical DNA sequence context. We found that *1,N*⁶-ethenoadenine and hypoxanthine were excised relatively efficiently, whereas other damaged and undamaged bases were not. The opposing pyrimidine base had a significant effect on the kinetics of excision and

DNA binding affinity of hypoxanthine, but a small effect on those for *1,N⁶*-ethenoadenine.

We also report that human AP endonuclease 1(APE1) stimulates the turnover of human alkyladenine DNA glycosylase. However, using a variety of techniques including gel retardation assay, co-immunoprecipitation, and two-hybrid analysis, it was not possible to detect evidence for a complex including substrate DNA, hAAG, and APE1 proteins.

CHAPTER 1 BACKGROUND AND SIGNIFICANCE

Chemical Instability of DNA

Although DNA contains the genetic information required for survival of all cells, it has an inherently limited chemical stability. Nucleic acids undergo spontaneous decomposition in solution, with ribonucleic acid (RNA) being especially vulnerable. Because of a 2'-hydroxyl group on ribose, the phosphodiester bonds of RNA molecules are very susceptible to hydrolysis, particularly in the presence of divalent cations such as Mg^{2+} and Ca^{2+} (55). The absence of this 2'-hydroxyl group on deoxyribose results in a stronger phosphodiester bond compared to ribose, however this also results in a much more labile *N*-glycosidic bond. Because of this the glycosylic bonds of ribonucleosides are much less susceptible to hydrolysis than those of deoxyribonucleosides.

The bases of DNA, which make up the genetic code, are comprised of purine (adenine and guanine) and pyrimidine (thymine and cytosine) molecules. Because of their chemical structure, purines represent better leaving groups than pyrimidines. Therefore, purines are spontaneously hydrolyzed from DNA more often than pyrimidines. Adenine and guanine are released at similar rates, although guanine is slightly more rapid. There is only a small difference in depurination rates between single-stranded and double-stranded DNA, therefore the double helical structure of DNA provides little protection against depurination (59). Cytosine and thymine are released at

a rate approximately 5% that of the purines (61). In human cells it has been estimated that there are approximately 2,000-10,000 hydrolytic depurinations per cell per day (59, 107).

Spontaneous base loss resulting from the inherent instability of glycosyl bonds is not the only daunting challenge facing DNA; the bases of DNA are subject to alteration or damage. A few examples of DNA base damage are hydrolytic deamination, oxidation, alkylation, and ionizing radiation-induced base damage, just to name a few. Cytosine residues are especially susceptible to hydrolytic deamination which has been extensively studied using *in vitro* and *in vivo* assays as well as genetic reversion approaches (30, 54, 59, 107). It is estimated that there are approximately 500-2,000 cytosine residues deaminated per human cell per day. By comparison the deamination rates for purine residues are approximately 3-5% of cytosine deamination rates (42). Unlike the depurination rates, which are similar for single-stranded and double-stranded DNA, cytosine deamination rates in double-stranded DNA are approximately 1% that of single-stranded DNA (32). Cytosine deamination, as well as deamination of other base residues, can also be enhanced by various chemical agents and steric factors. For example, UV radiation-induced cyclobutane dimers, certain alkylating agents, and various mismatched bases or alkylated bases opposite cytosine are all known to enhance cytosine deamination rates (29, 52, 74, 114).

Another major source of DNA base damage in aerobically growing cells is oxidative damage. Various oxidant by-products are generated during normal cellular metabolism, such as superoxide radicals, hydrogen peroxide, and hydroxyl radicals, all of which have been shown to cause extensive damage to DNA. In double-stranded DNA

the major base lesion generated by reactive oxygen species is 8-oxoguanine. Nuclear magnetic resonance (NMR) studies revealed that 8-oxoguanine tends to favor a *syn* conformation and because of this can form a stable Hoogsteen base pair with adenine (46, 65). If left unrepaired 8-oxoguanine preferentially base pairs with adenine rather than cytosine during DNA replication and thus generates G • C → T • A transversion mutations. These transversion mutations are the second most common somatic mutation found in human cancers and are especially prevalent in the mutational spectrum of the tumor suppressor gene *p53* (41). The frequency at which 8-oxoguanine arises in DNA is estimated to occur at approximately the same frequency as cytosine deaminations (500-2,000 per human cell per day). However, the data published for this rate has been imprecise and varies considerably (3, 32, 55).

Other Types of DNA Base Damage

Experiments involving UV radiation-induced DNA damage mark the birth of the DNA repair field (32). The exposure of a wide variety of cell types to UV radiation is arguably the best studied and most extensively used model system for discovering the biological consequences of UV induced DNA damage repair.

The two major classes of DNA lesions formed from solar UV radiation are cyclobutane dimers and pyrimidine-pyrimidone (6-4) photoproducts (Figure 1-1). When DNA is exposed to wavelengths approaching its maximum absorption (~ 260 nm), adjacent pyrimidines become covalently linked by the formation of a four-membered ring structure resulting from saturation of their respective 5,6 double bonds (32, 60, 116). The resulting structure is referred to as pyrimidine dimer or cyclobutane dipyrimidine. Studies show that in DNA thymine-thymine dimers are more common than other

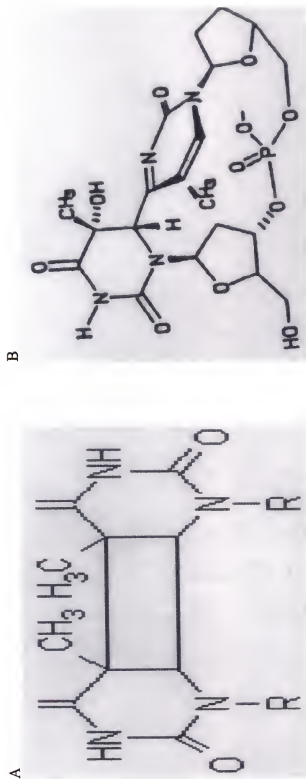


Figure 1-1. Structures of pyrimidine dimers. A) Structure of a cyclobutane pyrimidine dimer; the cyclobutane dimer is formed in DNA by covalent interaction of two adjacent pyrimidines in the same polynucleotide chain resulting in the formation of a four-membered cyclobutyl ring. B) Structure of a thymine-thymine photoproduct produced by linkage between the C-6 position of one thymine and the C-4 position of the adjacent thymine.

pyrimidine dimers. Irradiated plasmid and human DNA show a ratio of T-T to C-T to T-C to C-C of 68:13:16:3, for DNA irradiated at 254 nm (71, 115). The formation of cyclobutane dimers in DNA is not a random process. The Haseltine laboratory showed that pyrimidine dimer formation is influenced by the sequence context surrounding potential dimer sites (33). In the past cyclobutane dimers were considered to be bulky, DNA helix distorting lesions, which are noncoding since a base cannot be inserted during replication that can form stable hydrogen bonds. More recent evidence suggests these lesions can be accommodated inside the double helix with little distortion (32, 112), however replicative DNA polymerases are not capable of by-passing these lesions. Recently a new class of DNA polymerases have been identified which can replicate past pyrimidine dimers (16, 123).

Lesions at positions of cytosine located 3' to pyrimidine nucleosides are also present in UV irradiated DNA. These lesions are simply referred to as (6-4) photoproducts. These lesions introduce a major distortion in the DNA double helical structure. The (6-4) lesions of T-C and C-C are more common than T-T and there are not any reports of C-T (6-4) lesions (32). The (6-4) photoproducts usually occur at a frequency several fold lower than that of pyrimidine dimer formation. Also there is limited evidence suggesting that (6-4) lesions are influenced by DNA sequence context (11).

Ionizing radiation, another source of DNA damage, has been studied as extensively as UV radiation. However, at present various man-made therapeutic, diagnostic, and occupational sources of ionizing radiation are of far greater importance (32).

Ionizing radiation causes a wide variety of damage to DNA and also to other cellular components. Ionizing radiation is known to generate reactive oxygen species that then damage DNA. The DNA base damage arising from ionizing radiation has been studied *in vitro* using free bases, nucleosides, oligonucleotides, and DNA in aqueous solution (32, 113). A list of several common oxidative DNA base damages formed by ionizing radiation is shown in Table 1-1. In addition to causing DNA base damage, it is well documented that certain types of ionizing radiation can induce damage to the sugar residues of the DNA molecule and cause DNA strand breakage. It is estimated that X-rays (γ rays) at 1.0 Gy can result in 600-1,000 single-strand breaks and 16-40 double-strand breaks in human DNA (32, 113).

The bases of DNA are also susceptible to alkylation damage. Alkylated DNA bases can arise from endogenous or exogenous sources. The Seeberg laboratory recently showed the normal methyl-group donor of enzymatic transmethylation events, S-adenosylmethionine (SAM), can also react with DNA *in vivo* to produce alkylated DNA bases (107). The transmethylation reactions with SAM are estimated to generate several hundred alkylated DNA bases per human cell per day (98). A variety of environmental agents have been shown to alkylate DNA, such as *N*-methyl-*N'*-nitro-*N*-nitrosoguanidine (MNNG), methyl methanesulfonate (MMS), chemicals associated with cigarette smoke, dietary nitrites and nitrates, and various drugs used to treat cancer (37, 66, 98).

The N¹, N³, and N⁷ positions of adenine and the N¹, N², N³, N⁷, and O⁶ positions of guanine are especially susceptible to alkylation damage. This is because most alkylating agents are electrophilic compounds with affinity for nucleophilic centers (32).

Table 1-1. Oxidative lesions generated by γ radiation.

Product	No. of molecules/ 10^5 DNA bases
FaPyguanine	34.4
8-oxoguanine	23.3
5-hydroxyhydantoin	23.2
Thymine glycol	10.2
FaPyadenine	10.0
8-oxoadenine	5.5
5-hydroxycytosine	4.7
5-hydroxymethyluracil	2.8
5-hydroxyuracil	1.8

A list of common oxidative DNA base damages formed in chromatin of cultured human cells after treatment with γ radiation (420 Gy) (20).

The nitrogens of DNA bases, especially adenine and guanine, are nucleophilic and thus are reactive to alkylating compounds. Table 1-2 shows a variety of alkylating compounds and the plethora of alkylated lesions resulting from exposure to these agents. Lastly, the alkylation reaction involving alkylating compounds and DNA bases appears to be nonrandom in terms of DNA sequence and the relative distribution of alkylation damage may play a role in the generation of mutational hotspots (32). Support for this is given by the observation that the negative electrostatic potential of the N⁷ position of guanine is enhanced if this guanine is flanked by other guanine residues and will preferentially undergo electrophilic attack (32, 92).

Although DNA has limited chemical stability and is constantly being assaulted by endogenous and exogenous agents, the spontaneous mutation rate for most cells is very low. This is because cells have evolved elaborate pathways to counter the mutagenic and sometimes lethal effects of DNA damage. However, as with most things in life, not everything is perfect. The spontaneous decay of DNA and the accumulation of DNA damage in cells over time are likely to be major factors in mutagenesis, carcinogenesis, aging, as well as a variety of other human diseases (55).

Limiting Genomic Instability

The source of genomic instability is unfaithful transmission of genetic material from a cell to its progeny (105). This may occur from a breakdown in essential cellular functions that ensure the accuracy of DNA transactions, such as DNA replication, DNA damage repair, cell-cycle checkpoints, or mitotic chromosome distribution. A variety of human diseases can be viewed as diseases of underlying genetic instability. For the most part, all human cancers display some type of genetic instability, including subtle DNA

Table 1-2. A list of several known DNA alkylating agents.

DNA Source	Alkylating Agent	Resulting DNA Base Lesion
Salmon sperm	MeMS	7-MeG, 3-MeA, 1-MeA
Salmon sperm	Me ₂ SO ₄	7-MeG, 3-MeA, 1-MeA
Salmon sperm	MeNNG	7-MeG, O ⁶ MeG, 3-MeA
Salmon sperm	MeNU	7-MeG, 3-MeA, 7-MeA, O ⁶ MeG
HeLa cells	Et ₂ SO ₄	7-MeG, 3-MeA, 7-MeA, 3-MeG, 1-MeA, O ⁶ MeG
HeLa cells	EtNU	7-MeG, 3-MeA, 7-MeA, 3-MeG, 1-MeA, O ⁶ MeG
T7 phage	Mustard gas	7-MeG, 3-MeA

MeMS = methyl methanesulfonate, Me₂SO₄ = dimethyl sulfate, MeNNG = N-methyl-N'-nitro-N-nitrosoguanidine, MeNU = N-methyl-N-nitrosourea, Et₂SO₄ = diethyl sulfate, EtNU = N-ethyl-N-nitrosourea, Mustard gas = bis(2-chloroethyl) sulfide.

sequence alterations, gross chromosomal rearrangements, aneuploidy, and gene amplifications (105).

This review focuses on recent advances in the base excision repair pathway and discusses our biochemical studies of human base excision repair. For comparison I briefly discuss nucleotide excision repair (NER). The NER pathway represents a complex of proteins functioning to purge the genome of certain types of DNA base damage. Collectively these DNA repair pathways function to maintain genome stability by eliminating DNA base damage.

Nucleotide Excision Repair

The nucleotide excision repair (NER) pathway excises bulky DNA lesions from DNA and is evolutionary conserved from bacteria to man. As mentioned earlier, environmental sources of DNA base damage have been the subject of intense research. In addition to the previously mentioned UV-induced DNA lesions several other types of DNA damages arise from UV exposure, such as thymine glycols and pyrimidine hydrates. For the most part these lesions are bulky and often DNA helix distorting. As with other types of DNA damage, cells have evolved mechanisms to counter the mutagenic and lethal effects of these bulky adducts. The nucleotide excision repair (NER) pathway is the primary mechanism that recognizes these types of damages and excises them from DNA. NER is also responsible for eliminating a variety of other lesions from DNA including bulky chemical DNA adducts such as large polycyclic aromatic hydrocarbons (compounds found in cigarette smoke), interstrand crosslinks induced by various chemotherapeutic agents and some types of oxidative DNA damage

(10). Initial studies of NER in *E. coli* provided a foundation for NER experiments in other organisms.

Genetic experiments in *E. coli* identified three genes (*uvrA*, *uvrB*, and *uvrC*) that are required for excision of pyrimidine dimers from DNA. Subsequent studies revealed that these gene products are required for endonucleolytic incision of DNA containing pyrimidine dimers (97, 108). These initial and seminal experiments were followed by complex genetic and biochemical analyses, which identified other proteins, such as UvrD, required for efficient prokaryotic NER. The basic mechanism in bacteria is removal of a small single-stranded stretch of DNA (12-13 nucleotides) containing the substrate lesion by dual incision of the damage-containing DNA strand (10). Gap-filling DNA repair synthesis, using the complementary DNA strand as the template, is required to restore the initial genetic information. Although this type of mechanism is seen in higher eukaryotes, such as humans, the prokaryotic and eukaryotic NER proteins share very little homology, and mammalian NER is quite a bit more complex.

In eukaryotes, initial recognition of a NER substrate is carried out by the XPC/hHR23B complex. This initial recognition serves to recruit essential downstream NER components to the site of DNA damage. In addition to recognizing the initial damage, the XPC/hHR23B complex may also serve to increase the single-strandedness at the site of DNA damage (75). Additional proteins, such as XPE and XPA, may also function in initial DNA damage recognition for some types of lesions. In fact, XPA may be needed for proper organization of downstream NER components for efficient repair. XPA has been shown to interact with other NER components, such as RPA (single-stranded binding protein), the TFIIH transcription complex, and the ERCC1/XPF

endonuclease complex (10, 53, 84). After initial recognition local unwinding of the DNA helix and segregation of the DNA strand containing the lesion takes place. This process is dependent upon ATP, XPB, XPD, and the helicases of the TFIIH complex (26). The unwound DNA consist of a single-stranded oligonucleotide approximately 24-32 nucleotides in length that contains the substrate lesion. The endonuclease XPG incises this oligonucleotide on the 3' side of the open complex. ERCC1/XPF complex cuts on the 5' side of the single-strand and double-strand DNA junction. In theory, either of these endonucleases could possibly incise the undamaged strand; however both endonucleolytic events are coordinated by RPA, which binds to the undamaged DNA strand with a defined polarity (10). The final step in NER is gap-filling DNA synthesis and ligation. Nucleotide excision repair DNA synthesis requires RPA, RF-C, PCNA, and DNA polymerase δ or ϵ . The reaction is completed by the action of DNA ligase I (5).

The NER mechanism explained above is termed global genome nucleotide excision repair (GG-NER). Another type of NER has been identified that preferentially removes lesions from the transcribed strand of actively transcribed genes. This type of repair has been designated transcription-coupled repair (TC-NER) (67). Instead of using the XPC/hHR23B complex for initial recognition, TC-NER damage recognition is signaled by a stalled RNA polymerase II complex and CS-A and CS-B proteins (75). Both processes are essentially the same with the exception being in initial damage recognition (Figure 1-2).

There are several human diseases associated with defects in NER proteins. The most notable and well studied are xeroderma pigmentosum (XP), Cockayne's syndrome (CS), and trichothiodystrophy (TTD). Mutations in *XPA*, *XPB*, *XPD*, and *XPG* have been

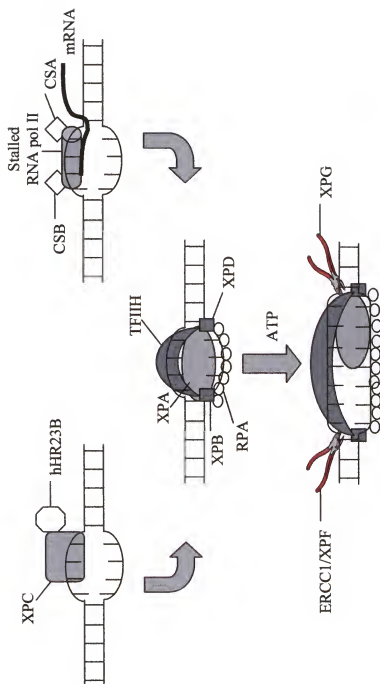


Figure 1-2. Model for GG-NER and TCR-NER. The only difference between the two pathways is in the initial recognition of the damage. Damage recognition can occur either by the XPC/hHR23B complex or by the RNA polymerase and the CSA and CSB proteins.

found to be associated with these diseases. The XP patients are highly sensitive to UV exposure and UV exposure generally results in degenerative alterations of the skin and eyes (10). Furthermore, XP patients have approximately a 20-fold increase in developing internal cancers by the age of 20. The CS patients display photosensitivity and CS cells display hypersensitivity to a variety of DNA damaging agents (5, 10). The CS patients normally display early onset progressive neurological degeneration and mental retardation. Brittle hair and ichthyosis (scaling of the skin) are hallmarks of TTD patients and these patients are also severely photosensitive. Most of the disease states associated with NER occur during early childhood, which may suggest a role for NER during development.

Base Excision Repair

The base excision repair pathway (BER) is an organism's primary defense against alkylated, deaminated, or oxidized DNA base damages. The pathway is called base excision repair because the chemically modified bases are released as free bases. The pathway is initiated by DNA glycosylases, which are damage-specific enzymes that recognize chemically modified DNA bases. The DNA glycosylases cleave the glycosidic bond connecting the base residue to the DNA sugar molecule with subsequent release of the free base. The resulting abasic sugar residue is processed by apurinic/apyrimidinic endonuclease (AP endonuclease) resulting in cleavage of the DNA phosphate backbone on the 5' side of the abasic site. The remaining deoxyribose phosphate residue is removed by a phosphodiesterase and DNA polymerase fills in the resulting gap and the strand is sealed by DNA ligase (Figure 1-3). Base excision repair is one of several pathways that also functions to remove abasic sites generated by spontaneous base loss

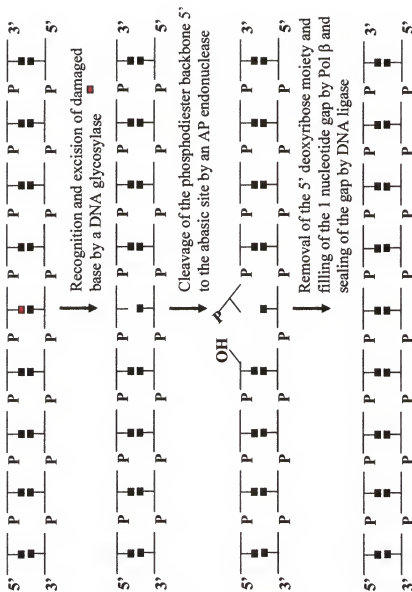


Figure 1-3. Representation of the base excision repair pathway. The pathway is dependent upon the action of DNA glycosylases, which must locate damaged DNA bases amid a vast excess of normal DNA bases.

during normal cellular metabolism. Base excision repair is an ancient DNA repair mechanism and has been identified in all organisms. Recent evidence suggests the primary function of BER may be to protect the long-term integrity of the genome over several generations (78).

The first DNA glycosylase identified was uracil DNA glycosylase (UDG), encoded by a gene designated *ung* (57). This enzyme was initially discovered in *E. coli*, but is also found in viruses, other bacteria, and eukaryotes. UDG is strictly specific for uracil residues, which arise in DNA via cytosine deamination or incorporation of dUMP during DNA replication. Uracil DNA glycosylase is highly conserved with approximately 40% amino acid sequence identity between the herpes simplex virus type 1 (HSV1), *E. coli*, and human UDG proteins (66). Intriguingly, UDG has not been detected in extracts of *Drosophila melanogaster* or in other insects that undergo pupation during development (32). This has led scientists to suggest that DNA containing large amounts of uracil might be required for normal developmental stages of pupating insects (21, 32). All UDGs isolated thus far are monomeric proteins (19-35 kDa), none of which can recognize uracil as a substrate in RNA molecules. Since the initial discovery of UDG, there have been a variety of DNA glycosylases identified in prokaryotes and eukaryotes. Most DNA glycosylases are damage specific enzymes recognizing only one type of damaged DNA base, but some of these newly identified DNA glycosylases are capable of recognizing several types of DNA damaged bases in DNA. For instance, the *E. coli* AlkA DNA glycosylase is capable of removing 3-methyladenine, 3-methylguanine, 7-methylguanine, and a variety of other alkylated DNA bases from DNA (66).

Characteristics of DNA Glycosylases

All of the DNA glycosylases identified to date are relatively small proteins ranging in molecular mass from 16-42 kDa. They do not require metal cofactors or exogenous energy sources for activity (32). All known DNA glycosylases show a strong preference for double-stranded DNA except for one, uracil DNA glycosylase (18, 32).

The DNA glycosylases can be subdivided into two groups: monofunctional and bifunctional DNA glycosylases. The monofunctional DNA glycosylases only catalyze hydrolysis of the glycosidic bond between the substrate base residue and the DNA sugar moiety. For the most part monofunctional DNA glycosylases utilize a water molecule in the enzyme active site for nucleophilic attack of the glycosidic bond. The active site water molecule of monofunctional DNA glycosylases is proposed to be activated (deprotonated) by the carboxyl side chain of an acidic catalytic amino acid residue, either aspartate or glutamate. The resulting incipient hydroxide ion can then be used for attack of the glycosidic bond.

Bifunctional DNA glycosylases utilize an active site enzyme amino group, usually a lysine residue, which has been activated by an aspartate residue as the nucleophile for attack of the glycosidic bond. In addition to being able to sever the glycosidic bond, bifunctional DNA glycosylases also contain an associated AP lyase activity that is capable of cleaving the DNA phosphodiester backbone. In these instances the activated amino group forms a Schiff base with C1' followed by β -elimination to cleave the phosphodiester backbone on the 3' side of the abasic site (32).

Spectroscopic and crystallographic studies show that DNA glycosylases employ a nucleotide flipping mechanism to expose substrate bases to the enzyme active site (40,

66, 73, 111). Nucleotide flipping, commonly referred to as base flipping, was first illustrated for the cytosine methyltransferases *HaeIII* and *HhaI* (45, 91). The suggested mechanism of rotating substrate bases out of the DNA helix exposes the substrate to the enzyme active site and provides tight control of substrate solvation and stereochemistry (40). Some argue that it remains to be seen whether base flipping is an active process carried out by DNA glycosylases upon binding to substrates or a passive event in which the enzyme captures spontaneously rotated nucleotides (40, 66, 73). However, our studies involving binding and excision of human alkyladenine DNA glycosylase (hAAG) to substrate bases opposite abasic residues suggest that hAAG may actively find and flip nucleotides out of DNA in order to expose them to the enzyme active site (1). In this study, we showed that hAAG could not excise or bind substrate bases when placed opposite an abasic site residue. The lack of base-pairing opposite an abasic site is likely to increase the frequency of transient spontaneous base-flipping. However, hAAG was not capable of recognizing substrates under these conditions which suggest that hAAG recognizes base pairs rather than just a damaged base before flipping occurs.

Human Alkyladenine DNA Glycosylase

DNA glycosylases capable of excising alkylated DNA bases from DNA have been identified in bacteria, yeast, plants, rodents, and humans (12, 13, 22, 56, 57, 99, 100). These enzymes were initially shown to excise 3-methyladenine from DNA hence they came to be known as 3-methyladenine DNA glycosylases. However, more detailed experiments revealed that most of these enzymes are capable of excising a diverse range of damaged bases in DNA, including 3-methyladenine, 7-methylguanine, 3-methylguanine, hypoxanthine, 1 N^6 -ethenoadenine, and various damages induced from

chemotherapeutic agents (37, 39, 81, 99, 101). This feature is quite unique because most DNA glycosylases are damage-specific, removing only one type of damaged base from DNA.

Human alkyladenine DNA glycosylase (hAAG) is a monofunctional DNA glycosylase comprised of 298 amino acid residues and is currently the only known human DNA glycosylase that excises alkylation-damaged bases from DNA. hAAG is a single domain protein of mixed α and β structure containing seven α helices and eight β strands. Eukaryotic hAAG homologues show a high degree of sequence and structural similarities. Despite the high degree of similarities between the eukaryotic enzymes, each enzyme shows a distinct substrate preference for damaged bases. For example, there is approximately 81% sequence similarity between mouse AAG and hAAG, however mouse AAG excises 3-methyladenine and 7-methylguanine 5-fold better than hAAG. Conversely, hAAG removes 1 N^6 -ethenoadenine 10-fold better than mouse AAG (19, 96). The exact nature for these differences is not understood.

Three crystal structures have been solved for hAAG (50, 51). The first structure reported was of hAAG complexed to a double-stranded oligonucleotide containing a central pyrrolidine abasic site nucleotide analog. The pyrrolidine nucleotide mimics the transition state of the glycosylase reaction and hAAG has been shown to bind very tightly to the pyrrolidine nucleotide. The second structure was of a catalytically inactive mutant (Glu125Gln) complexed to a double-stranded oligonucleotide containing a central 1 N^6 -ethenoadenine • T pair. The last structure shows the wild-type enzyme complexed to the same oligonucleotide as the Glu125Gln mutant. When all three crystal structures are superimposed upon one another there is very little structural difference between the

bound DNAs, the water molecules, and the protein residues in each complex. This suggests that the shape of the enzyme active site is predetermined rather than being induced by substrate binding.

Surprisingly, in the wild-type enzyme-DNA complex, the glycosylic bond is intact despite the fact that the crystals were grown for several days at room temperature. It was subsequently shown that high concentrations of magnesium used during crystal growth prevented glycosylase activity. Unexpectedly, there is not any electron density seen in the crystal structure that can be ascribed to bound magnesium. The exact nature of why magnesium inhibits hAAG activity is still unclear.

In the pyrrolidine containing structure, the pyrrolidine is flipped out of the DNA duplex into a pocket on the protein surface. The pyrrolidine nucleotide is secured in the proposed active site by protein contacts to the flanking phosphates. hAAG makes extensive contacts to both DNA strands to similar extents. A protruding β hairpin ($\beta 3\beta 4$) inserts into the minor groove of the bound DNA. Tyr162, which resides on the β hairpin, intercalates into the minor groove where its side chain fills the space vacated by the flipped nucleotide (Figure 1-4). Tyr162 acts as a surrogate base presumably stabilizing the nucleotide targeted for repair in an extrahelical conformation (50). It is hypothesized that Tyr162 is required for efficient nucleotide flipping. In the active site a bound water molecule is present that is poised for attack of the flipped-out nucleotide. The geometry of the water molecule is consistent with a direct, in-line displacement of a damaged base from the DNA backbone (40). The water molecule is at the center of a hydrogen bonding network that links the pyrrolidine nucleotide to the side chains of Glu125 and Arg182 and the main chain carbonyl of Val262 (Figure 1-5) (50). The close proximity of the water

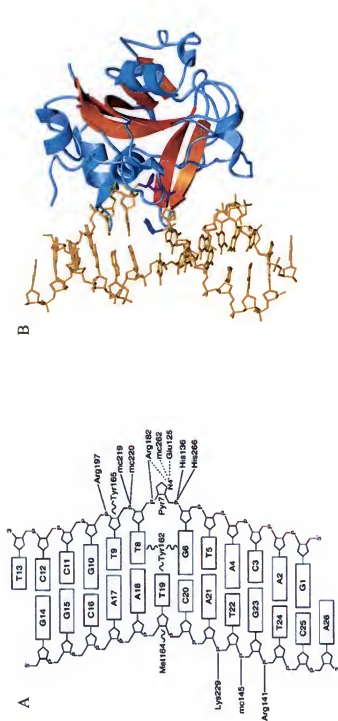


Figure 1-4. A) Schematic diagram of the hAAG-DNA contacts. The pyrrolidine abasic nucleotide is in an extrahelical conformation and hAAG makes contacts with both DNA strands. B) Crystal structure representation of hAAG complexed to DNA containing a pyrrolidine abasic nucleotide. hAAG binds in the minor groove and flips the abasic nucleotide (purple) into the active-site pocket. Tyr162 (blue) intercalates in the hole left by the flipped out nucleotide.

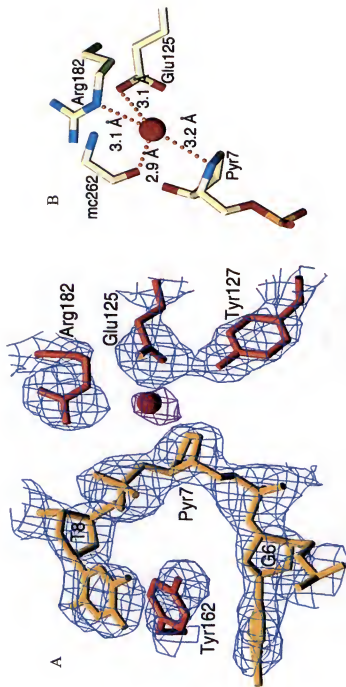


Figure 1-5. Electron density map of the flipped-out pyrrolidine abasic nucleotide. A) Difference electron density calculated with phases from the model refined with the water omitted, clearly shows a bound water molecule. B) The active site water hydrogen bonds with Glu125, Arg182, and the main chain carbonyl of Val262, and N4' of the pyrrolidine abasic nucleotide.

molecule with these residues suggest that Glu125 acts as a general base to deprotonate the water for backside attack of the glycosidic bond. Additionally, Arg182 is proposed to assist this attack by stabilizing the incipient hydroxide ion. In support of this, the substitution of Glu125 with glutamine results in a catalytically inactive mutant that is still capable of binding and flipping damaged substrates. Lastly, support for this model of nucleotide flipping and base excision is given by the strict conservation of Tyr162, Glu125, and Arg182 amongst all hAAG homologues.

The wild-type enzyme-DNA complex containing a central 1 N^6 -ethenoadenine • T pair suggests how some damaged bases are distinguished from normal DNA bases. The 1 N^6 -ethenoadenine substrate is flipped out of the DNA helix and into the enzyme active site where it stacks between the aromatic side chains of Tyr127 on one side and His136 and Tyr159 on the other side (51). It is proposed that base-stacking interactions between electron deficient damaged bases and aromatic side chains may provide the basis for hAAG substrate recognition. In addition, in the wild-type enzyme-DNA complex Tyr127 donates a hydrogen bond to Glu125, thereby stabilizing it in the active site. The ethenoadenine moiety fits snugly into the active site and a hydrogen bond exists between the main chain amide of His136 and the N^6 of 1 N^6 -ethenoadenine, which offers an acceptor lone pair that is unique to the alkylated adduct (50). The N^6 of normal adenine is protonated and would instead be repelled by the main chain amide of His136. Modeling of other suspected DNA substrate bases show that these can be accommodated in the enzyme active site.

These structures show an elegant means of exposing a nucleotide for base excision as well as the network of residues that could catalyze the in-line displacement of

a damaged base from the phosphodeoxyribose backbone (50). Although the structures do not definitively answer all of the questions regarding BER initiation, they do serve as a foundation for understanding base recognition, nucleotide flipping, and catalytic mechanisms employed by DNA glycosylases to excise damaged bases. A major question that still remains is how DNA glycosylases locate their substrates. Are they actively scanning the DNA for substrates? Do some glycosylases bind DNA and begin to flip nucleotides in search for substrates? Are they part of larger BER complexes? Do they associate with the DNA replication machinery or transcription factors in order to find substrates? The answer to these questions is not known. The only way to find out is to continue building on the foundation with more genetic, biochemical, and structural experiments.

hAAG Substrate Specificity

hAAG has been shown to have a broad substrate specificity and has been reported to remove various structurally unrelated damaged bases from DNA including, 3-methyladenine (12, 20, 80, 95, 99, 101), 7-methylguanine (4, 12, 80, 95, 99), hypoxanthine (4, 69, 102), *IN*⁶-ethenoadenine (4, 19, 20, 101), 7,8-dihydro-8-oxoguanine (9), etheno adducts of guanine (19), and undamaged purines (8, 125) (Figure 1-6). Several laboratories report conflicting results concerning substrate recognition and excision of hAAG substrates. A possible reason for the discrepancy in results may be due to the different oligonucleotide sequences used by each laboratory to examine substrate specificity. Additionally, some experiments have used excessively high enzyme concentrations compared to substrate concentrations in order to observe substrate recognition and excision. However, where a direct comparison was made examining two

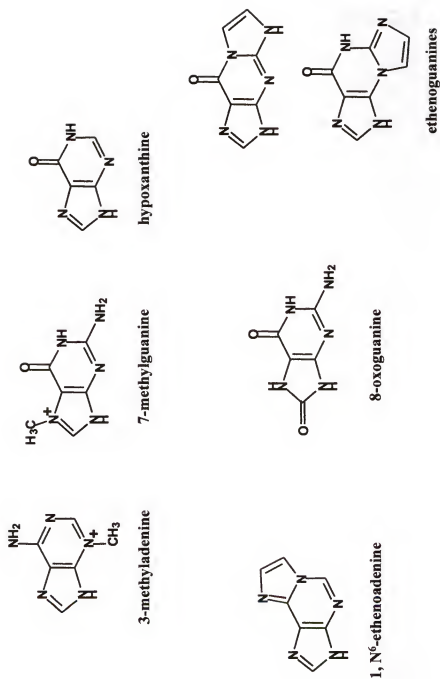


Figure 1-6. hAAG substrate bases. Damaged DNA bases reported to be excised from DNA by hAAG.

DNA adducts by two different laboratories, the results were very dissimilar. One laboratory reported that *IN*⁶-ethenoadenine to be excised 10-fold more efficiently than 3-methyladenine (20), while the other laboratory reported 3-methyladenine to be excised 3-7-fold more efficiently than *IN*⁶-ethenoadenine (101). Therefore, there is a 30-70-fold difference in reported results.

To more clearly define the substrate range of hAAG, we chose to measure kinetics of excision and DNA binding affinities for several different DNA damaged bases within the same DNA sequence context under the same assay conditions. Additionally, the effects on excision rates and binding affinities of varying the base paired with a damaged DNA base were examined. The goal was to try and elucidate any structural features that hAAG might use during substrate recognition and excision. Under our assay conditions, we found that *IN*⁶-ethenoadenine and hypoxanthine were excised efficiently by hAAG whereas 7,8-dihydro-8-oxoguanine, O⁶-methylguanine, adenine, and guanine were not. *IN*⁶-ethenoadenine and hypoxanthine represent damages to adenine. Both of these damaged bases have two hydrogen bond acceptors that project into the major groove *N*⁷ for both and an exocyclic nitrogen at the 6 position for *IN*⁶-ethenoadenine and an exocyclic oxygen at the 6 position for hypoxanthine. These are unique features to these damaged bases and may be exploited by hAAG.

The structural data for hAAG shows the active site pocket is preformed and not induced by substrate binding (40, 50, 51). Based upon these data and substrate modeling studies it is difficult to understand how some of the suggested substrates would be excised by hAAG notably, 7,8-dihydro-8-oxoguanine, etheno adducts of guanine, and 7-methylguanine. In support of the structural data, as well as our excision data, hAAG

knock-out experiments show excision of 7-methylguanine and 7,8-dihydro-8-oxoguanine are not affected in cells lacking hAAG activity. These studies do show that hAAG activity is required for removal of IN^6 -ethenoadenine, hypoxanthine, and 3-methyladenine from DNA.

Our results reveal that for some damaged bases, the opposing base can affect binding and excision. We show that IN^6 -ethenoadenine excision is relatively unaffected by the opposing base whereas hypoxanthine excision is greatly affected. This is more than likely due to the hydrogen-bonding interactions that each damaged base makes with the opposing base. IN^6 -ethenoadenine is not capable of hydrogen-bonding with any base because the etheno group bridges N^1 and the exocyclic amino group of adenine. If nucleotide flipping is important in substrate recognition the lack of hydrogen-bonding with IN^6 -ethenoadenine may make it easier to flip regardless of which base opposes it. In contrast, hypoxanthine is excised most efficiently opposite thymine. Hypoxanthine forms a wobble base-pair with thymine and uracil and a Watson-Crick base-pair with cytosine. These differences in hypoxanthine base-pairing more than likely contribute to differences in hypoxanthine excision efficiencies. These results are quite surprising based upon the structural data which shows that hAAG does not make specific contacts with the opposing base.

These studies were aimed at understanding the substrate specificity of hAAG. This DNA glycosylase is unique in that it is capable of excising several different damaged bases from DNA. Most of the previous studies involving broad substrate specific DNA glycosylases have focused on the damaged base alone, but our studies indicate that hAAG recognizes base pairs and not just the damaged base alone in DNA.

This feature of recognizing damaged bases within a certain base pairing context probably has an important biological role in helping to insure that the damaged base is repaired correctly. For example, hypoxanthine is excised more efficiently when opposite thymine than opposite cytosine. Hypoxanthine is initially formed opposite thymine, however once in DNA, hypoxanthine is mutagenic and miscodes for cytosine during DNA replication. If hAAG only recognized the damaged base alone, then removal of hypoxanthine opposite cytosine would result in a G • C mutation.

Human Apurinic/Apyrimidinic Endonuclease

Apurinic/apyrimidinic sites (AP sites), commonly referred to as abasic sites, are generated in all cells via spontaneous DNA base loss and by the activities of DNA glycosylases. Approximately 10,000 AP sites are generated per human cell per day (55, 58, 59). AP sites are chemically unstable in that they autolytically degrade into abnormal DNA strand breaks and are known to disrupt several essential cellular processes (55, 82). AP sites engage in suicide reactions with topoisomerase I, which results in permanent DNA damage and premature cell death (88). AP sites can form stable complexes with topoisomerase II which cause DNA double-strand breaks that are conducive to binding poly (ADP-ribose) polymerase resulting in faulty cell cycle arrest checkpoints and apoptosis (44, 82, 89). This presents an intriguing dilemma in that AP sites generated by DNA glycosylases are usually more cytotoxic than the original DNA damaged base. In order to survive cells have evolved apurinic/apyrimidinic endonucleases (AP endonucleases) to process AP sites and avoid cell death.

The major AP endonuclease found in mammalian cells, including humans, is human apurinic/apyrimidinic endonuclease 1 (APE1). This essential DNA repair protein

is also known as HAP-1 and APEX, and as an activator of DNA binding activity for some oxidized transcription factors, it is also called Ref-1 (64). APE1 cleaves the DNA sugar-phosphate backbone on the 5' side of AP sites, via a hydrolytic reaction involving Mg^{2+} , in order to prime DNA synthesis at these sites (24). Additionally, APE1 contains an associated 3' phosphodiesterase and 3' phosphatase activities. If BER is initiated by monofunctional DNA glycosylases, APE1 leaves a nick with a 3'-OH and a 5'-deoxyribose 5-phosphate (dRP). If BER is initiated by bifunctional glycosylases, APE1 generates a 1 nucleotide gap flanked by 3'-OH and 5' phosphate ends (78). The 3' OH group generated by APE1 serves as a substrate for DNA polymerases.

Recent structural studies of three cocrystals of human APE1 complexed to double-stranded oligonucleotides containing central abasic residues have provided insight into substrate binding and phosphodiester bond cleavage of AP sites by APE1 (72). The crystal structure of APE1 alone was previously solved (34) and its structure is very similar to the three cocrystals complexed with AP site containing DNA, suggesting that APE1 does not undergo an extensive protein conformational change upon DNA binding and catalysis (120). The r.m.s. deviation is only ~ 0.5 Å between $C\alpha$ atoms of the apoenzyme and those of the DNA-bound structures (72). The crystal structures reveal that APE1 has a rigid, preformed DNA binding surface that is dominated by positively charged amino acid residues that kink the DNA helix and surround the AP-DNA strand (72). The DNA binding surface of APE1 spans the abasic site and several flanking nucleotides. APE1 inserts loops into both the major and minor grooves of DNA causing a severe bending ($\sim 35^\circ$) of the DNA (Figure 1-7). The APE1-bound DNA complex shows a flipped-out abasic site residing in a pocket that excludes normal DNA bases. It is

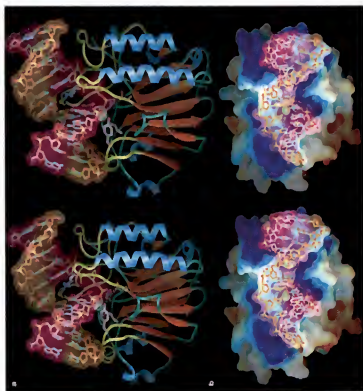


Figure 1-7. Crystal structure of APE1. A) Stereo view of APE1 complexed to a double-stranded 11 base-pair oligonucleotide containing a central abasic site. APE1 contacts both DNA strands and the abasic residue is rotated out of the DNA and inserted into the active site pocket. B) APE1 binding to DNA viewed looking down on the enzyme-DNA interface. APE1 binding to abasic site containing DNA causes a bend in the DNA $\sim 35^\circ$.

suggested that the insertion of these loops into DNA results in a flipping of the AP site into an extra helical conformation resembling that of DNA glycosylases. Although nucleotide flipping is characteristic of DNA glycosylases and other DNA binding proteins, it is not obviously required by AP endonucleases. However, several structural studies of other AP endonucleases also show a bound abasic residue that is rotated out of the DNA helix.

In all three of the APE1-bound complexes the sugar is in an alpha anomeric conformation rather than a beta anomeric conformation. This is noteworthy because crystal structures of hUDG complexed to product DNA also shows the abasic residue sugar in an alpha anomeric position (72, 120). These observations have led to a hypothesis of an enzyme-product hand-off between DNA glycosylases and AP endonucleases. The researchers suggest that the extensive DNA binding surface of APE1, along with the distortion of the bound DNA, permit displacement of DNA glycosylases that are bound to their respective abasic site products. If APE1 retains the distorted conformation after cleaving the DNA phosphate backbone, it may be able to hand-off the product to the next enzyme in the BER, polymerase beta (pol β). In fact studies have shown that APE1 and pol β are capable of binding one another in the presence of abasic site DNA (64).

Stimulation of DNA Glycosylase Activity by APE1

Several *in vitro* studies show that some DNA glycosylases bind tightly to abasic sites on DNA (85, 90, 118). In most instances these glycosylases bind more tightly to the abasic site than to their respective damaged substrates. For instance, the affinity of human 8-oxoguanine DNA glycosylase (hOGG1) for an AP site opposite cytosine is

approximately 2.8 nM; whereas its affinity for its substrate 8-oxoguanine opposite cytosine is approximately 24 nM (38, 117). Another example is human thymine DNA glycosylase (hTDG) which displays an affinity for AP sites approximately 100-1000-fold greater than for its mismatched substrate (G • T) (118). In these instances, the overall BER pathway would be slowed unless other factors could stimulate enzyme turnover or eliminate the reaction product generated by DNA glycosylases. Recent studies indicate that APE1 is capable of promoting enzyme turnover of these glycosylases by displacing the glycosylase from the abasic site (38, 90, 117, 118). Also, it has been shown that these glycosylases have a higher affinity for non-cleaved AP sites than for the cleaved DNA product generated by APE1. Therefore, this would shift the equilibrium towards the free glycosylase and allow for multiple enzyme turnovers.

In contrast to these DNA glycosylases, our studies show that hAAG binds substrates with greater or equal affinity compared to abasic site products. However, our data does indicate that APE1 stimulates hAAG turnover. These data suggest that APE1 is not stimulating the catalytic activity of hAAG, but is somehow allowing hAAG to perform multiple enzyme turnovers. These studies will be followed by more extensive kinetic experiments in order to determine the exact nature of hAAG stimulation by APE1. We are also interested in the affect that other BER components might have on human DNA glycosylase activity as well as the affect that human DNA glycosylases might have on APE1 activity.

Human Polymerase Beta and DNA Ligase

In the BER pathway of mammalian cells, the concerted action of DNA glycosylases and APE1 results in a DNA strand that contains a 3'-OH end and a 5'-sugar

phosphate. In mammalian cells, the DNA synthesis step of BER is carried out by DNA polymerase β (pol β). Pol β is the smallest of the nuclear DNA polymerases with a molecular weight of approximately 39 kDa. Pol β consists of two domains, an N-terminal 8-kDa domain that contains deoxyribosephosphate lyase activity and a C-terminal domain that possesses nucleotidyl transfer activity (104). Pol β is classified as an error-prone DNA polymerase and it has been estimated that pol β 's error frequency is approximately 1 in every 2,000 nucleotides incorporated (6).

The DNA synthesis step in BER can proceed by either a short-patch or long-patch pathway. In the short-patch pathway, pol β adds one nucleotide to the 3'-OH end and then removes the 5'-deoxyribose phosphate (dRP) moiety (86). The resulting nick is sealed by either DNA ligase I or through the XRCC1 protein complexed with DNA ligase III. The exact DNA ligase that functions in mammalian BER is still unclear. There is genetic and biochemical evidence suggesting both DNA ligase I and DNA ligase III participates in BER. Cells deficient in either DNA ligase I or DNA ligase III are hypersensitive to alkylating agents, and extracts from these cells are defective in BER (110). Regardless of which DNA ligase is responsible for end joining, removal of the dRP moiety is absolutely required for DNA ligase to seal the nick. Short-patch BER constitutes between 75-90% of all BER in human cells (78, 109). Genetic and biochemical studies show that short-patch BER exclusively requires pol β .

Long-patch BER involves the synthesis of between 2-8 nucleotides and is useful for cases when the dRP moiety is resistant to pol β excision. In these instances strand displacement DNA synthesis results in a flap structure that contains the dRP moiety. Strand displacement DNA synthesis can be accomplished with pol β , pol δ , or pol ϵ .

Proliferating cell nuclear antigen (PCNA) stimulates pol β strand displacement synthesis, but is not required for long-patch BER initiated by pol β (78). The resulting flap formed from strand displacement DNA synthesis is removed by flap endonuclease 1 (FEN1). PCNA aids in this reaction by positioning FEN1 at the flap-DNA hinge and stimulates the nuclease activity of FEN1 to release a short oligonucleotide containing the dRP moiety (78). Pol β deficient cells have been shown to be deficient in short-patch BER but proficient in long-patch repair, thus pol δ or pol ϵ is believed to be responsible for long-patch BER (109).

Genetic Studies of BER Proteins

There are not any known human diseases associated with a defect in a BER protein. Regardless of this, any system that is conserved throughout evolution and functions to purge cellular genomes of DNA base damage must be of utmost importance. There have been quite a few genetic studies in mice examining various BER enzyme deficiencies. Using mouse knockout technology several BER enzymes have been inactivated in order to gain more insight into the genetic nature of faulty BER. The mouse is an ideal organism for comparing BER with humans because most of the mouse BER enzymes show an exceptionally high degree of sequence similarity as well as structural conservation.

DNA glycosylase knockouts were the first to be constructed and yielded somewhat surprising results. Mice deficient in AAG activity show no increase in spontaneous mutation frequency and only a 3-fold enhancement in mutation frequency when exposed to alkylating agents (23). UDG deficient mice show less than a 2-fold increase in mutation frequency in all tissues examined (79). It was subsequently

discovered that UDG was responsible for removing uracil from newly replicated DNA and that another protein (SMUG) was responsible for removing uracil generated via cytosine deamination (79). OGG1 deficient mice show a 6-fold increase in spontaneous mutation frequency in some tissues analyzed whereas other tissues did not show a significant increase above control tissues (70). Thus far, none of these mice have developed tumors in any tissues and there are not any other signs of disease formation in spite of the accumulation of DNA base damage resulting from deficiencies in DNA glycosylase activity. However, the accumulation of these DNA base damages seems to be considerably less than would be expected. These observations are in contrast to the prokaryotic DNA glycosylase deficient strains that show a substantial increase in mutation frequency and some strains show a decrease in cell viability, suggesting that a back up system for repair may be present.

Genetic knockouts of components downstream of DNA glycosylases in the BER pathway have yielded completely opposite results. Experiments show that a deficiency in any component downstream of DNA glycosylases results in an embryonic lethal phenotype (31). One explanation for this phenotype might be that the DNA glycosylases generate repair intermediates that if not repaired lead to cellular death. Another plausible explanation is that some of the downstream components, namely APE1, XRCC1, and pol β have also been shown to play a role in development. If the former explanation is correct then one would assume that inactivation of the major DNA glycosylases, in addition to inactivation of downstream BER components, would rescue the lethal phenotype. However, these experiments have not been completed.

These limited genetic studies have raised some interesting questions regarding the importance of mammalian BER. Why would DNA glycosylases be so strongly conserved throughout evolution when inactivation of individual DNA glycosylases seem to have little affect upon genome stability? Does BER play a role in disease avoidance? As stated previously knockouts involving individual DNA glycosylases showed only a modest increase in mutation frequency, but more intriguingly is the observation that the accumulation of DNA base damage is not as high as expected. This may suggest that other repair systems are correcting the DNA base damage. Additionally, some of these base damages are known to induce mutations and block replication yet these mice show no signs of disease. Therefore, a possibility of another DNA repair system functioning to eliminate base damages is a strong possibility. Also a small reduction in fitness would be hard to detect under most laboratory settings, but may have a profound effect on long-term fitness (78). Along these same lines it very well may be that in order to see a significant increase in mutation frequency several DNA glycosylases need to be inactivated. It has been suggested that BER may actually be involved in protecting the long-term integrity of cellular genomes. The BER pathway was established before diseases encroached upon eukaryotic organisms. It has been stated that prevention of cancer is not a function of DNA repair, but cancer may be a consequence of inadequate repair (78). It seems likely that any system that is dedicated to purging the genome of potential mutagenic and lethal consequences would be important for disease avoidance. Just because there is not a known disease associated with a BER defect does not necessarily mean that a disease state does not exist. Additionally, mutations in other genes that eventually leads to disease formation may actually have a root in faulty BER.

The fact of the matter is that a considerable number of human diseases can already be traced back to faulty DNA repair pathways.

Summary

The purpose of our research has been aimed at understanding how DNA glycosylases function in BER. To this end, we have focused our attention on the broad substrate specific DNA glycosylase, hAAG. Our goal has been to illuminate the biochemical mechanisms that allow for complete and efficient repair of damaged bases via the BER pathway. Since DNA glycosylases initiate BER they are key to the overall effectiveness of the pathway. Our results have provided seminal insights into how hAAG recognizes and excises damaged substrates from DNA. We have also shown that APE1 stimulates hAAG turnover *in vitro*. These results suggest that there is some type of coupling between hAAG activity and APE1 activity in the BER pathway. Knowledge obtained from our studies could be extremely valuable. Since many unrepaired DNA lesions are pre-mutagenic they have the potential to cause mutations. This is of special medical interest because mutations generated during DNA replication of damaged bases are thought to be the root of several human diseases, including various cancers.

Lastly, the chemical instability of the covalent structure of DNA coupled with the enormous amount of endogenous and exogenous damage to DNA that occurs each day is startling. But even more startling is the fact that cells have been able to counter this massive assault by evolving elaborate DNA repair mechanisms in order to avoid dire consequences. All eukaryotic DNA repair mechanisms have a prokaryotic counterpart. This strong conservation of DNA repair mechanisms throughout evolution underscores the importance of these systems. More than likely during evolution, cells quickly

acquired DNA repair processes in order to avoid genome damage. The wealth of knowledge that has been obtained from genetic, biochemical, and structural experiments have provided a firm foundation in understanding some of these processes. Even so, more questions remain today than compared to thirty years ago.

CHAPTER 2 EXPERIMENTAL PROCEDURES

Purification of Human Alkyladenine DNA Glycosylase (hAAG)

Protein Expression

Escherichia coli BL21 (DE3) (Novagen) cells were transformed with pET-14b expression plasmids containing wild-type or mutant hAAG genes. The wild-type hAAG gene was spliced from a pLM1 vector containing wild-type hAAG and placed into the pET-14b expression vector. The pLM1-hAAG construct was a generous gift from Dr. Tom Ellenberger (Harvard University). Transformed cells were plated on 2xYT plates containing 100 µg/mL ampicillin and grown for 16-18 hours at 37°C. Only transformed colonies that were less than one week old were used for culturing. A 10 mL aliquot of 2xYT containing 100 µg/mL ampicillin was inoculated with a single colony of transformed cells. Cells were grown at 37°C with vigorous shaking (200 rpm) to $A_{600} = 0.5-1.0$ and stored at 4°C overnight. The next day the cells were washed twice (10 mL per wash) with fresh 2xYT containing 100 µg/mL ampicillin by spinning the cells down and discarding the supernatant and resuspending the cell pellet in fresh media. The washed cells were used to inoculate 6 liters of 2xYT containing 100 µg/mL ampicillin. Cells were grown at 37°C with vigorous shaking (200 rpm) to $A_{600} = 0.5$. The cells were cooled in ice to 15°-20°C and the culture allowed to equilibrate at room temperature for 30 minutes with shaking. Cells were induced with 1 mM (final concentration) isopropyl β -D-thiogalactopyranoside (IPTG) and were incubated at room temperature with

vigorous shaking (200 rpm) for an additional 8 hours. Cells were harvested by centrifugation at 8,000g for 30 minutes and the cell pellets stored overnight at -80°C.

Protein Isolation and Purification

The cell pellets were weighed (typically 20-25 g/6L) and resuspended on ice with 3 mL/g in cold buffer A (50 mM sodium phosphate (pH 7.4), 0.5% 2-mercaptoethanol, 1 mM EDTA, 10% (w/v) glycerol, 70 mM NaCl, 1 µg/mL pepstatin A (Sigma), 1 µg/mL leupeptin (Sigma), and 0.1 mg/mL PMSF (Sigma)). Aliquots of the cell suspension were placed into cold 50 mL conical tubes and lysed by sonication using a Branson Sonifier 450 equipped with a 3/8 inch tip. Four 30 second pulses with the power level between 6 and 7 at 30-40% duty were delivered at 3 minute intervals in an ice bath. The crude extract was dispensed into cold 30 mL plastic tubes and spun at 27,000 g for 45 minutes at 4°C in a JA-20 Beckman rotor. The supernatant, containing soluble protein, was pooled and placed into a pre-chilled sterile 250 mL Erlenmeyer flask and placed on ice. All subsequent purification steps were performed at 4°C using an Amersham Pharmacia Biotech FPLC system.

A 175 mL diethylaminoethyl cellulose (Sigma) (DE52) anion exchange column (26 cm x 40 cm) was utilized to remove nucleic acids from the supernatant. As the DE52 column is slow to equilibrate in buffer A approximately 1000 mL of 250 mM sodium phosphate (pH 7.4) was run at 2 mL/minute over the packed column. After this several column volumes of 1X buffer A without protease inhibitors was run over the column until the pH of the effluent was 7.4.

The supernatant from the crude extract was loaded at 2 mL/minute onto the DE52 column. After the sample was applied the column was rinsed with one column volume of

buffer A. hAAG does not bind to the DE52 column in buffer A; therefore the column flow-through fractions were collected in a 500 mL pre-chilled sterile Erlenmeyer flask on ice. The pooled fractions were loaded at 1.5 mL/minute onto a 5 mL HiTrap sulfopropyl sepharose cation exchange column (Amersham Pharmacia Biotech) equilibrated in buffer A and the column was rinsed with 3 column volumes of buffer A. Although hAAG should bind to the HiTrap column under these conditions the flow through from this column was also collected as a precaution. An 88 mL gradient from 70 to 500 mM NaCl in buffer A was used to elute hAAG from the HiTrap column. hAAG Δ 79 typically eluted from the HiTrap column at approximately 250-300 mM NaCl and hAAG-FL typically eluted at 400-450 mM NaCl. Fractions (1.5 mL) were collected in 2 mL plastic tubes. Fractions containing hAAG were identified by SDS-PAGE analysis and pooled. This pool was concentrated to approximately 2-3 mL by centrifugation using a Centricon-10 (10,000 molecular weight cutoff) device (Amicon). The concentrated pool was loaded at 0.5 mL/minute onto a 90 mL Sephacryl S-200 HR gel filtration column (Amersham Pharmacia Biotech). The column was developed isocratically at 1.0 mL/minute with buffer B (25 mM Tris (pH 7.5), 200 mM NaCl, 1 mM EDTA, 1 mM dithiothreitol, and 5% (w/v) glycerol). Fractions (1.5 mL) were collected in 2 mL plastic tubes and those fractions (typically fractions 20-30) containing hAAG were identified by SDS-PAGE analysis and pooled. This pool was concentrated to approximately 0.5-1.0 mL by centrifugation using a Centricon-10 device. The concentrated, purified hAAG protein was dialyzed against pre-chilled hAAG storage buffer (50 mM HEPES (pH 7.5), 100 mM NaCl, 1 mM EDTA, 1 mM dithiothreitol, and 37.5% glycerol) at 4°C and aliquots were

dispensed into sterile plastic tubes and stored at -80°C. Typically 6 liters of cells yielded approximately 15-20 mg of hAAGΔ79 and 3-5 mg of hAAG-FL protein.

Oligonucleotide Synthesis and Purification

Synthetic unmodified and modified oligonucleotide substrates were either purchased from Sigma-Genosys or prepared by solid phase synthesis on an Applied Biosystems Incorporated 392 DNA synthesizer using standard β -cyanoethylphosphoramidite chemistry and reagents from Glen Research. Using standard procedures, the oligonucleotides were cleaved from the solid support by treatment with fresh concentrated ammonium hydroxide and the column effluent was forced into a collection vial by argon flush. The collection vial contained a crude mixture of base-protected product and failure sequence oligonucleotides in ammonium hydroxide. The base-protecting groups were removed from the oligonucleotides by placing the vial into a 55°C sand bath for 12-16 hours. The deprotected oligonucleotide mixture was transferred to 2 mL plastic tubes and concentrated to approximately 250 μ L using a Savant Hi-Speed centrifugal vacuum system. An equal volume of 50% glycerol was added to the concentrated oligonucleotide mixture and an A_{260} of the samples was determined.

The samples were resolved on a 30 cm (width) X 40 cm (height) X 1.5 mm (thick) 16% polyacrylamide gel containing 8 M urea. The gel was pre-run at 6 watts for an hour at room temperature in 1X TBE buffer (90 mM Tris, 90 mM boric acid, 1 mM EDTA). After pre-running the gel, the wells were flushed extensively using a needle and syringe. Approximately 10-20 μ L of bromophenol blue/xylene cyanol FF loading dye was loaded into the first well and 40-50 μ L of the oligonucleotide mixture was loaded

into each of the additional wells. To avoid warming of the gel and the possibility of heat damaging the oligonucleotides, the samples were run for 16-18 hours at 6 watts. The gel apparatus was disassembled and the gel covered on both sides with plastic wrap, making sure to avoid bubbles between the plastic wrap and the gel. The wrapped gel was placed on a TLC plate that contained a fluorescent dye indicator and a hand held UV source was used to produce a shadow of the bands on the TLC plate. The bands were circled on the plastic wrap with a black permanent marker quickly, so that the DNA was not exposed to the UV light for an extended period. The bands were cut from the gel using new razor blades and placed into a sterile 50 mL conical tube. Approximately 8-10 mL of sterile NTE (50 mM Tris-HCl (pH 7.5), 50 mM NaCl, and 1 mM EDTA) was added to the gel slices and the tube gently shaken for approximately 8 hours at room temperature. The liquid was removed from the tube and transferred to another sterile 50 mL conical tube and placed at 4°C. An additional 5 mL of NTE was added to the DNA-containing slices. This mixture was gently shaken overnight and the next day the solution was combined with the first DNA elution. The pooled solution was dialyzed using Spectropor Dialysis tubing (3500 molecular weight cutoff) 3X against 4 L water, changing the solution every 6 hours. In order to remove gel debris the solution was passed through a 0.2 μ M syringe filter (Acrodisc) after dialysis. The filtered oligonucleotide solution was dispensed into sterile 2.0 mL plastic tubes and concentrated to approximately 500 μ L using a Savant Hi-Speed centrifugal vacuum system. An A_{260} of each sample was determined and the concentrations of the purified single-stranded oligonucleotides were calculated using extinction coefficients (27) derived for each oligonucleotide at 260 nm. Oligonucleotide samples were dispensed into sterile plastic tubes and stored at -80°C.

³²P DNA hAAG Excision Assay

Labeling and Annealing of ³²P DNA Substrates

Single-stranded oligonucleotide substrates containing a central undamaged or damaged nucleotide were 5'-end-labeled with [γ -³²P]-ATP (Amersham Pharmacia Biotech) using bacteriophage T4 polynucleotide kinase (PNK) (Invitrogen). Typical labeling reactions (40 μ L) contained 2.5 μ M substrate DNA, 50 mM HEPES (pH 8.0), 100 mM NaCl, 1 mM EDTA, 8 mM MgCl₂, 1 unit of T4 PNK, and 250 nM [γ -³²P]-ATP. Labeling reactions were performed at 37°C for 1 hour. Subsequently the reaction mixture was heated to 95°C for 10 minutes to heat inactivate the T4 PNK. Ten μ L of complement DNA (12 μ M) was added to the labeled substrate and mixed thoroughly. The two complementary strands were annealed to each other by incubation in an 80°C water bath for several minutes, then cooling the water bath slowly to room temperature. No further purification of the labeled double-stranded substrate was required.

Excision Assays

hAAG base excision was measured using a chemical cleavage/gel assay. Typical excision reaction mixtures included 50 nM ³²P-labeled oligonucleotide duplex DNA, 50 mM HEPES (pH 8.0), 100 mM NaCl, 10 mM EDTA, 1 mM DTT, 9.5% glycerol, and various concentrations of hAAG in a total volume of 40 μ L. Before the addition of enzyme all components were placed in a 0.5 mL plastic tube and allowed to equilibrate in a 37°C water bath for 3 minutes. Excision reactions were initiated by addition of enzyme and incubation of the mixture at 37°C. At several time points during the excision reaction, an aliquot (4 μ L) of the reaction mixture was quenched by placing the aliquot into another 0.5 mL plastic tube that contained 1 μ L of 1 M NaOH (0.2 M NaOH final

concentration) followed by pipeting the solution up and down several times to mix. Quenched reactions were immediately placed on ice and kept cold until completion of the experiment. The quenched reactions were then placed in a 90°C heat block for 5 minutes in order to cleave DNA strands containing abasic sites. After heating, the samples were centrifuged using an Eppendorf microfuge (13,000g for 5 seconds) and diluted with 2 volumes (8 μ L) of loading buffer consisting of 95% formamide and 20 mM EDTA. The substrates and products were resolved by electrophoresis on a 12% polyacrylamide gel containing 8M urea in 1X TBE buffer. Before loading the samples, the gel was pre-run at 1600 volts for 45 minutes, followed by extensive flushing of the wells using a needle and syringe. Bromophenol blue/xylene cyanol FF loading dye (4 μ L) was loaded into the first well followed by loading 4 μ L of each sample into the additional wells. Samples were electrophoresed at 1600 volts for 1 hour. After electrophoresis the gel was placed on filter paper, trimmed and dried on a Savant vacuum gel drier at 80°C for 45 minutes. The dried gel was exposed to a phosphorimager screen for approximately 6-8 hours and analyzed quantitatively using a Molecular Dynamics Storm PhosphorImager and ImageQuant software.

Electrophoretic Mobility Shift Assay (EMSA) Using 32 P DNA

hAAG binding to undamaged or damaged DNA bases was measured using electrophoretic mobility gel shift assays (EMSAs). The DNA strand containing the damaged base was 5'-end-labeled with [γ - 32 P]-ATP and annealed to a complementary strand containing either T, C, or U opposite the damaged base. The EMSA buffer is identical to the excision reaction buffer and typical binding reactions contained 50 nM 32 P-labeled oligonucleotide duplex, 50 nM HEPES (pH 8.0), 100 mM NaCl, 10 mM

EDTA, 1 mM DTT, 9.5% glycerol, and increasing concentrations of hAAG in a total volume of 20 μ L. Before the addition of substrate or enzyme all the other components were placed in a 0.5 mL plastic tube and allowed to equilibrate to 4°C in a cold room for approximately 1 hour. After the addition of substrate and enzyme the reaction mixtures were incubated at 4°C for 10 minutes. Five μ L of the reaction mixture was then loaded directly onto a 6% nondenaturing polyacrylamide gel and electrophoresis was performed at 4°C for 180 minutes at 8 V/cm. Afterwards the gel was dried on a Savant vacuum gel drier at 80°C for 25 minutes and exposed to a phosphorimager screen for approximately 3-4 hours. Amounts of bound and free 32 P-labelled DNA probe were determined by quantitative analysis of dried gels using a Molecular Dynamics Storm PhosphorImager and ImageQuant software.

Apparent binding constants ($K_{d,app}$) for hAAG binding to DNA substrates were calculated using Equation 1 for a simple two-state binding model where E_o is the total enzyme concentration, D_o is the total DNA concentration, and ED^{total} is the total concentration of all enzyme-bound species.

$$[ED^{total}] = E_o + D_o + K_{d,app} - \frac{\sqrt{(E_o + D_o + K_{d,app})^2 - 4 E_o D_o}}{2} \quad (\text{Eq. 2-1})$$

Yeast Two-Hybrid Analysis

Yeast Media Preparation

Yeast extract/peptone/dextrose (YPD) medium and YPD agar medium were prepared by combining 20 g/L peptone, 10 g/L yeast extract, with or without 20 g/L agar into 930 mL of deionized water and adjusting the pH to 5.8 with hydrochloric acid (HCl). The media was sterilized in an autoclave for 30 minutes and cooled to approximately 60°C. Next 50 mL/L of sterile 40% dextrose (glucose) and 15 mL/L of filter sterilized

0.2% adenine hemisulfate were added to the media solution. This rich medium was used only for the initial streaking of yeast freezer stocks, maintaining yeast strains, and mating experiments.

Synthetic dropout (SD) medium was the yeast minimal medium used in yeast transformations and for testing specific yeast phenotypes. SD medium was prepared by combining 6.7 g/L of yeast nitrogen base without amino acids, the appropriate “dropout” supplement containing specific amino acids, with or without 20 g/L agar into 950 mL of deionized water and adjusting the pH to 5.8. The media was sterilized in an autoclave for 30 minutes and cooled to approximately 60°C. The medium was supplemented with 50 mL/L of sterile 40% dextrose (glucose) and where appropriate 20 mg/L of X- α -galactosidase (Clontech) dissolved in dimethylformamide (DMF) where appropriate.

Yeast Transformation

Freezer stocks of yeast strains were streaked onto YPD plates and grown at 30°C for 3-5 days. To make competent cells, 1 mL of YPD medium was inoculated with several 2-3 mm diameter colonies from platings 1-2 weeks old. This provided the best transformation efficiencies. The 1 mL cultures were grown for 24 hours at 30°C, then the cells were transferred to a 500 mL flask containing 50 mL of sterile YPD medium and grown at 30°C for 16-18 hours with vigorous shaking (250 rpm) ($OD_{600} > 1.5$). A volume of this overnight culture was transferred to a 1 L flask containing 300 mL of YPD medium so that an $OD_{600} = 0.2-0.3$ was achieved. The cells were incubated at 30°C for 3-4 hours with shaking (250 rpm) until the $OD_{600} = 0.5 \pm 0.1$. The cells were then centrifuged at 2,000g for 10 minutes at room temperature. The resulting supernatant was discarded and the cell pellets resuspended in 30 mL of sterile TE (10 mM Tris-HCl (pH

7.5) and 1 mM EDTA) and centrifuged at 2,000g for 10 minutes at room temperature. The supernatant was discarded and the cell pellets were resuspended in 1.5 mL of freshly prepared, sterile TE/LiAc (10 mM Tris-HCl (pH 7.5), 1 mM EDTA, and 100 mM lithium acetate (pH 7.5). Transformation efficiency was greatest when the cells were used within a few hours of preparation; however it is also possible to freeze the cells at -80°C in 100 µL aliquots at this stage. For all transformations 0.1 µg of plasmid construct, 0.1 mg herring testes carrier DNA (boiled for 20 minutes prior to use), and 100 µL of yeast competent cells were mixed in a 1.5 mL tube by vigorous vortexing. Six-hundred µL of freshly prepared, sterile PEG/LiAc (40% PEG 3350 and 100 mM lithium acetate (pH 7.5)) solution was added to each transformation tube and vigorously vortexed for several seconds. Subsequently, the tubes were incubated at 30°C for 30 minutes with shaking (200 rpm). Following incubation 70 µL of dimethyl sulfoxide (DMSO) was added to each tube and the tubes were mixed by gentle inversion. The tubes were incubated in a 42°C water bath for 15 minutes to heat shock followed by chilling on ice for 5 minutes. The chilled samples were centrifuged at >13,000 rpm for 1 minute at room temperature and the supernatants discarded. The cell pellets were resuspended in 0.1-0.5 mL of TE and plated on the appropriate SD agar plates, which were grown at 30°C for 7-10 days.

Yeast Mating

Saccharomyces cerevisiae strain AH109 was transformed with the pGBKT7 vector carrying the full-length hAAG gene. AH109 is not capable of growing on media lacking tryptophan (Trp); however, pGBKT7 contains a Trp gene and yeast transformants containing this plasmid are capable of growth on media lacking Trp. These transformants served as the bait during yeast two-hybrid analysis. One large 2-3 mm diameter colony

containing the bait construct was used to inoculate 50 mL of SD/-Trp minimal media and grown at 30°C for 20-24 hours with shaking (250-270 rpm), to an $OD_{600} > 0.8$. The saturated culture was centrifuged at 2,000g for 10 minutes at room temperature and the supernatant discarded and the cells resuspended in 3 mL of SD/-Trp liquid medium.

A 1 mL aliquot of a Y187 pretransformed MATCHMAKER human liver cDNA library (Clontech) was thawed on ice and gently vortexed. The cDNA library is cloned into the pACT2 plasmid, which contains a leucine (Leu) marker. Y187 is auxotrophic for Leu, but because the Y187 pretransformed strain contains the pACT2 vector it is capable of growing on media lacking Leu. The entire AH109 bait construct culture and the 1 mL library culture was mixed together in a 2 L flask containing 45 mL of 2X YPD/Kan (kanamycin) medium. Kanamycin is used to prevent bacterial growth in the culture. The tube containing the cDNA library culture was rinsed twice with 1 mL of 2X YPD/Kan medium and the tube containing the bait culture was rinsed once with 3 mL of 2X YPD/Kan medium, and the rinses were added to the 2L incubation flask. The mating mixture was incubated at 30°C overnight for 20-24 hours with gentle swirling (30 rpm). The flask needed to be at least 2 L to permit sufficient aeration of the culture and low-speed swirling was necessary to keep the cells from settling to the bottom of the flask. Mating efficiency was calculated by using equation 2-2.

$$\frac{\text{cfu (each plate)} \times 1000 \mu\text{l/ml}}{\text{vol. plated } (\mu\text{l}) \times \text{dilution factor}} = \text{viable cfu/ml} \quad (\text{Eq. 2-2})$$

$$\frac{\# \text{ cfu/ml of diploids}}{\# \text{ cfu/ml limiting partner}} \times 100 = \text{mating efficiency}$$

Selection of Positive Clones

The mated cells were transferred to a sterile 250 mL centrifuge bottle, centrifuged at 2,000g for 10 minutes at room temperature and the supernatant discarded. During centrifugation, the mating flask was rinsed twice (50 mL each) with 2X YPD/Kan and these rinses were used to resuspend the cell pellet. The resuspended cells were again centrifuged at 2,000 g for 10 minutes at room temperature and the supernatant discarded. This cell pellet was resuspended in 10 mL of 0.5X YPD/Kan medium and the total volume of cells and medium was measured. One-hundred μ L aliquots of 1:10,000, 1:1,000, 1:100, and 1:10 dilutions of the mating mixture were plated on 100 mm diameter plates of SD/-Leu, SD/-Trp, and SD/-Leu/-Trp media. These plates were grown at 30°C for 4-8 days and used to calculate transformation efficiency. The remaining mating mixture was plated on approximately 50 large 150 mm diameter plates SD/-Leu/-Trp/-His/X- α -galactosidase plates (low stringency selection) at 200 μ L per plate. In theory, because each yeast strain requires a protein-protein interaction to activate transcription of the *HIS* gene only mated cells that contain interacting proteins are capable of growing on this media. The plates were incubated at 30°C for approximately 4-8 days or until colonies appeared, although it was usually necessary to incubate plates for at least 7 days to allow visualization of slower-growing colonies. After colonies appeared on the low stringency SD/-Leu/-Trp/-His/X- α -galactosidase plates, the blue colonies were patch plated onto SD/-Leu/-Trp/-His/-Ade/X- α -galactosidase (high stringency selection) medium and grown for 7-10 days at 30°C in order to eliminate some of the false positives from the low stringency selection. This type of selection eliminates false positives because the *ADE* and *HIS* genes are both GAL4 responsive and located in different places

on the chromosome. Therefore, upstream and downstream sequences for each would be different and only proteins with a specific interaction would be capable of activating transcription of both reporter genes. The initial clones from the high stringency selection may contain more than one library construct, which may complicate analysis of putative positive clones. Therefore, putative positive colonies were purified by restreaking 3 times onto SD/-Leu/-Trp/-His/X- α -galactosidase plates to allow loss of non-interacting library plasmids. In most instances, blue and white colonies were observed which is indicative of segregation. Blue colonies were selected and maintained on SD/-Leu/-Trp/-His/X- α -galactosidase medium.

Yeast Colony PCR Analysis of Putative Clones

Positive candidate yeast colonies isolated and purified from the high stringency selection were placed into tubes containing 25 μ L of yeast lysis buffer (50 mM Tris-HCl (pH 8.0), 0.1% SDS, 0.3% β -mercaptoethanol, 1 mM EDTA, and 1:50 β -glucuronidase). Each tube was vigorously vortexed for 1 minute and placed into a 37°C water bath for 1-2 hours. Every 30 minutes, the tubes were removed from the water bath and vigorously vortexed for several seconds and placed back into the water bath. Following incubation 100 μ L of sterile deionized water was added to each tube and each tube was vortexed for several seconds. Five μ L of the crude lysis mixture was added to sterile 0.5 mL thin-walled microfuge tubes. Ninety-five μ L of yeast colony PCR cocktail solution was added to each tube. Each aliquot of the cocktail contained the components listed in Table 2-1. The tubes were transferred to a MJ Research Incorporated thermocycler and subjected to the PCR cycle listed in Table 2-2. After the cycle was complete 10 μ L of each PCR product was mixed with 1 μ L of 10X loading buffer (0.25% bromophenol

blue, 0.25% xylene cyanol FF and 25% Ficoll 400). The entire sample (11 μ L) was loaded into an agarose gel (0.85-1.0%) and electrophoresed at 100 volts for 1-2 hours. After electrophoresis, pictures were taken of the gels using a Kodak digital electrophoresis documentation system. The PCR products were grouped by size and 10 μ L of the PCR product was digested with either *Alu* I or *Hae* III. These two restriction

Table 2-1. PCR cocktail.

10 X PCR buffer	10 μ L
1.25 mM dNTPS	16 μ L
25 mM MgCl ₂	6 μ L
oligonucleotide primers	25 pmoles of each
<i>Taq</i> polymerase	.250 μ L
sterile water	to 100 μ L

Table 2-2. PCR conditions.

PCR Step	Step Conditions
1	94°C for 5 minutes
2	94°C for 1 minute
3	50°C for 1 minute
4	72°C for 3.5 minutes
5	29X back to Step 2

enzymes were chosen because they are four-base cutters and would likely yield a digestion pattern for all samples analyzed. The products of those digests were resolved

on a 1.5% agarose gel and sorted by their restriction digest sizes to eliminate duplicate clones. PCR products were purified using Qiagen PCR purification kit and subjected to sequencing analysis. The resulting sequences were examined using BLAST analysis (NCBI).

Isolation of Plasmid DNA from Yeast

Fresh yeast colonies (2-4 day-old) were used to inoculate 10 mL of the appropriate SD liquid minimal medium. Each culture was vigorously vortexed to avoid any clumping of cells. The tubes were incubated at 30°C for 18-24 hours with shaking (250 rpm). The cells were then collected by centrifugation and the supernatant discarded. The cell pellets were resuspended in 100 µL of 1X TE buffer and transferred to sterile 2.0 mL plastic tubes. One-hundred µL of lyticase solution (Sigma) was added to each sample and the tubes were thoroughly vortexed (1-2 minutes). The samples were incubated in a 37°C water bath for 90 minutes. Every 15 minutes, the tubes were vigorously vortexed for several seconds and placed back into the water bath. Following incubation 100 µL of 20% SDS was added to each sample and the samples were vigorously vortexed for 1 minute. Each sample was then placed into a -20°C freezer for 30 minutes and then thawed at room temperature. The samples were vortexed for an additional 1 minute to ensure complete lysis of the cells. Two-hundred µL of phenol:chloroform:isoamyl alcohol (25:24:1) was added to the samples and each sample was vortexed for 5 minutes at the highest speed. Each tube was then centrifuged at 14,000 rpm at room temperature for 15 minutes. The aqueous phase (upper) from each sample was transferred to a sterile 1.5 mL plastic tube. Ten µL of 10 M ammonium acetate and 500 µL of 95-100% ethanol was added to each sample and the tubes were

placed into a -70°C freezer for 1 hour and the samples were centrifuged at 14,000 rpm at 4°C for 15 minutes. The supernatants were discarded and the pellets dried at room temperature using a Savant Hi-Speed centrifugal vacuum drier. Each sample was resuspended in 20 µL of 1X TE buffer. The amount of plasmid DNA cannot be measured because it is relatively small compared to the contaminating genomic DNA in each sample. Therefore, as a rule of thumb 5 µL of yeast plasmid solution is used to transform 100 µL of chemically competent *Escherichia coli* cells in order to propagate the yeast plasmid of interest.

Western Blot Analysis

SDS-PAGE and Protein Blotting to Nitrocellulose

Purified proteins and crude extracts were subjected to SDS-PAGE on 12% polyacrylamide gels. Polyacrylamide gel electrophoresis was performed at room temperature at 125 volts for approximately 90 minutes. The gels were equilibrated in Towbin buffer (25 mM Tris, 192 mM glycine, 20% methanol; the pH should be approximately 8.3) by immersing the gels 3 times for 5 minutes each. The gels were measured with a ruler and 6 pieces of filter paper and 1 piece of nitrocellulose membrane corresponding to 2 mm larger than the gel were cut for each gel. The nitrocellulose membrane was soaked in Towbin buffer for approximately 15 minutes before use. Transfer sandwiches were set-up on an Owl Scientific semi-dry blotter in the following order: 3 pieces of filter paper soaked briefly in Towbin buffer, 1 SDS-PAGE gel, 1 piece of nitrocellulose membrane, and 3 pieces of filter paper soaked briefly in Towbin buffer. A 15 mL Corex tube was used after each step to roll out any air bubbles from the sandwiches. The gels were transferred to the nitrocellulose membrane at room

temperature at 0.8 mA/cm^2 of membrane for approximately 90 minutes. After the transfer the membranes were placed in blocking solution (1X TBS (25 mM Tris, 25 mM boric acid, 150 mM NaCl), 5% non-fat dry milk, 0.05% Tween-20) and blocked at 4°C overnight with gentle shaking.

Membrane Probing and Chemiluminescent Detection

The membranes were allowed to equilibrate at room temperature with shaking. The membranes were washed 3 times for 5 minutes in 1X TBS and 0.05% Tween-20 and probed with the appropriate primary antibody in blocking solution for 1 hour at room temperature with gentle shaking. The antibody dilutions were made as described by the manufacture's instructions. Afterwards the membranes were washed 5X for 5 minutes each in 1X TBS and 0.05% Tween-20. The membranes were probed with the appropriate secondary antibody, which was horseradish peroxidase conjugated, for 1 hour at room temperature with gentle shaking. The secondary antibody dilutions were made in blocking solution as described by the manufacture's (Pierce Chemical Company) instructions. The membranes were washed 5 times for 5 minutes each in 1X TBS and 0.05% Tween-20 and the membranes were developed using the SuperSignal West Pico chemiluminescent substrate detection kit from Pierce Chemical Company. Briefly, the membranes were rinsed for 10 minutes with a 1:1 mix of luminol/enhancer solution and stable peroxide solution at 0.125 mL/cm^2 of membrane surface. The blots were removed and covered in plastic wrap being sure to avoid any air bubbles between the plastic wrap and the blot. The membranes were exposed to Fuji Super RX film for various times (a recommended first exposure time of 60 seconds) and the film was developed using a Kodak M35A X-OMAT processor.

Protein Phosphorylation Assays

Casein Kinase II Assay

Purified casein kinase II and casein kinase II peptide substrate were purchased from Promega Corporation. Purified hAAG proteins were used during *in vitro* casein kinase II phosphorylation assays at various concentrations (2-10 μ M). Typical assays (20 μ L) were carried out using 1 unit of casein kinase II in buffer containing 25 mM Tris-HCl (pH 7.5), 1 mM EDTA, 1 mM DTT, 200 mM NaCl, 10 mM $MgCl_2$, and 0.15 mM [γ - ^{32}P]-ATP. The reaction mixture was incubated at 37°C for 30 minutes. Following incubation the samples were diluted with 3 volumes of 2X SDS-gel loading buffer and boiled for 10 minutes in a water bath. Four μ L of each sample was subjected to SDS-PAGE on a 12% polyacrylamide gel. Polyacrylamide electrophoresis was performed at room temperature at 120 volts for 2 hours. The gels were dried on a heated Savant vacuum gel drier and autoradiography was performed as previously described.

Protein Kinase C Assay

Purified protein kinase C was purchased from Promega Corporation and protein kinase C peptide substrate was purchased from Sigma. Purified hAAG proteins were used during *in vitro* protein kinase C phosphorylation assays at various concentrations (2-10 μ M). Typical assays (20 μ L) were carried out using 1 unit of protein kinase C in buffer containing 20 mM HEPES (pH 7.5), 1.7 mM $CaCl_2$, 1 mM DTT, 10 mM $MgCl_2$, 0.6 mg/mL phosphatidyl serine, and 0.15 mM [γ - ^{32}P]-ATP. The reaction mixture was incubated at 30°C for 30 minutes. Following incubation the samples were diluted with 3 volumes of 2X SDS-gel loading buffer and boiled for 10 minutes in a water bath. Four μ L of each sample was subjected to SDS-PAGE on a 12% polyacrylamide gel.

Polyacrylamide electrophoresis was performed at room temperature at 120 volts for 2 hours and the gels were dried on a heated Savant vacuum gel drier and autoradiography was performed as previously described.

CHAPTER 3
BASE EXCISION AND DNA BINDING ACTIVITIES OF HUMAN
ALKYLADENINE DNA GLYCOSYLASE (hAAG)

Introduction

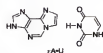
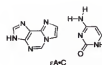
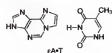
Human alkyladenine DNA glycosylase (hAAG) is the only DNA glycosylase identified in human cells to date that excises bases damaged by alkylation. This glycosylase has been shown to have a broad substrate specificity and has been reported to excise at least 12 different damaged bases including 3-methyladenine (12, 19, 80, 96, 99, 101), 7-methylguanine (4, 12, 80, 96, 99), 1,*N*⁶-ethenoadenine (4, 19, 20, 102), etheno adducts of guanine (19), 8-oxoguanine, (9), hypoxanthine (4, 69, 102), and undamaged purines (8, 124). These damaged purine bases are structurally diverse and contain modifications to groups involved in base pairing and to both the major and minor groove sides of base pairs. For example, the methyl group of 3-methyladenine projects into the minor groove, whereas that of 7-methylguanine projects into the major groove, but neither of these methyl groups interrupts hydrogen-bonding interactions with its base-pairing partner. On the other hand, hydrogen-bonding interactions are disrupted for ethenoadenine and the etheno adducts of guanine. Deamination of adenine to form hypoxanthine alters base pairing and converts a Watson-Crick base pair with T to a wobble base pair, whereas 8-oxoG is still capable of forming a Watson-Crick base pair with C. Given these different base and base pair structures, it is difficult to formulate one model for the structural and mechanistic bases of recognition and excision of these chemically diverse substrates.

To begin to define the mechanistic basis for substrate recognition and excision by hAAG, kinetics of excision and DNA binding affinities were measured for DNA containing different damaged DNA bases within the same sequence context. We used a deletion mutant of hAAG that is missing the first 79 amino acids from the N-terminus (hAAG Δ 79) in all of these studies. Deletion of this nonconserved N-terminal region has been shown to have no effect on either base excision or DNA binding activities of the enzyme, but the truncated enzyme is more soluble at low ionic strength. In addition, the effects on excision rates and binding constants of varying the base paired with a damaged DNA base were examined. Although the alkylated DNAs processed by hAAG appear to have few characteristics in common, the goal of our experiments is to determine whether there are common underlying structural features that are recognized by hAAG. Base excision and DNA binding by hAAG were measured for than 20 different base pair combinations. Figure 3-1 illustrates structures of some of the base pairs that were incorporated into DNA substrates. We found ethenoadenine (ϵ A) and hypoxanthine (Hx) to be the most efficiently excised; however, excision of Hx was affected dramatically by its base-pairing partner.

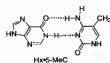
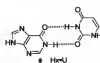
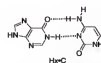
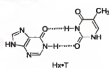
Results

Excision of Damaged and Undamaged DNA Bases by hAAG

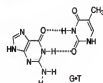
A survey was done of the excision activity of hAAG on several different damaged and undamaged DNA bases to determine which of these bases were most efficiently excised by hAAG. Damaged DNA bases were incorporated at a single site in the center of synthetic oligonucleotides, 25 nucleotides in length, using standard β -cyanoethyl phosphoramidite chemistry. Duplex DNA substrates were made by annealing the

1,N⁶-Ethenoadenine Base Pairs

Hypoxanthine Base Pairs



Guanine Base Pairs



Adenine Base Pairs

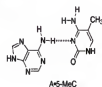


Figure 3-1. Structures for some of the damaged DNA base pairs tested as substrates for hAAG. When paired opposite T, εA and Hx were excised most rapidly. Changing the base opposite εA had only modest effects on base excision rates, whereas changing the base opposite Hx had a dramatic effect on base excision and DNA binding.

complementary oligonucleotide and were identical in sequence except for the central “damaged” base pair. Excision activity was measured in time course assays by incubating these ^{32}P -labeled DNA substrates (50 nM) with hAAG Δ 79 (400 nM) at 37 °C for periods up to 160 minutes. A chemical cleavage/gel assay was used to measure the amount of excision of each damaged base at several times during the course of the excision reaction. In this assay, DNA products containing apurinic sites were chemically cleaved by heating in 0.2 M NaOH at 90 °C for 5 minutes. Cleaved DNA products were then separated from uncleaved substrates by denaturing polyacrylamide gel electrophoresis and quantitated by phosphorimaging. Time courses for excision of several of the bases that were tested as substrates are shown in Figure 3-2 (see Figure 3-1 for structures of base pairs). Of the damaged DNA bases tested, Hx and ϵA were excised most efficiently; excision of Hx was nearly complete in 10 minutes and excision of ϵA was nearly complete in 80 minutes. In contrast, significant excision of 8-oxoG and O^6 -methylguanine (O^6 -MeG) did not occur over a period of 160 minutes. Changing the base opposite 8-oxoG and O^6 -MeG from C to T did not affect excision rates (data not shown). It has been reported that hAAG is capable of excising undamaged purines (8, 124); however, under our assay conditions, significant excision of A and G were not observed when present as correct pairs or when present as G•T and A•C mispairs.

Single Turnover Kinetics of Excision of 1,N⁶-ethenoadenine and Hypoxanthine

The kinetics of excision of ϵA and Hx were examined in more detail. Because excision kinetics were extremely slow under steady-state kinetic conditions and the enzyme loses activity with prolonged incubation at 37 °C, single turnover kinetics of excision were measured. (Note: When hAAG is incubated with DNA under conditions

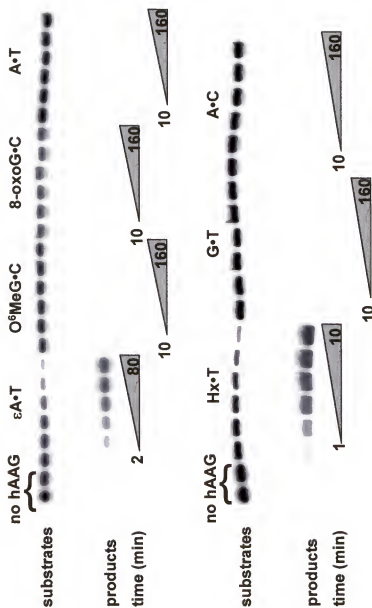


Figure 3-2. hAAG excision assays. Time course assays for several of the damaged DNA bases tested as substrates for hAAG. DNA duplexes, 25 nucleotides in length and of identical sequence except for the central base pair, were incubated with hAAG at 37°C for periods up to 160 minutes.

where DNA binding occurs, the enzyme is protected from heat inactivation at 37°C (Abner and Bloom, unpublished). For these assays, the 25 nucleotide DNA duplex substrates above containing a central $\epsilon A \cdot T$ or $Hx \cdot T$ base pair were used. In these experiments, 50 nM DNA was incubated with increasing concentrations of hAAG Δ 79 up to 800 nM in separate reactions. Aliquots were withdrawn at several time points during each reaction, quenched with 0.2 M NaOH, and analyzed by the chemical cleavage/gel assay method described above. For each concentration of hAAG Δ 79, two or three separate time course reactions were performed. The averages and standard deviations for time courses at 400, 600, and 800 nM concentrations of hAAG Δ 79 are plotted in Figure 3-3. For both damaged base pairs, $\epsilon A \cdot T$ and $Hx \cdot T$, reaction time courses are essentially the same at these three enzyme concentrations, demonstrating that the concentration of enzyme is saturating, and reaction kinetics are not a function of enzyme-substrate binding rates.

Individual time course reactions at each enzyme concentration were fit to an exponential rise (Equation 3-1) to determine values for k_{obs} .

$$y = a(1 - e^{-k_{obs}t}) \quad (\text{Equation 3-1})$$

For ϵA , k_{obs} values were 0.080 ± 0.003 , 0.075 ± 0.001 , and $0.076 \pm 0.001 \text{ min}^{-1}$ for duplicate measurements at concentrations of 400, 600, and 800 nM enzyme, respectively. Calculated values of k_{obs} were 4 to 5 times greater for Hx and were 0.31 ± 0.01 , 0.32 ± 0.01 , $0.37 \pm 0.01 \text{ min}^{-1}$ for triplicate measurements at 400, 600, and 800 nM enzyme, respectively.

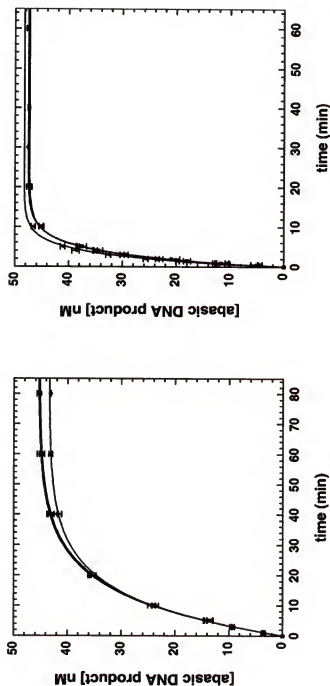


Figure 3-3. Single-turnover kinetics of excision of ϵA and Hx when paired opposite thymine. DNA duplexes containing either a central $\epsilon A \cdot T$ (left panel) or Hx·T (right panel) base pair were incubated with 400 (circles), 600 (squares), and 800 (triangles) nM hAAG Δ 79 in separate reactions. Two or three separate time course reactions were done at each enzyme concentration, and the average values and S.D. are plotted.

Effects of Base Pairing Partners on Excision of ϵ A and Hx

To determine whether the base paired opposite ϵ A or Hx had any effect on the efficiency of hAAG catalyzed excision, thymidine (T) was replaced with both 2'-deoxycytidine (C) and 2'-deoxyuridine (U). The pyrimidine base paired opposite the damaged base had a larger effect on excision of Hx than on excision of ϵ A. Time course assays (Figure 3-4) were done in duplicate using 400 nM hAAG and 50 nM "damaged" DNA as above. Replacing T with a C resulted in little if any effect on the observed rate (k_{obs}) of excision of ϵ A, which was 0.066 min^{-1} , but decreased k_{obs} for Hx by a factor of about 5 to 0.062 min^{-1} . Surprisingly, replacing T with U resulted in a decrease in the rates of excision of both ϵ A and Hx. Again, the effect on the rate of excision of ϵ A was smaller and was reduced by a factor of 1.7 to 0.045 min^{-1} . Excision of Hx was reduced by a factor of about 15 to 0.022 min^{-1} when T was replaced with U. As a control, the DNA strand that contained U was labeled and excision was measured in assays using both hAAG Δ 79 and *E. coli* uracil DNA glycosylase. No uracil DNA glycosylase activity was observed in reactions with hAAG Δ 79, whereas quantitative excision of U was seen in reactions with uracil DNA glycosylase (data not shown). The effect of replacing T with U is striking because U differs from T in that it simply lacks the 5-methyl group, which extends into the major groove. To determine if a 5-methyl group affects base excision by hAAG, C was replaced with 5-methylcytosine (5-MeC) in base pairs with ϵ A and Hx. In this case, the 5-methyl group had no effect and excision was the same for base pairs with C and 5-MeC (data not shown).

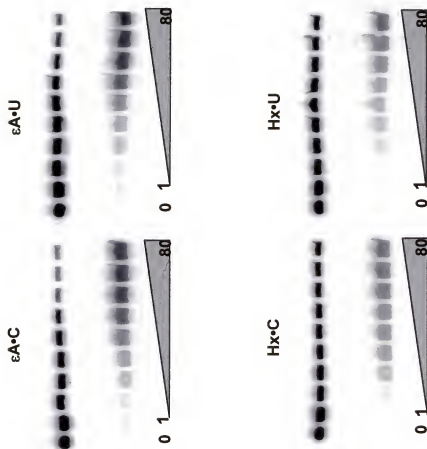


Figure 3-4. Excision of ϵA and Hx when paired opposite cytosine and uracil. Time course assays were carried out with 50 nM duplex DNA and 400 nM hAAGA79 at 37°C as in Figure 3-2.

Binding of hAAG Δ 79 and a Catalytically Inactive Mutant to DNA Containing an ϵ A•T Base Pair

To better define the interactions between hAAG and different damaged DNA bases, the binding affinity of hAAG to DNA duplexes containing different damaged DNA bases was measured. For these experiments, a catalytically inactive mutant of hAAG, hAAG Δ 79E125Q, was used so that binding to DNA substrates could be measured in the absence of excision. In this mutant, glutamic acid 125 was replaced by glutamine. This glutamic acid residue has been proposed to act as a general base to activate water for hydrolysis of the glycosidic bond (50). In excision assays with ϵ A and Hx paired opposite T, hAAG Δ 79E125Q was unable to excise either ϵ A or Hx over a period of 80 minutes under conditions as in Figure 3-2 (data not shown).

To determine whether mutation of Glu125 to glutamine affected binding activity, binding of wild-type hAAG Δ 79 and hAAG Δ 79E125Q to DNA duplexes containing an ϵ A•T base pair were measured. Incubation of hAAG Δ 79 with ϵ A containing DNA at 4 °C significantly reduces the rate of excision of ϵ A, so that binding to this substrate can be measured in the absence of significant product formation. The same 25 nucleotide duplex DNA substrates used in excision assays were used in binding assays and the DNA strand containing the damaged base was 5' end-labeled with 32 P. Binding experiments were done by incubating the ϵ A•T containing DNA duplex with different concentrations of enzyme at 4 °C for 10 minutes. After 10 minutes, an aliquot of these reaction mixtures was removed and analyzed using an electromobility shift assay (EMSA). Two additional aliquots of each reaction mixture were removed: the first when the EMSA gel was loaded and the second after the gel was completed. These additional aliquots were

immediately quenched with 0.2 M NaOH and analyzed to determine the amount of excision of ϵ A that occurred during the time course of the EMSA.

Results from EMSAs are shown in Figure 3-5A for hAAG Δ 79 and Figure 3-6A (upper panel) for hAAG Δ 79E125Q. Binding isotherms for the wild type and catalytically inactive mutant are virtually identical (Figure 3-5B), indicating that the point mutation reduces excision activity while having little if any effect on DNA substrate binding. For wild type hAAG Δ 79, only about 16% of the substrates were converted to abasic DNA products during the time course of the EMSA at the highest enzyme concentration.

Binding of hAAG Δ 79E125Q to DNA Substrates Containing Different ϵ A and Hx Base Pairs

The catalytically inactive mutant, hAAG Δ 79E125Q, was used to measure the binding affinity of the enzyme to DNA substrates containing different damaged DNA bases. Electrophoretic mobility shift assays were done as above using the same damaged duplex DNA substrates used in excision assays. Representative phosphorimager scans of binding data are shown in Figure 3-6A for DNA duplexes containing ϵ A and Hx base pairs with T, C, and U. In general, hAAG binds with greater affinity to DNA containing ϵ A base pairs than Hx base pairs. The base-pairing partner has a significant effect on the enzyme's affinity for DNA substrates containing Hx base pairs. For each DNA substrate, three separate EMSA experiments were performed and quantitated. Binding isotherms showing the average and standard deviation of these three independent experiments are shown in Figure 3-6B. Data were fit to a simple two state binding model shown in equation 3-2 using a quadratic equation (see *Experimental Procedures*) to determine an apparent dissociation constant ($K_{d,app}$) where ED^{total} represents all species of ED

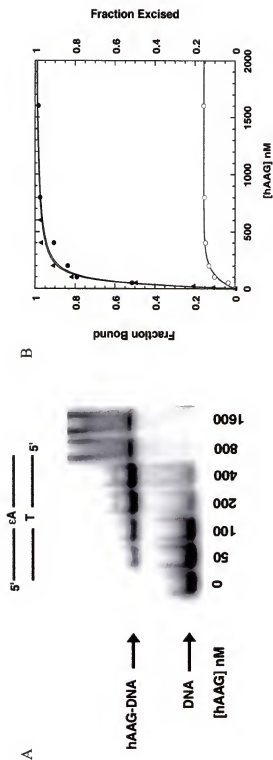


Figure 3-5. hAAGΔ79 binding to damaged DNA. A) An EMSA gel is shown for binding of catalytically active hAAGΔ79. An EMSA gel for hAAGΔ79E125Q is shown in Figure 3-6A, for comparison. B) The fraction of εA excised during the EMSA time course (open circles) was quantitated and is plotted along with the fraction of εA·T DNA bound by hAAGΔ79 (filled circles) and hAAGΔ79E125Q (filled triangles).

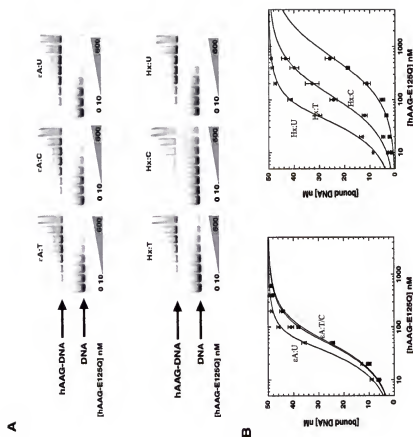


Figure 3-6. Binding of hAAG Δ 79E125Q to DNA containing ϵ A and Hx base pairs. A) DNA duplexes containing ϵ A or Hx paired with thymine (T), cytosine (C), or uracil (U) were incubated with increasing concentrations of enzyme. EMSAs were used to calculate the fraction of DNA bound by protein. B) Binding isotherms of the respective data.

complexes formed (i.e. both complexes where the damaged nucleotide are flipped (ED^{flp}) and not flipped (ED^{un})).



Apparent dissociation constants calculated for ϵ A base pairs were 20 ± 2 , 23 ± 2 , and 6.3 ± 1.0 nM for base pairs with T, C, and U, respectively. Dissociation constants for DNA duplexes containing Hx base pairs were affected to a much greater extent by changing base pairing partners. Apparent dissociation constants were 92 ± 2 nM and 12 ± 2 nM for Hx•T and Hx•U base pairs, respectively. For the duplex containing Hx•C base pairs, $K_{d,app}$ is approximately 600 nM and is too great to accurately determine because at high enzyme concentrations bands smear on EMSA gels, probably due to nonspecific binding of the enzyme to undamaged DNA.

In addition to measuring binding to DNA containing ϵ A and Hx lesions, hAAG binding was measured to DNA containing each of the base pairs that were used in excision assays. These base pairs included O⁶-MeG opposite C and T, 8-oxoG opposite C and T, G opposite T, C, and U, and A opposite T, C, U, and 5-MeC. Significant binding to these DNA substrates was not observed (data not shown). Although U opposite a lesion increased binding to DNA containing ϵ A and Hx, it had no effect when placed opposite G or A.

Binding of hAAG Δ 79 to DNA Duplexes Containing Abasic Sites

Several DNA glycosylases including *E. coli* MutY (94), human thymine DNA glycosylase (50), and human methyl-CpG-binding endonuclease 1(85) have been shown to bind very tightly to the products of their excision reactions. To determine whether hAAG has a high affinity for the apurinic DNA products, binding of hAAG Δ 79 to duplex

DNA substrates containing a synthetic abasic site was measured. A synthetic reduced abasic site was used in place of the natural abasic site because this substrate is more stable and can be incorporated at a specific site using standard synthetic chemistry. As a control, binding of hAAG Δ 79 to DNA containing a natural abasic site was measured (data not shown) and found to be similar to binding to a reduced abasic site, as has been observed by others (69). Results from EMSA experiments with DNA substrates containing abasic sites are shown in Figure 3-7. As with damaged bases, the binding affinity of the enzyme is affected by the base opposite the abasic site. The enzyme only binds duplexes that contain pyrimidines opposite the abasic site. Apparent binding constants calculated for substrates with pyrimidines opposite the abasic site were 140, 300, and 56 nM for T, C, and U, respectively. Interestingly, when either ϵ A or Hx were placed opposite the abasic site, the enzyme did not bind DNA duplexes, suggesting that the enzyme cannot recognize these damaged bases unless a base is paired opposite them.

Discussion

The human alkyladenine DNA glycosylase has been shown to have a broad substrate specificity excising damaged purines, particularly alkylated purines. Studies have shown that hAAG is capable of excising 3-methyladenine (12, 20, 80, 96, 99, 101), 7-methylguanine (4, 12, 80, 96, 99), 1, N^6 -ethenoadenine (4, 19, 20, 101), etheno adducts of guanine (19), 8-oxoguanine (9), hypoxanthine (4, 69, 102), and undamaged purines (8, 124). However, the relative efficiencies of excision of all of these damaged bases have not been firmly established by direct comparison of excision kinetics for each within the same DNA sequence context. This study examines the structural and mechanistic principles for recognition and excision of damaged DNA bases by hAAG. In essence,

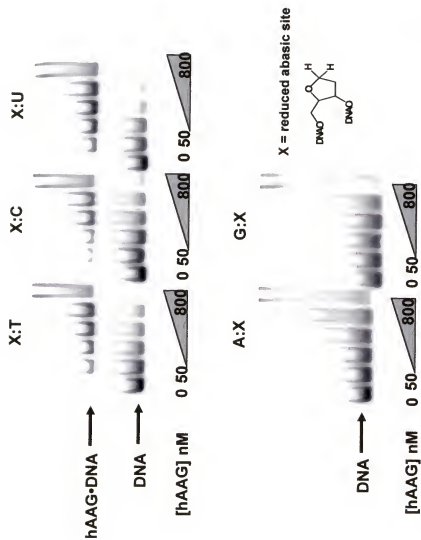


Figure 3-7. Binding of hAAGΔ79 to DNA containing abasic sites. A reduced abasic site analog was used in place of the natural abasic site in these assays. hAAGΔ79 binds DNA containing an abasic site opposite pyrimidine bases, but is not capable of binding to DNA containing abasic sites opposite a purine base, even if the purine base is εA or Hx.

our approach was to perform “site-directed mutagenesis” on damaged base pairs to determine which structural features of a base pair were important in binding and excision. Much of the previous work in the field has focused largely on the damaged base alone, but more recent evidence suggests that its base-pairing partner plays a role (4, 101, 102, 124, 125). Our results demonstrate that for some damaged bases, the opposing base can have a dramatic effect on binding and excision. This result is surprising based on the structural data available for the enzyme-DNA complex, which shows no specific contacts between the enzyme and opposing base.

The crystal structure of hAAG complexed with DNA containing a pyrrolidine abasic site analog (50) and a more recent structure of hAAG bound to ϵ A-containing DNA (51) have revealed that this enzyme, like other DNA glycosylases, flips a damaged nucleotide out of the DNA helix and into an enzyme binding pocket where hydrolysis takes place. A β hairpin projects into the minor groove and widens the minor groove at the site of damage and at base pairs immediately 3' to the pyrrolidine, suggesting that the enzyme may scan DNA from the minor groove to detect damage. A tyrosine residue (Tyr162) projects from this β hairpin and intercalates in the DNA helix in the “hole” where the damaged base would have been. In contrast to cocrystal structures of uracil DNA glycosylase with DNA, little compression of the sugar-phosphate backbone is seen in the hAAG-DNA complexes (82, 83). For hAAG, “pushing” the damaged nucleotide out of the helix may be accomplished by the action of Tyr162 along with other residues of the β hairpin without assistance of “pinching” due to backbone compression that is seen for uracil DNA glycosylase. Although the binding site of uracil DNA glycosylase has a geometry that provides a “tight fit” for uracil through specific amino acid-uracil

interactions (103), the binding site of hAAG must be able to accommodate a structurally diverse group of damaged bases. Aromatic amino acid side chains, including Tyr127, are present in the active site of hAAG that stack with the damaged base. It has been proposed that base-stacking interactions between electron-deficient damaged bases and aromatic side chains may provide the basis for recognition and excision by hAAG (50, 51) and *E. coli* 3-methyladenine DNA glycosylase II (49, 50, 127). In addition, interactions between a hydrogen bond donor on hAAG and a hydrogen bond acceptor at position 6 of a damaged purine may play a role in recognition (51). Although these structures have provided significant insights into the mechanism of recognition and excision by hAAG, questions about substrate specificity remain to be answered.

To gain further insight into the structural and mechanistic principles for excision of damaged DNA bases, excision and binding activities of hAAG were measured for different damaged substrates within an identical DNA sequence context. Initial assays were done to qualitatively compare the excision of four damaged bases, *IN*⁶-ethenoadenine, hypoxanthine, 7,8-dihydro-8-oxoguanine, and *O*⁶-methylguanine, as well as undamaged purines both correctly paired and mispaired with pyrimidines. Hypoxanthine and *IN*⁶-ethenoadenine, both paired opposite T, were the only bases excised during the 160-minute time courses of these assays. Another study using full-length His-tagged hAAG also found that 8-oxoG was not excised (4). It is possible that undamaged purines, 8-oxoG, and *O*⁶-MeG may be excised after much longer times, but since excision of these bases was so inefficient, further characterization was not done. Neither 3-methyladenine nor 7-methylguanine were examined in this study because 3-MeA cannot be incorporated site-specifically into DNA, and 7-MeG is relatively labile.

A comparison of the structures of these base pairs, shown in Figure 3-1, highlights structural similarities and differences that may be important in the excision reaction. Both ϵ A and Hx have two hydrogen bond acceptors that project into the major groove, N^7 for both and an exocyclic nitrogen at the 6 position for ϵ A and an exocyclic oxygen at the 6 position for Hx. However, the base pair that each forms with T is different. The exocyclic etheno group of ϵ A creates a more bulky base and prevents hydrogen-bonding interactions with T. NMR studies show that to accommodate the larger size of ϵ A, an ϵ A•T pair adopts a conformation where both bases are stacked in the helix but skewed relative to one another so that they do not form a planar base pair (47). Hypoxanthine hydrogen bonds with T but forms a wobble pair rather than a Watson-Crick-type pair. This wobble pair differs from a Watson-Crick pair in that the purine is shifted into the minor groove, and the pyrimidine is shifted into the major groove. If hAAG scans the minor groove, it may detect either of these distortions. The fact that Hx forms hydrogen bonds with T and ϵ A does not may make ϵ A easier to flip, whereas the smaller size of Hx may increase the rate of excision by a better fit in the binding pocket.

It is interesting that excision of G was not observed when placed opposite T because a G•T pair forms a wobble base pair very similar in structure to Hx•T, the major difference being the 2-amino group that is present of G but not on Hx. Perhaps the 2-amino group is not accommodated within the enzyme active site or it misaligns the nucleotide in the active site so that hydrolysis of the glycosylic bond is not efficient (51). In contrast, 7-MeG also has a 2-amino group but is excised by hAAG (4, 12, 80, 96, 99). The 7-methyl group acts to increase the lability of the purine base and may also serve to

enhance the efficiency of hydrolysis of the glycosidic bond in the enzyme active site even though alignment of the nucleotide may not be optimal.

To further characterize the excision of ϵ A and Hx, single turnover kinetics were performed to establish the maximal rate for excision of each base. When paired opposite T, the observed rate constant (k_{obs}) for excision of Hx (0.33 min^{-1}) was about 4-fold greater than that for ϵ A (0.077 min^{-1}). Since observed rates in these experiments are not limited by the rate of enzyme-DNA binding and the assay measures both enzyme-bound products and free products, k_{obs} values reflect the rate of conversion of an enzyme-substrate complex to an enzyme-product complex. Depending on the kinetic mechanism, this rate could be limited by the rate of nucleotide flipping or the actual rate of hydrolysis of the glycosidic bond but in any case reflects the rate of conversion of enzyme-bound substrates to products.

The pyrimidine base opposing the lesion has a much greater affect on excision of Hx than ϵ A. For both lesions, excision rates decreased in the order $T > C > U$. For Hx, changing from T to C and T to U reduced the observed rates by factors of 5 and 15, respectively. Replacing T with U resulted in a more modest 1.7-fold decrease in excision of ϵ A. A similar study done by Asaeda *et al.* (4) using full-length His-tagged hAAG also found that excision of Hx was affected to a much greater extent by its base-pairing partner than excision of ϵ A. The fact that the base-pairing partner has a much larger effect on excision of Hx than ϵ A may be due to differences in hydrogen-bonding interactions in the base pairs. Because the etheno group bridges N^1 and the exocyclic amino group of adenine, ϵ A is prevented from making hydrogen-bonding interactions with T, C, and U (Figure 3-1). If nucleotide flipping is important in the mechanism of

excision, the lack of hydrogen-bonding interactions may simply make ϵ A relatively easy to flip regardless of which base opposes it. It is important to note that although excision of ϵ A by hAAG is relatively insensitive to the base opposite ϵ A, a base is required. The fact that hAAG does not excise either ϵ A or Hx when placed opposite an abasic site further suggests that hAAG does not simply capture damaged bases that transiently assume extrahelical positions but instead actively finds and flips damaged bases. The lack of base-pairing interactions at an abasic site is likely to increase the frequency of transient spontaneous flipping of a damaged DNA base.

The effects that the pyrimidine base-pairing partner has on excision rates for Hx is somewhat surprising, particularly when a T is replaced by a U. The major difference between a T and U base-pairing partner is the presence or absence of a 5-methyl group that extends into the major groove (Figure 3-1). The fact that the enzyme discriminates between Hx•T and Hx•U suggests that the structure of the base pair rather than simply the damaged DNA base plays a role in the mechanism of recognition and excision by hAAG. Two possible explanations are that the enzyme either initially interacts with both the damaged base and its partner or that the base-pairing partner affects the interaction of the enzyme with the damaged base in some way. Although it is possible that the enzyme could interact with both the damaged base and its partner by binding DNA at the major groove before flipping the damaged base from the minor groove, it seems unlikely. Instead, the crystal structure suggests that the presence of uracil opposite the lesion could affect the alignment of the flipped base in the enzyme active site. Intercalation of Tyr162 into the space formerly occupied by the damaged base may help push the nucleotide into the enzyme active site so that the glycosidic bond is aligned

properly for hydrolysis. Uracil opposite hypoxanthine may reduce the rate of catalysis by preventing Tyr162 from intercalating into the DNA far enough to push the damaged nucleotide into the enzyme active site in the proper alignment. The unpaired uracil may shift back into the helix toward the minor groove to maximize base stacking interactions, and this shift may prevent Tyr162 from intercalating into the DNA far enough to push the damaged base into its proper orientation. The 5-methyl group on T may prevent T from shifting as far back into the helix due to its bulkiness and unfavorable steric interactions with the bases above and below T. In the crystal structure, the T opposite the damaged base is also pushed into the major groove by about 1.5 Å (50).

The effect of the base-pairing partner on excision efficiency may have an important biological role in helping to ensure that the damage is repaired correctly. Hypoxanthine is excised more efficiently when placed opposite T than opposite C. Initially, Hx would be formed in DNA from deamination of A opposite T. Once in DNA, Hx is mutagenic, miscoding for C so that if replication occurs before repair, then an Hx•C pair may be formed. Once an Hx•C pair is formed, excision of Hx and repair by base excision repair would create a G•C mutation. The structural basis for this difference may be due to the fact that Hx•C forms a Watson-Crick-like base pair, whereas Hx•T or Hx•U form wobble base pairs (Figure 3-1). The addition of a 5-methyl group to C does not enhance the excision of Hx as does replacing U with T. Perhaps, the normal Watson-Crick-type structure of the base pair masks the presence of the Hx.

To further characterize the interaction of hAAG with damaged DNA bases, binding to DNA containing damaged bases was also measured with a catalytically inactive mutant, hAAG Δ 79E125Q. In general, DNA binding and base excision activities

were correlated. For damaged bases that were poorly excised by hAAG such as 8-oxoG, O⁶-MeG, and undamaged G and A, significant binding was not observed. There was one exception to this rule; binding to ϵ A•U and Hx•U pairs was relatively strong. Overall, hAAG had a greater affinity for DNA containing ϵ A ($K_d = 20$ nM for ϵ A•T, as also reported by Kartalou *et al.* (43) than for DNA containing Hx ($K_d = 92$ nM for Hx•T). Binding affinities decreased with the base opposing the lesion in the order U > T > C, and the effect was much greater for Hx than ϵ A. Binding to DNA containing Hx pairs was 7.6-fold greater for Hx•U than Hx•T and at least 50-fold greater for Hx•U than Hx•C, whereas the affinity of hAAG for DNA containing ϵ A•U was 3.2- and 3.6-fold greater than for DNA containing ϵ A•T and ϵ A•C, respectively. The same trend was seen for hAAG binding to DNA containing abasic sites. hAAG does not bind to abasic site DNA containing purine residues opposite the abasic site even if these purine residues are damaged ϵ A and Hx. The magnitude of the binding interactions to DNA products containing an abasic site is on the same order of magnitude as binding to DNA substrate containing an Hx•T base pair and about 7-fold weaker than binding to DNA containing an ϵ A•T base pair. This result seems to imply that hAAG may not remain tightly bound to DNA products after excision, as has been found for some other DNA glycosylases including *E. coli* MutY (87), human thymine DNA glycosylase (118), and human methyl-CpG-binding endonuclease 1 (85).

Which is the better substrate for hAAG, ϵ A or Hx? To some extent this depends on the base opposite the lesion, because for Hx both DNA binding and excision are affected significantly by the opposing base. Both damaged bases are likely to be initially formed opposite a T since they arise from damage to A. Hx opposite T is excised about 4

times more rapidly than ϵ A opposite T; however, this rapid excision rate is balanced by a greater binding affinity of hAAG for DNA containing ϵ A. hAAG binds DNA containing an ϵ A•T pair about five times better than DNA containing Hx•T. So when ϵ A and Hx are paired with T, they are about equally good substrates for hAAG.

Based on these initial experiments, we have developed a working model for damaged base recognition and excision by hAAG. In this model, there are two important criteria for efficient base excision, initial identification of the damaged DNA base and proper alignment of this damaged nucleotide in the enzyme active site for cleavage of the glycosidic bond. Initially, the enzyme must find the damaged base amid the vast excess of undamaged DNA bases. Initial recognition of damage may depend on recognition of structural distortions in DNA induced by the damage followed by nucleotide flipping, which checks for fit of the damaged base in the enzyme active site. If the damaged base does not fit properly into the enzyme active site then it will not attain the proper geometry for hydrolysis to take place and excision will be inefficient. The base opposite a damaged base might affect excision by influencing either the initial recognition of damage and/or substrate alignment in the enzyme active site. For example, a C opposite Hx may mask Hx from efficient recognition because it forms a Watson-Crick-type base pair, whereas U opposite Hx may affect how Hx is aligned in the enzyme active site.

CHAPTER 4

HUMAN AP ENDONUCLEASE 1 (APE1) STIMULATES THE TURNOVER OF HUMAN ALKYLADENINE DNA GLYCOSYLASE (hAAG)

Introduction

hAAG is proposed to attack the glycosylic bond of damaged bases with an activated nucleophilic water molecule (50) with subsequent release of the free base. Base removal by hAAG produces an abasic site residue which is actually another type of DNA base damage. Abasic sites can also be generated in DNA from the spontaneous hydrolysis of glycosylic bonds. Abasic sites in DNA have been shown to be cytotoxic (6, 44), therefore repair of abasic sites is required to ensure cell survival.

The removal of abasic site residues is initiated by apurinic/apyrimidinic (AP) endonucleases. APE1 is the major endonuclease in human cells responsible for repair of abasic sites. APE1 incises the DNA phosphodiester backbone on either the 5' or 3' side of abasic sites. APE1 creates substrates for human DNA polymerase β which is the polymerase responsible for gap filling in the base excision repair pathway. After gap filling, base excision repair is completed by DNA ligase.

The human base excision repair pathway has been reconstituted *in vitro* (17, 48, 77), but it is still unclear how base excision repair enzymes function to coordinate repair *in vitro* and *in vivo*. Functional repair complexes have been demonstrated for other DNA repair pathways, such as nucleotide excision repair, but there is not any evidence for a functional base excision repair complex. A few models of base excision repair have been proposed based upon these *in vitro* experiments, as well as genetic and structural

experiments. The latest model suggests base excision repair enzymes function like runners in a relay race--passing a baton from one runner to the next (120). The model is dependent upon each enzyme remaining bound to its respective product and this binding is thought to distort the DNA in a way that serves as a signal to efficiently pass the resulting DNA product along to the next enzyme. This model is speculative and complicated by the fact that each base excision repair enzyme can also bind to DNA substrates free in solution (120).

Recent evidence suggests there may be coordination in the initial steps in base excision repair. Several *in vitro* studies have shown that some DNA glycosylases bind tightly to abasic sites on DNA ((36, 90, 106, 118), thus reducing glycosylase turnover. For some DNA glycosylases, such as human thymine DNA glycosylase and human methyl-CpG-binding endonuclease 1, the binding to abasic site is 10-20 times greater than the substrate base. The overall base excision repair process would be slowed in these instances unless other factors were recruited to stimulate enzyme turnover or eliminate the reaction product (117). APE1 has been shown to stimulate enzyme turnover of several DNA glycosylases *in vitro* (38, 90, 117, 118) by displacing the bound glycosylase from the abasic site. Additionally, these glycosylases show a greater affinity for abasic site compared with the cleaved product generated by APE1, therefore these glycosylases can carry out multiple rounds of damaged base excision in the presence of APE1.

In this study, we investigated the effect of APE1 on hAAG excision to test the possibility that APE1 may stimulate the excision activity of hAAG. Since APE1 stimulation of hAAG activity may be mediated through protein•protein interactions, the

full-length protein was used in initial studies. After observing stimulation, we used a deletion mutant of hAAG that is missing the first 79 amino acids from the N-terminus (hAAG Δ 79) to determine whether the N-terminus was required for protein•protein interactions. Deletion of this unconserved N-terminal region has been shown to have no effect on base excision (50, 80, 94), but the truncated enzyme is more soluble at low ionic strength.

Our binding assays suggested that hAAG binds DNA containing abasic sites relatively weak however, in excision assays only one or two turnovers of substrate to product were observed suggesting that hAAG may stay bound to its product. Addition of APE1 to these assays increased the number of rounds of enzyme turnover. This stimulation of hAAG turnover was dependent upon APE1 concentration, the presence of full-length hAAG, and magnesium in the reaction buffer.

The requirement of magnesium in the assay buffer for stimulation of hAAG turnover suggests the possibility that the stimulation is due to APE1 cleavage of abasic site DNA since magnesium is required for APE1 catalyzed incision. Removing the abasic site products would reduce product inhibition and increase the rate of substrate turnover by hAAG. This simple mechanism for stimulation of hAAG activity would not necessarily require protein•protein interactions between hAAG and APE1, but the fact that the activity of full-length hAAG and not hAAG Δ 79 was enhanced by APE1 suggests that a protein•protein interaction is occurring.

Stimulation of hAAG activity was observed in assays where the concentrations of DNA substrates were in excess of hAAG. In single-turnover experiments, no stimulation

of hAAG activity was observed, therefore we conclude that APE1 is not enhancing turnover by increasing hAAG catalytic activity.

The observation that APE1 affected hAAG-FL and not hAAG Δ 79 turnover might suggest that APE1 is interacting with the N-terminal portion of hAAG. To test this hypothesis, we utilized wild-type hAAG-FL protein and a catalytically inactive mutant of hAAG-FL, hAAGE125Q-FL. This mutant is proficient in binding damaged DNA substrates, but is not capable of cleaving the glycosylic bond between the substrate base and the DNA sugar. This mutant was used to try and detect a ternary complex between APE1, hAAG, and damaged DNA. However, using a variety of techniques including electrophoretic mobility shift assay, western blot analysis of EMSA gels, co-immunoprecipitation, and yeast two-hybrid analysis we were unable to detect a complex between hAAG and APE1, even in the presence of damaged DNA.

Results

Excision of Damaged DNA Bases by hAAG Δ 79 and hAAG-FL Protein

Previous reports have shown that deletion of the unconserved N-terminal portion of hAAG does not affect base excision activity (50, 80, 95), but increases protein solubility at low ionic strength. We tested the excision activity of hAAG Δ 79 and hAAG-FL proteins on two damaged substrate bases, *I*,*N*⁶-ethenoadenine and hypoxanthine. These damaged bases were site specifically incorporated in the center of synthetic oligonucleotides 25 nucleotides in length, identical in DNA sequence except for the central damaged base, as described in the material and methods section. Double-stranded DNA substrates were made by annealing to the complementary oligonucleotide. Both

*I,N*⁶-ethenoadenine and hypoxanthine are damages to adenine residues, therefore they are paired opposite thymine in all studies.

Base excision was measured using a chemical cleavage/gel assay. Assays contained 1000 nM ³²P-labeled DNA and were initiated by the addition of 100 nM hAAG-FL or hAAGΔ79 protein. Reactions were performed at 37°C for 120 minutes and excision was measured for several time points during the course of the assay. Abasic sites generated by hAAG were chemically cleaved by heating in 0.2 M NaOH at 90°C for 5 minutes and substrates and products were resolved on a 12% denaturing polyacrylamide gel. Results from the time course assays are shown in Figure 4-1. Hypoxanthine containing DNA is excised more efficiently than *I,N*⁶-ethenoadenine containing DNA as previously shown (1).

In earlier work, we investigated the single turnover kinetics of excision of these same two damaged bases by hAAGΔ79 (1). In this study, we investigated the single turnover kinetics of excision of *I,N*⁶-ethenoadenine and hypoxanthine by hAAG-FL protein in order to compare it with hAAGΔ79. In these experiments, 50 nM ³²P-labeled substrate DNA was incubated with 400 nM hAAG-FL protein at 37°C for 80 minutes. Aliquots of the reaction mixture were withdrawn at several time points during the course of the excision reaction and quenched in 0.2 M NaOH and treated as previously described. Reaction time courses are plotted in Figure 4-2 and are essentially the same as hAAGΔ79. Collectively, these data support the work of others demonstrating that there is no difference in excision activity between hAAGΔ79 and longer hAAG constructs.

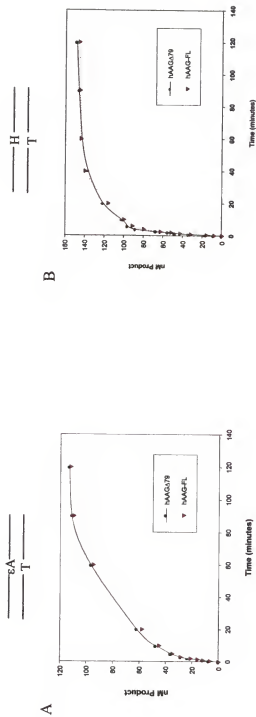


Figure 4-1. Plots showing hAAG-FL and hAAG Δ 79 excision. A) Excision of 1,N⁶-ethenoadenine by hAAG-FL and hAAG Δ 79 proteins. B) Excision of hypoxanthine by hAAG-FL and hAAG Δ 79 proteins. For both plots the DNA concentration = 1000 nM and the enzyme concentration = 100 nM.

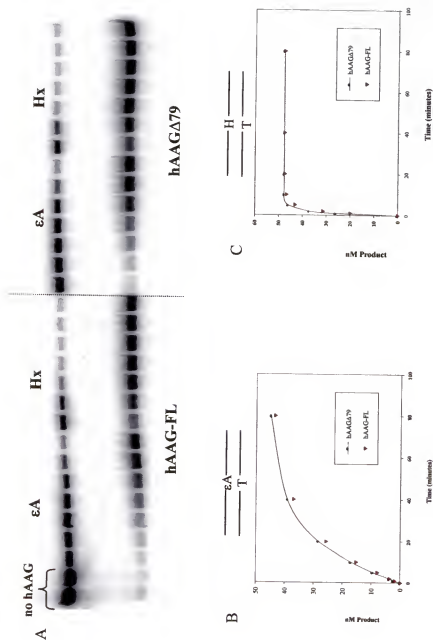


Figure 4-2. Single turnover excision assays. A) Representative gel showing excision of I, N^6 -ethanoadenine and hypoxanthine. B) Excision of I, N^6 -ethanoadenine by hAAG-FL and hAAG Δ 79 proteins under single turnover conditions. C) Excision of hypoxanthine by hAAG-FL and hAAG Δ 79 proteins under single turnover conditions. For each set of reactions the DNA = 50 nM and the enzyme = 400 nM.

The Effect of APE1 on hAAG Glycosylase Activity

Recently studies have indicated that APE1 stimulates turnover of several DNA glycosylases (38, 90, 117, 118). This stimulation was attributed to APE1's ability to displace DNA glycosylases that bound tightly to abasic site product generated during damaged base removal. In order to investigate whether APE1 affects hAAG glycosylase activity, we performed excision assays in the presence of APE1. Excision assays contained 1000 nM ^{32}P -labeled DNA substrate, 100 nM hAAG Δ 79 or hAAG-FL protein, and 0, 250, 500, and 1000 nM APE1. Time course experiments were carried out at 37°C for 120 minutes. Aliquots of the reaction mixtures were withdrawn at several time points during the assay and treated as previously described. Data from these experiments (data not shown) are identical to those shown in Figure 4-1 and shows that under these conditions there is no stimulation of hAAG glycosylase activity in the presence of APE1. These experiments were carried out in reaction buffer lacking magnesium because a high concentration of magnesium was previously shown to inhibit hAAG glycosylase activity (51). However, APE1 requires magnesium as a cofactor in order to incise DNA at abasic site residues (7, 64). Because of this, we decided to perform the experiments again in the presence of increasing concentrations of magnesium. The results are depicted in Figure 4-3 and reveal that APE1 stimulates multiple turnovers of hAAG-FL protein in a magnesium dependent manner, but does not stimulate hAAG Δ 79 protein under these conditions. The optimal magnesium concentration was found to be 10 mM (data not shown) and there is no further increase in hAAG-FL turnover at higher magnesium concentrations. The increased rate of damaged base excision was not due to contamination of APE1 by hAAG-FL protein because addition of APE1 alone did not

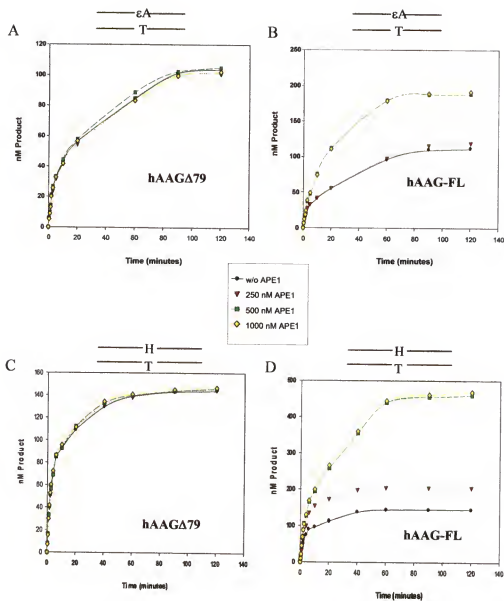


Figure 4-3. APE1 stimulates hAAG-FL turnover. A & C) The addition of APE1 does not stimulate hAAG Δ 79 excision of substrates. B & D) APE1 stimulates multiple turnovers of hAAG-FL protein. These reactions were performed in the presence of 10 mM magnesium chloride.

excise either damaged bases (data not shown). Because hypoxanthine is cleaved more rapidly from DNA than *1,N*⁶-ethenoadenine, hAAG-FL is capable of performing more turnovers on hypoxanthine containing DNA in the presence of APE1.

Effect of Magnesium on hAAG Glycosylase Activity

Because we have shown that magnesium is required for APE1 to stimulate hAAG-FL turnover, we decided to study the effect of 10 mM magnesium on hAAG-FL activity in the absence of APE1. Excision reactions were performed using 1000 nM ³²P-labeled DNA substrate, 100 nM hAAG-FL protein, and 10 mM magnesium chloride. Reactions were performed at 37°C for 120 minutes. Reaction aliquots were withdrawn at various time points during each reaction and quenched in 0.2 M NaOH as previously described. Figure 4-3B and D (w/o APE1 plots) shows that hAAG-FL protein is still active and only modestly affected in the presence of 10 mM magnesium chloride.

The nature of hAAG stimulation by APE1

In order to discern if APE1 was stimulating hAAG-FL protein turnover in the same manner as other DNA glycosylases, we performed electrophoretic mobility shift assays (EMSA) to examine hAAG-FL binding to abasic site containing DNA. A synthetic reduced abasic site was used in place of the natural abasic site because this substrate is more stable and can be site specifically incorporated using a commercial DNA synthesizer. This is the same abasic site used by other laboratories that investigated APE1 stimulation. Binding experiments were done by incubating ³²P-labeled abasic site duplex DNA with increasing concentrations of hAAG-FL protein at 4°C for 10 minutes. After incubation, an aliquot of each reaction mixture was loaded onto a 6% nondenaturing gel and electrophoresis was performed at 8V/cm in TBE buffer (pH 8.3)

for 3 hours. Under these conditions and using EMSA, hAAG-FL protein did not bind damaged DNA (data not shown). In contrast, in the same experiment hAAG Δ 79 was shown to have an apparent dissociation constant equal to 20 nM for the same substrate (*1,N*⁶-ethenoadenine).

Single turnover kinetics of excision of *1,N*⁶-ethenoadenine and hypoxanthine were measured in the presence of APE1 to determine if APE1 was enhancing the catalytic activity of hAAG-FL. Under single turnover conditions the excision rate is not limited by enzyme-DNA binding and the assay measures both enzyme-bound products and free products, therefore the rate reflects conversion of an enzyme-substrate complex to an enzyme-product complex. Excision reactions were performed using 50 nM ³²P labeled-DNA substrate, 400 nM hAAG-FL protein, 0 and 1000 nM APE1, and 10 mM magnesium chloride. The results in Figure 4-4 show that *1,N*⁶-ethenoadenine and hypoxanthine excision are not affected under single enzyme turnover conditions in the presence of APE1. This means that APE1 is not stimulating hAAG-FL by a mechanism that increases the rate of conversion of enzyme-substrate complexes to enzyme-product complexes.

EMSA, Western Blot Analysis of EMSA Gels, Co-immunoprecipitation, and Yeast Two-Hybrid Analysis to Test the Possible Interaction between APE1 and hAAG-FL Protein

The fact that full-length hAAG activity is stimulated by APE1, but hAAG Δ 79 is not suggests there may be an association between APE1 and the N-terminal region of hAAG-FL protein. To test this hypothesis we utilized hAAG-FL wild-type protein and a catalytically inactive mutant hAAGE125Q-FL protein. In this mutant, glutamic acid 125 is replaced with glutamine. Glu125 has been proposed to act as a general base to activate

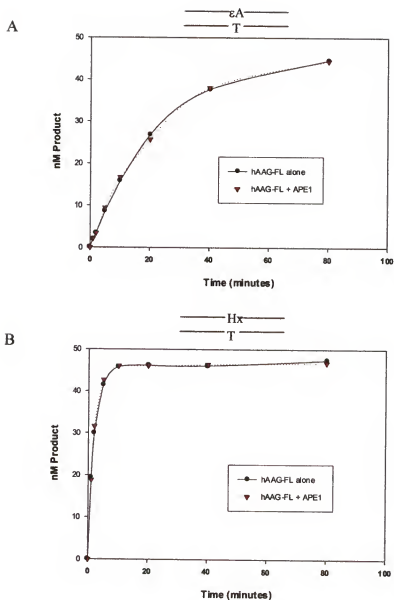


Figure 4-4. Single turnover excision assays in the presence of APE1. A) The addition of APE1 has no effect on hAAG-FL excision of ethenoadenine (ϵA) under single enzyme turnover conditions. B) APE1 does not effect hAAG-FL excision activity of hypoxanthine (Hx) under single enzyme turnover conditions.

a water molecule for hydrolysis of the glycosidic bond (50). The catalytically inactive hAAGE125Q Δ 79 mutant has been shown to be proficient in DNA binding and nucleotide flipping, but this has not been determined for hAAGE125Q-FL.

EMSA was performed as previously described using wild-type hAAG-FL and hAAGE125Q-FL proteins in the presence of *I,N*⁶-ethenoadenine, hypoxanthine, and abasic site containing DNA substrates and various concentrations of APE1. We used various EMSA gel conditions in order to detect a hAAG-FL (mutant and wild-type hAAG) • DNA complex and we only observed weak binding of hAAG-FL to DNA substrates in contrast to earlier results where damage-specific protein•DNA bands were observed in EMSA's with hAAG Δ 79. Additionally, our attempts failed to detect a supershift in any of the ³²P labeled-DNA substrates in the presence of hAAG and APE1. We also performed western blot analysis on the EMSA gels that contained substrate DNA, hAAGE125Q-FL protein, and APE1. These blots were probed with hAAG antibody in an attempt to see a shift in the mobility of hAAG in the presence of APE1. However, all attempts to detect a shift in hAAG mobility in the presence of APE1 failed.

Because we were unable to detect DNA binding by hAAG-FL in EMSA's both in the presence and absence of APE1, we tried alternative methods for measuring protein•protein interactions. The first approach was to use hAAG antibodies to co-immunoprecipitate a hAAG-APE1 complex. In these assays, 200 nM hAAG-FL was incubated with 1000 and 4000 nM APE1 prior to the addition of 5 μ g of polyclonal anti-hAAG antibody. Protein A bound to sepharose beads was added to precipitate the antibody complex. The precipitated and soluble fractions were separated and analyzed by SDS-PAGE. The precipitated fraction contained only hAAG protein and the soluble

fraction contained APE1 protein. These results suggest that either the protein•protein interaction is too weak to survive the precipitation and washing conditions or the protein•protein interaction may require DNA.

As a second approach, a yeast two-hybrid analysis was used to detect an interaction between catalytically active hAAG-FL protein and APE1 in the absence of damaged DNA substrates. The two hybrid proteins GAL4-BD-hAAG and GAL4-AD-APE1 were simultaneously expressed in diploid yeast cells *in vivo*. Co-expression of these fusion proteins did not reconstitute a functional transcriptional activator showing that hAAG does not bind APE1 in this assay. However, it is possible that the DNA binding domain and affinity tag fused to the N-terminus of hAAG may interfere with binding of this region of the protein to APE1. A control experiment showed that overexpression of both proteins in the yeast cells was not toxic. Therefore the lack of an interaction was not due to toxicity generated by overproducing each protein.

Discussion

The base excision repair pathway is one of several DNA repair pathways employed by an organism to maintain genome stability. Unlike other repair pathways, a fully functional base excision repair complex has not yet been detected. In order for base excision repair to be efficient, there must be some type of coordination between the activities of each enzyme involved in the pathway. Recently, several laboratories have shown the potential coordination of the initial steps in base excision repair (38, 90, 117, 118). In these studies, hTDG and hOGG1 had apparent dissociation constants of 4 pM and 2.8 nM respectively, for the product of their glycosylase reactions (abasic site). The apparent dissociation constants for damaged substrate bases for hTDG is approximately

40 nM and 24 nM for hOGG1. This tight binding to abasic site was shown to slow multiple enzyme turnovers for each DNA glycosylase. However, these DNA glycosylases are capable of performing multiple turnover events more rapidly in the presence of APE1. These data suggest that DNA glycosylases and APE1 may act together to coordinate the early steps of base excision repair.

We show here that APE1 is also capable of promoting hAAG protein turnover *in vitro*. In our studies, we used a full-length hAAG protein and an N-terminal deletion mutant that is missing the first 79 amino acids. Deletion of this unconserved N-terminal region is shown to have no effect on base excision activity, but results in more soluble protein under low ionic strength. We found that APE1 could stimulate multiple turnovers of hAAG-FL protein, but had no effect on hAAG Δ 79 protein. The finding that this stimulation of hAAG-FL protein by APE1 required magnesium is somewhat surprising. APE1 binds rather tightly ($K_d \sim 0.8$ nM) to abasic site containing DNA in the absence of magnesium (119). However, magnesium has been shown to act as a required cofactor for APE1 processing of abasic sites. If APE1 binds to abasic site DNA relatively tightly in the absence of magnesium, then our results might suggest that APE1 binding to abasic site alone is not enough to stimulate hAAG-FL protein turnover, thus it seems stimulation of hAAG-FL protein requires processing of the abasic sites by APE1. Because hAAG Δ 79 is not stimulated by APE1 the N-terminal region of hAAG may be required for APE1 stimulation.



Our working model for hAAG activity is pictured above. In single turnover experiments where all of the substrate is bound by hAAG either flipping or excision can

be rate limiting because we are measuring the rate of going from an enzyme-substrate complex to an enzyme-product complex. To rule out the possibility that APE1 was enhancing the catalytic activity of hAAG-FL protein we performed single enzyme turnover kinetic assays in the presence and absence of APE1. Under these conditions there was no difference in the excision rates of *1,N*⁶-ethenoadenine and hypoxanthine in the presence of APE1. Therefore, APE1 is not increasing hAAG-FL turnover by affecting flipping or excision. In hAAG-FL excision experiments where substrate is in excess DNA binding is not rate limiting. Therefore, any of the other steps in the model could be affected by APE1. Collectively, our data suggest that hAAG-FL protein turnover is somehow limited by dissociation and that APE1 in the presence of magnesium stimulates this dissociation. However, this idea does not explain why hAAG Δ 79 is not stimulated by APE1.

Both hAAG-FL and hAAG Δ 79 proteins are shown to have identical base excision repair activities in the absence of APE1. The fact that hAAG-FL protein is stimulated by APE1 and hAAG Δ 79 protein is not, suggests APE1 may somehow interact with the N-terminal region of hAAG. In order to test this hypothesis, we used several different techniques including, EMSA, western blot analysis of EMSA gels, co-immunoprecipitation, and yeast two-hybrid analysis to detect an interaction between hAAG-FL protein and APE1. Additionally, we utilized a catalytically inactive mutant, hAAGE125Q-FL, in order to detect the formation of a ternary complex between hAAGE125Q-FL protein, APE1, and substrate DNA. Our results have shown no evidence for an interaction between hAAG-FL protein and APE1. Several possibilities exist that could explain the lack of detection for an interaction. APE1 only stimulates

hAAG-FL protein activity when present in excess amounts. This alone suggest that the interaction is very weak or unstable and cannot be detected using the techniques that we have employed. All other APE1 stimulation studies have had to use excess APE1 as well, in order to stimulate DNA glycosylase turnover. APE1 may actually stimulate hAAG-FL protein turnover indirectly by binding DNA and changing the confirmation of the DNA helix, thus causing dissociation of hAAG and allowing for APE1 binding. Several other attempts by various laboratories to detect an interaction between APE1 and human DNA glycosylases have also failed (38, 90, 117, 118). These laboratories have used EMSA, surface plasmon resonance, co-immunoprecipitation, western blot analysis, and yeast two-hybrid analysis.

In conclusion, the stimulation of hAAG-FL protein by APE1 suggest hAAG activity is somehow coordinated with APE1 activity, as has been shown for several other DNA glycosylases. It will be interesting to find out if other base excision repair enzymes can affect DNA glycosylase activity and if DNA glycosylases can affect other base excision repair enzyme activities.

CHAPTER 5

IDENTIFICATION OF NOVEL PROTEIN INTERACTIONS WITH hAAG USING YEAST TWO-HYBRID ANALYSIS TO SCREEN A LIVER cDNA LIBRARY

Introduction

The commercially available yeast two-hybrid system is a powerful assay for probing protein-protein interactions in a variety of biological systems. The central idea for the yeast two-hybrid system, as described by Fields and Song (28), was recognized by experiments on the regulation of yeast transcription factors. Some transcription factors were shown to contain two distinct and separable domains (e.g. GAL4 and GCN4). The domains can be divided into a site-specific DNA-binding domain and an acidic domain that is required for transcriptional activation (2). In these initial studies, functionally active chimeric proteins were constructed that contained the DNA binding domain of yeast transcription factors combined with activation domains of different transcription factors. These chimeras could interact and activate transcription just as efficiently as their wild-type counterparts. Subsequent studies revealed that proteins known to interact could be separately fused to the DNA binding domain and activation domain of the yeast GAL4 transcription factor and when the two interacting proteins bound one another the result was activation of transcription of GAL4 target genes in yeast (35). In these instances gene expression was a result of reconstitution of a functional transcription factor by the association of the two hybrid proteins. Hybrid proteins that did not interact could not activate transcription. It was discovered later that activation could be

monitored by the activation of a reporter gene such as β -galactosidase. In order to assist the application of the two-hybrid approach, the endogenous *GAL4* activator gene and the *GAL80* repressor gene have been deleted from yeast strains used in screening (35).

The two-hybrid system was initially designed to investigate the interaction of pairs of proteins and later used to search for novel protein-protein interactions. With the yeast two-hybrid system a cDNA library can be screened for novel proteins that interact with either a known “bait” protein or confirm interactions between known proteins. The principle of the yeast two-hybrid analysis is shown in Figure 5-1. In the past, the two-hybrid approach was met with skepticism because it was unknown if the method could distinguish between interactions that were physiologically relevant from the lower-affinity interactions that were not biologically important and today many scientists are still hesitant to use this approach. However, after several years of use in the scientific community and a plethora of control experiments measuring protein-protein interactions and affinities it was revealed that >75% of the bait proteins used revealed a physiologically relevant interacting protein (25). The yeast two-hybrid system has been extensively used to identify novel interacting proteins in bacteria, yeast, viruses, plants, and animals. Two-hybrid experiments have been carried out with a large number of proteins from a variety of cellular locations. Cytoplasmic, nuclear and membrane-associated proteins from a variety of organisms have been successfully used to screen for novel interacting proteins (2).

The yeast two-hybrid approach has also been used to deduce which protein residues are important for a specific interaction. This has been accomplished by generating deletion hybrid constructs in one gene of interest and assaying for reporter

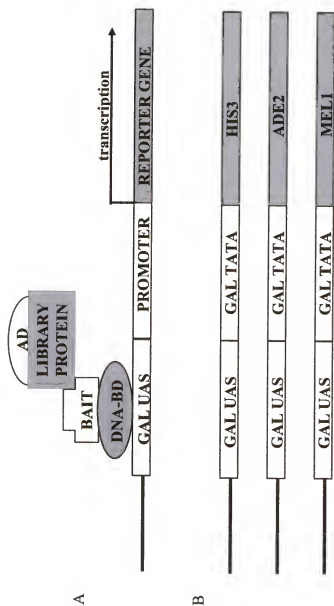


Figure 5-1. The yeast two-hybrid principle. A) The bait and library proteins are expressed as fusion proteins containing the yeast GAL4 DNA-binding domain and activation domain, respectively. When the binding domain and activation domain come in close proximity of one another they are capable of activating transcription of reporter genes. B) Reporter constructs in the yeast strains AH109 and Y187. The reporter genes are integrated into the chromosome and are under the control of distinct GAL4 upstream activating sequences and TATA boxes. These promoters yield strong and specific responses to GAL4. Both yeast strains have deletions in the *TRP*, *LEU*, and *GAL4* genes.

gene activation (2). This approach has been widely used to map a number of regions responsible for protein-protein interactions. The two-hybrid approach provides a sensitive assay to detect proteins suspected of interacting based upon other experimental evidence. Probably the most important feature of the two-hybrid approach is the ability to rapidly isolate novel genes encoding proteins that associate with a known protein of interest (2, 14). Conventionally, this has required extensive biochemical and genetic experiments. By using a single “bait” protein a cDNA library containing thousands of possible interacting proteins can be screened in a relatively short amount of time and at minimal cost.

The yeast two-hybrid commercial assay is sensitive enough to detect dissociation constants equal to 70 μM (128). This capability exceeds other methods used to detect protein-protein interactions, such as co-immunoprecipitation. However, a downside to this sensitivity is that some protein-protein interactions may not be able to be confirmed with secondary assays. The sensitivity of the two-hybrid system results from: 1) over production of hybrid proteins by strong promoters on high-copy number vectors, which favors complex formation, 2) a measured signal that is roughly proportional to the equilibrium concentration of the heterodimeric species, 3) enhancement of the stability of the hybrid protein complex by the interaction of the activation domain with proteins from the transcriptional initiation complex, which also associate with promoter DNA, 4) an increase in the stability of the hybrid protein complex on forming a ternary complex with DNA and 5) amplification of the signal by producing chimeric mRNA molecules that generate multiple stable reporter enzymes per transcript (2).

Clontech MATCHMAKER Yeast Two-Hybrid System 3

The Clontech yeast two-hybrid assay uses the *Saccharomyces cerevisiae* yeast strain AH109 that includes four reporter genes (*ADE2*, *HIS3*, *lacZ*, and *MEL1*/ α -galactosidase) integrated into the host genome in different regions and each having distinct GAL4 responsive upstream activating sequences (UAS) and TATA boxes. These distinct promoter elements eliminate three major categories of false positives: those caused by proteins that interact upstream of the reporter construct, that interact directly with the sequences flanking the GAL4 binding site, and that interact with transcription factors bound to specific TATA boxes. AH109 contains deletions in the tryptophan (*TRP*) synthetase and leucine (*LEU*) synthetase genes. Because of this, and the previously mentioned transcriptional regulation of the *ADE2* and *HIS3* gene products, AH109 is not capable of growing on minimal media lacking these nutrients. In addition, AH109 expresses α -galactosidase which allows for blue/white colony selection on minimal media containing X- α -Gal, the substrate of α -galactosidase.

AH109 is a compatible mating partner with *S. cerevisiae* strain Y187. Y187 contains the same four reporter genes as AH109 and they are under the exact same GAL4 UASs and TATA boxes. Y187 also contains deletions in the *TRP* and *LEU* genes. The mating compatibility between AH109 and Y187 allows for one strain to contain the bait protein of interest and the other strain to contain the cDNA library to be screened. Mating two strains together significantly reduces the time and labor needed to co-transform a single strain with thousands of cDNA library constructs and reduces the time needed to screen a cDNA library.

Because the four reporter genes of AH109 and Y187 are under the control of GAL4 promoters they cannot be activated (transcribed) unless two interacting proteins bring the GAL4 activation domain and GAL4 DNA binding domain in close proximity to one another. In theory, this can only happen when the bait protein, fused to the GAL4 binding domain, binds to another protein, which is fused to the GAL4 activation domain. In these instances, a protein-protein interaction can be deduced from growing mated cells on minimal media lacking adenine, histidine, which allow for selection of interacting proteins, supplemented with X- α -Gal, which allows for visual selection. The deletion in the *TRP* and *LEU* genes of each strain also allow for additional selection. These allow for selection of the strains transformed with plasmids carrying these genes.

The Clontech yeast two-hybrid system uses the pGBKT7 and pACT2 plasmids. The pGBKT7 vector contains the GAL4 DNA binding domain, to which the bait protein is fused, and the *TRP* gene. The pACT2 vector contains the GAL4 activation domain, which the cDNA library fragments are fused to, and the *LEU* gene. Since AH109 and Y187 lack the *TRP* and *LEU* genes, these plasmids allow for transformation selection on minimal media lacking these nutrients and also provide additional selection during yeast two-hybrid screening. The pGBKT7 vector encodes a c-Myc epitope tag, which is fused to the N-terminus of the bait protein. The pACT2 vector encodes a hemagglutinin (HA) tag, which is fused to the library protein. These tags eliminate the need to generate specific antibodies to new proteins and allow for the identification of fusion proteins.

While the two-hybrid approach is a powerful genetic tool for detecting protein-protein interactions it does have limitations. For example, hybrid proteins are targeted to the nucleus and interactions that require post-translational modifications that take place

within the endoplasmic reticulum may not occur (2). Additionally, other proteins may require phosphorylation to interact with a specific protein which might not occur in yeast. Additionally, some hybrid proteins are lethal or harmful to the yeast host strain when overexpressed. In these examples protein-protein interactions are not possible because of a reduction in cell viability. Another downside of the yeast-two hybrid approach is some proteins are known to activate transcription in the absence of a specific interaction. These examples are commonly referred to as false positives. New yeast strains have been developed that virtually eliminates false positives. These yeast strains have several reporter genes under the control of GAL4 activating sequences, which allow for tight control of transcriptional activation.

After performing a yeast two-hybrid analysis, it is necessary to confirm the interaction is real and determine if the interaction is of biological importance. Some protein-protein interactions may occur, but because of the cellular location of each protein they might not ever be able to associate *in vivo*. It is equally important to try and discern the biological relevance of the protein-protein interaction. Establishing this is normally the most time consuming due to experimental demands and in some instances the most difficult.

Several human BER proteins are known to interact with one another. For instance, pol β has been shown to interact with DNA ligase I, XRCC1, and APE1 (7, 48, 89). However, there is no evidence that shows that DNA glycosylases directly interact with any of the downstream BER components. Because the product of DNA glycosylase reactions, an abasic site, is cytotoxic some mechanism is likely to exist which links DNA glycosylase activity to downstream BER components. For these reasons, we have

decided to use the Clontech yeast two-hybrid system 3 to screen for proteins that might interact with hAAG. hAAG is abundant in the liver, so we chose to screen a human liver cDNA library to search for possible hAAG interacting proteins. Such proteins might link hAAG to other cellular processes such as DNA replication, transcription, or other DNA repair pathways. In addition, there may be proteins that enhance hAAG activity and link hAAG to downstream BER components, such as APE1 or link BER to other DNA repair pathways.

Results

Yeast Strains and Vector Constructs

Full-length hAAG was fused between the c-Myc epitope tag and the GAL4 DNA-binding domain (DNA-BD) of the cloning vector pGBKT7, thereby creating bait for yeast-two hybrid analysis. Also, full-length APE1 was fused in the same manner to pGBKT7 in order to determine if proteins that interacted with hAAG could also interact with APE1. The pGBKT7 vector contains a T7 promoter, a c-Myc epitope tag, *TRP* nutritional selection marker, kanamycin resistance, and can autonomously replicate in *E. coli* and *S. cerevisiae*.

A Y187 yeast strain transformed with a human liver cDNA library cloned into the pACT2 vector was purchased from Clontech. The cDNA inserts are between 0.5-4.0 kb in length and there are greater than 1×10^6 independent clones represented. The pACT2 vector contains a T7 promoter, HA epitope tag, *LEU* nutritional selection marker, ampicillin resistance, and can autonomously replicate in *E. coli* and *S. cerevisiae*. The vectors are depicted in Figure 5-2. These vectors are high copy number. The epitope

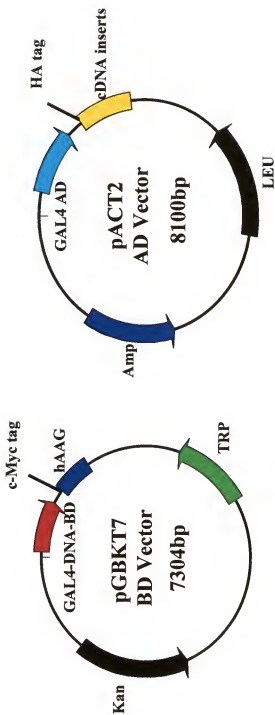


Figure 5-2. The pGBKT7 and pACT2 vectors. Both of these plasmids contain 17 promoters and bacterial and yeast origins of replication. In addition, each plasmid contains either a c-Myc or HA tag to facilitate immunodetection or protein purification.

tags on the proteins eliminate the need to generate specific antibodies to every protein shown to interact with each bait protein.

Yeast Transformations and Phenotypic Analysis of Strains

Strain AH109 was transformed with pGBKT7 vector, pGBKT7-p53 (control provided by Clontech), pGBKT7-hAAG, and pGBKT7-APE1. After transformation, the resulting strains, along with untransformed AH109, were plated on four different types of minimal synthetic dropout media (SD) deficient for one of the selectable markers: Adenine (Ade), histidine (His), leucine (Leu), and tryptophan (Trp) in order to test strain phenotypes before yeast two-hybrid analysis. After 7 days of incubation at 30°C, the plates were examined for growth. AH109 showed a small amount of leaky His expression, however when plated on media deficient for more than one marker there was no growth (data not shown). Representative plates for AH109 are shown in Figure 5-3. The transformants could only grow on plates lacking Trp (data not shown). These results demonstrate that the host strain AH109 and the transformants behave as predicted based on genotype and should not present a problem during yeast two-hybrid analysis.

Control Experiments to Measure Bait Toxicity, Bait Transcriptional Activation, and Mating Efficiency

In order to determine if hAAG or APE1 fusion proteins were toxic to the AH109 host strain, growth rates in rich liquid medium (YPD) were compared to AH109 alone and AH109 harboring pGBKT7 vector. Three colonies of each strain were used to inoculate 20 mL of liquid culture. The cultures were grown at 30°C for 10 hours with vigorous shaking (250 rpm). OD₆₀₀ measurements were taken at 1, 2, 4, 6, 8, and 10-hour time points and the results are shown in Figure 5-4. The results indicate that there is not a significant difference in growth rates between the transformants and the AH109 strain



Figure 5-3. Phenotypic analysis of AH109. AH109 was plated on yeast minimal media lacking a single amino acid in order to check the phenotype. There does seem to be a small amount of growth on the histidine deficient plates, however when these cells are re-plated on fresh media of any kind the cells are not viable.

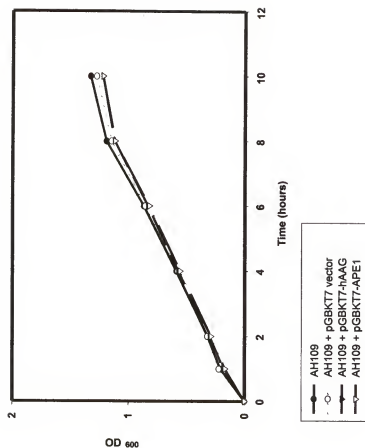


Figure 5-4. Comparative growth rates of AH109 and AH109 transformants. AH109, AH109-pGBKT7, AH109-hAAG, AH109-APE1 strains were used to inoculate 20 mL of liquid media and each culture was grown at 30°C for 10 hours. OD₆₀₀ measurements were taken at multiple time points and plotted in order to compare growth rates for each strain. The results show that the hAAG and HAP1 transformants are not toxic to the host strain.

alone. Therefore, hAAG and APE1 are not toxic to the host strain AH109 nor do they cause a reduction in observed growth rates.

In order for yeast two-hybrid analysis to work efficiently the bait protein must not activate transcription of the yeast reporter genes unless it is bound to the activation domain hybrid protein. Transformants containing pGBKT7, pGBKT7-hAAG, and pGBKT7-APE1 were plated on several types of minimal media supplemented with X- α -Gal but lacking Trp (SD/-Trp/X- α -Gal), lacking Trp and His (SD/-Trp/-His/X- α -Gal), and lacking Trp and Ade (SD/-Trp/-Ade/X- α -Gal). Growth on SD/-Trp/-His/X- α -Gal and SD/-Trp/-Ade/X- α -Gal would indicate that these fusion proteins could activate transcription in the absence of the activation domain. The transformants only grew on the SD/-Trp/X- α -Gal plates and they did not activate expression of the *MEL1* gene (Figure 5-5). Therefore, hAAG and APE1 cannot activate transcription of the endogenous yeast reporter genes by themselves.

Yeast mating is a practical method of introducing two plasmids into the same host cell, but some yeast strains have a reduction in mating efficiency when certain proteins are overexpressed. Therefore, mating control experiments were carried out to determine the mating efficiency of AH109 strains overexpressing hAAG and APE1. As a general rule of thumb yeast mating efficiency should be between 3-10%. AH109 transformants containing pGBKT7 vector, pGBKT7-p53, pGBKT7-hAAG, and pGBKT7-APE1 were mated with Y187 carrying a pACT2-TD1 plasmid. The TD-1 protein (SV40 large T antigen) is known to bind to p53 and served as an additional mating control. The mating experiments were carried out as described in the experimental procedures and 100 μ l aliquots of 1:10 and 1:100 dilutions of each mating mixture was plated on SD/-Leu/X- α -

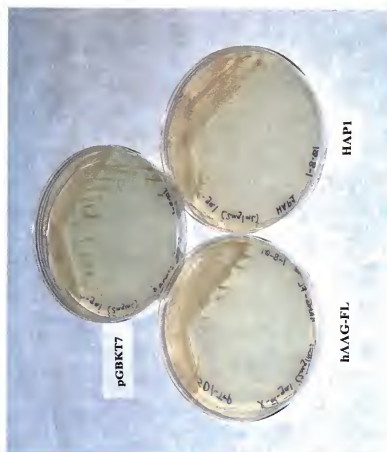


Figure 5-5. Transcriptional activation control experiments. The hAAG and APE1 transformants were plated on low and high stringency minimal media supplemented with X- α -gal, as well as minimal media lacking tryptophan. The transformants could only grow on media lacking tryptophan and they did not activate transcription of the *MEL1* gene as can be seen above (colonies are not blue).

Gal, SD/-Trp/ X- α -Gal, SD/-Leu/-Trp/X- α -Gal, and SD/-Leu/-Trp/-Ade/-His/X- α -Gal plates. Mating efficiencies were calculated for each cross as described in experimental procedures. The cross between the yeast strains carrying p53 and TD-1 yielded a mating efficiency of 6% whereas the mating efficiency for hAAG and APE1 crosses yielded a mating efficiency of approximately 5% for each. Additionally, the p53/TD-1 cells induced expression of the endogenous yeast reporter genes and resulted in blue colonies (Figure 5-6). The mating efficiencies of hAAG and APE1 compared to the control p53/TD-1 cross are not significantly different. These results, when compared with previous control experiments, suggest that hAAG and APE1 are suitable baits for use in a yeast two-hybrid experiment.

Screening a Human Liver cDNA Library Using hAAG as Bait

A single large colony of AH109/pGBKT7-hAAG maintained on SD/-Trp, approximately 6 days old, was used to inoculate 50 mL of SD/-Trp liquid medium. The culture was grown overnight (18-24 hours) at 30°C with vigorous shaking (250 rpm) to an OD₆₀₀ greater than 0.8. The cells were collected by centrifugation and resuspended in 5 mL fresh SD/-Trp liquid medium. A 1 mL aliquot of the pretransformed Y187 library strain was thawed and combined with the AH109/pGBKT7-hAAG cells and treated as described in the experimental procedures. The mating mixture was grown for 24 hours and the cells collected by centrifugation and resuspended in 10 mL of 0.5X YPD/kanamycin. A 100 μ L aliquot of a 1:10,000, 1:1,000, 1:100, and 1:10 dilution of the mating mixture was plated on SD/-Leu, SD/-Trp, and SD/-Leu/-Trp in order to calculate mating efficiency. The remaining mating mixture was plated on ~50 large 150 mm diameter SD/-Leu/-Trp/-His/X- α -Gal plates (low stringency selection) at 200 μ L per

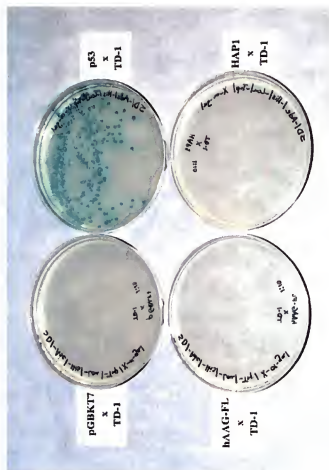


Figure 5-6. hAAG and APE1 do not activate yeast reporter genes. AH109 transformants were mated with the y strain Y187 that contained a pACT2 plasmid expressing TD-1 fused to the activation domain of GAL4 and the mating cultures were plated on minimal media lacking leucine, tryptophan, histidine, and adenine supplemented with X- α -Gal. p53 and TD-1 are known interacting proteins and activate transcription of the yeast reporter genes (blue colonies), whereas the other mating cultures were not capable of activating transcription. Control experiments showed that the other mating cultures were viable.



Figure 5-7. Typical yeast colony PCR. A 1.5% agarose gel stained with ethidium bromide depicting a typical yeast colony PCR reaction. The first lane contains a DNA marker and the second lane is a negative control containing no template DNA. All other lanes contain putative DNA interacting proteins. For specific assay conditions see the experimental procedures section.

plate. The plates were incubated colony side down at 30°C for 10 days. Blue colonies were selected and patch plated onto SD/-Leu/-Trp/-His/-Ade/X- α -Gal plates (high stringency selection). The blue colonies that resulted from this selection were re-streaked three additional times on SD/-Leu/-Trp/-His/X- α -Gal in order to eliminate clones that may contain more than one AD/library plasmid construct. A mixture of white and blue colonies indicated segregation. After segregation, the phenotypes of each blue colony were verified again on SD/-Leu/-Trp/-His/-Ade/X- α -Gal plates. Colonies with the correct phenotype were patch plated on SD/-Leu/-Trp/-His/-Ade/X- α -Gal plates and grown for 5 days at 30°C to generate working stocks. All plates were stored at 4°C after incubation. There were 121 blue colonies that resulted from the low stringency selection after mating. After plating onto higher stringency medium, re-testing phenotypes, and sorting colonies there were a total of 68 putative positive clones that interacted with hAAG.

Yeast Colony PCR to Eliminate Duplicates

It is possible that a high percentage of the putative interacting clones contain the same AD/library insert. It is common practice to isolate yeast plasmid DNA from each putative positive clone in order to perform PCR analysis to eliminate duplicates. However, we have devised a yeast colony PCR assay to eliminate duplicates (see experimental procedures). This method saves time and reduces the number of costly yeast plasmid isolations performed. This method is highly efficient and yields PCR products > 95% of the time. A typical yeast colony PCR reaction is illustrated in Figure 5-7. After PCR analysis, the products are digested with Alu I or Hae III and the fragments are sorted by size.

Of the 68 putative positive clones, 65 yielded PCR products. The three clones that did not yield PCR product were no longer viable for unknown reasons. PCR products were sorted by size and grouped together. Between 3 and 10 PCR products of each group were purified and subjected to DNA sequencing analysis as described in the experimental procedures using primers that are unique to the pACT2 vector. Each PCR product yielded approximately 175-300 nucleotides of DNA sequence. The resulting sequences were BLAST searched for identification and the results are listed in Table 5-1. All yeast colonies containing AD/library inserts that could possibly be relevant were grown and purified by the yeast plasmid isolation method in the experimental procedures. The resulting plasmids were propagated in *E. coli* followed by purification and storage at -20°C. In addition, freezer stocks of the yeast strains that contained these interacting clones were made as well.

Confirmation of Protein Interactions in Yeast

In order to confirm protein-protein interactions the DNA-BD/bait and purified AD/library plasmids were transformed simultaneously into AH109. The resulting transformants were plated onto SD/-Leu/-Trp/-His/-Ade/X- α -Gal plates and grown at 30°C for 1 week. All putative interactions were confirmed by these transformations.

Human MT-2A was shown to be a possible hAAG interacting protein. MT-2A is a metal binding protein and MT-2A protein expression is increased in response to certain alkylating agents. In order to try and map the site of interaction of MT-2A to hAAG, deletion constructs were made of hAAG and fused to the DNA-BD of pGBKT7 (Figure 5-8). The Y187 strain harboring the MT-2A containing plasmid was mated to the various AH109 strains carrying the hAAG deletion constructs. The mating mixture was plated

Table 5-1. A list of the possible hAAG interacting proteins.

Human Protein Identified	Number of Independent Clones
MT-2A	17
Ribosomal binding protein S20	5
Unknown protein—colon adenocarcinoma	3
Unknown protein—similar to aminoacylase	5
Unknown protein—chromosome 11	3
Unknown protein—chromosome 15	5
Fibronectin	11
Catalase	3
Carboxypeptidase	5
Zinc binding protein	3
Chloride channel protein	4

The unknown proteins represent possible open reading frames (ORFs) resulting from BLAST analysis of their respective cDNAs. Also shown is the number of independent clones for each protein identified.

A.A. Composition

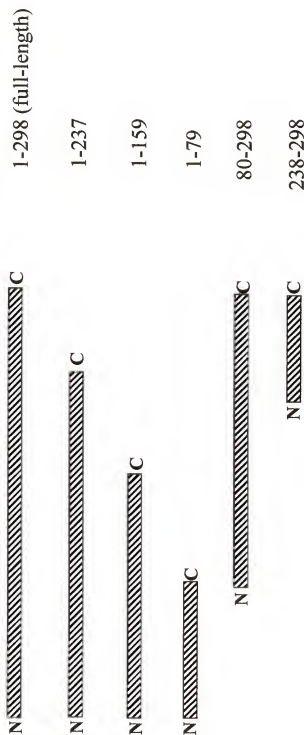


Figure 5-8. Representation of hAAG deletion constructs. Deletion constructs were made of hAAG and fused to the DNA-binding domain of pGBKT7 in order to try and discern the region of hAAG that interacts with MT-2A. The resulting plasmids were transformed into AH109 and mated with the Y187 strain expressing MT-2A.

onto SD/-Leu/-Trp/-His/-Ade/X- α -Gal plates and incubated at 30°C for 1 week. The results are shown in Table 5-2. Briefly, these data show that MT-2A interacts with the C-terminal portion of hAAG.

We performed the same mating experiment described above, but we used AH109 transformed with pGBKT7-APE1-BD fusion. The results showed that APE1 and MT-2A also interact.

Lastly, we performed a mating experiment with AH109 carrying the pGBKT7-hAAG-BD fusion and Y187 carrying the pACT2-APE1-AD fusion. Under these conditions we were unable to detect an interaction between hAAG and APE1. The resulting diploid cells from the mating experiment were able to grow on minimal media lacking Trp and Leu, which indicates that overexpression of each protein in the same cell is not toxic.

Discussion

The base excision repair and the nucleotide excision repair pathways are multistep processes that correct DNA base damage resulting from endogenous and exogenous sources. Exhaustive experiments have revealed that human nucleotide excision repair requires more than 30 proteins (121). In contrast to NER, BER requires fewer proteins and the individual BER proteins can accomplish *in vitro* reactions in the absence of other BER components (68). In spite of the fact that individual BER proteins do not require complex formation to catalyze *in vitro* reactions, such protein-protein interactions may occur for *in vivo* DNA repair. There are examples of protein-protein interaction amongst BER components. For instance, APE1 and pol β are shown to interact at DNA abasic sites and the result of this interaction increases the rate of dRP removal by pol β (7). A

Table 5-2. Mapping the interaction on hAAG of MT-2A binding.

hAAG Construct	Growth on SD/-Leu/-Trp	Growth on SD/-Leu/-Trp/-His/-Ade	MEL1 Production (blue colonies)
pGBKT7 vector	+	-	-
1-298	+	+	+
1-237	+	-	-
1-159	+	-	-
1-79	+	-	-
80-298	+	+	+
238-298	+	+	+

recent study has shown that hAAG is capable of interacting with human RAD23 proteins. This interaction was found by yeast two-hybrid analysis screening a human skin cDNA library. The human RAD23 proteins are known to function in the NER process. The authors suggest that the interaction between RAD23 proteins and hAAG might facilitate coupling of BER and NER. However, the authors do not provide any evidence to support this notion. In addition, human skin cDNA libraries are known to be enriched in NER proteins, therefore this interaction could be biased because of the screening procedure.

We decided to use yeast two-hybrid analysis to probe a human liver cDNA library for proteins that might interact with hAAG. hAAG is highly expressed in liver tissue compared to other tissues, therefore hAAG interacting proteins might also reside in liver tissue. We are interested in finding any proteins that might couple hAAG activity to other cellular processes, such as DNA replication, transcription, and other DNA repair pathways. Also, we are interested in any proteins that might link hAAG to downstream BER components or novel proteins that could facilitate catalysis by hAAG.

In our experiments, we have identified several proteins that may interact with hAAG. At first glance, none of these proteins appear to be directly involved in DNA repair processes. However, there is circumstantial evidence that supports the notion that a few of these proteins could be involved in DNA repair pathways.

Human MT-2A is a metallothionein protein known to bind various metals, including zinc and cadmium and is abundant in the liver. All eukaryotic cells described thus far contain some type of metallothionein protein(s). The cellular function of metallothionein proteins remains a mystery, but they are thought to be involved in metal detoxification. In humans there have been eight different isoforms of metallothionein

described. Human MT-2A consists of a single polypeptide chain of 61 amino acids, 20 of which are cysteine residues. Cadmium, mitomycin C, interferon, UV irradiation, alkylating agents, and ionizing radiation induce the cellular transcription of MT-2A (62). Experiments show that MT-2A is overexpressed in a number of solid tumors (76). Also, overexpression of MT-2A is known to protect mammalian cells from the cytotoxic effects of alkylating agents and ionizing radiation (62, 63, 93). Both of these agents have been shown to damage DNA and BER is a primary pathway for repairing these types of damages.

Human ribosomal protein S20 (RPS20) was also detected in the yeast two-hybrid analysis as a possible protein interacting with hAAG. RPS20 comprises a subunit of the 40s ribosomal subunit. This possible interaction is somewhat interesting because recently it was demonstrated that human ribosomal protein S3 (RPS3) also contains AP endonuclease activity (15). This novel activity of S3 was detected in XP patients that have a reduction in APE1 activity. In addition, experiments have revealed that D. melanogaster S3 protein contains 8-oxo-guanine DNA glycosylase activity as well as AP endonuclease activity (126). Human S3 is also part of the 40s ribosomal subunit.

In the past DNA glycosylase studies have concentrated on identifying proteins that excise various types of base damage from DNA. While these experiments are crucial to understanding BER, they fail to address any possible interplay between DNA glycosylases and other proteins *in vivo*. The studies that we have initiated are aimed at identifying other proteins that may be required for efficient DNA glycosylase activity or that might link DNA glycosylase activity to other essential pathways. These studies are

still in their infancy, but as more experiments are accomplished we will begin to unravel the cross talk, if any, between DNA glycosylases and other proteins.

CHAPTER 6

PROTEIN PHOSPHORYLATION OF hAAG BY PROTEIN KINASE-C AND CASEIN KINASE II

Introduction

All cells respond to their environment through dynamic post-translational modification of their existing proteins [Wells, 2001 #3061]. There have been more than 20 post-translational modifications described for eukaryotic proteins [Parekh, 1997 #3062]. These modifications have been shown to be important for cellular survival. Protein phosphorylation is one of the most well studied examples of cellular post-translational modifications. Most proteins are phosphorylated at serine, threonine or tyrosine residues. Proteins involved in transcription, DNA replication, DNA repair, cytoskeletal organization, cell-cycle checkpoints, signal transduction pathways, protein degradation, and a variety of other essential cellular processes have been shown to be phosphorylated [Hart, 1997 #3063; Wells, 2001 #3061]. Most of these phosphorylation events have been shown to regulate protein activity in some manner.

Several DNA repair proteins have been shown to be phosphorylated in response to DNA damage. Exposure of mammalian cells to ionizing radiation promotes ATM-dependent phosphorylation of p53 [Lee, 2001 #3064] in a DNA damage dependent manner. Experiments reveal that several BER enzymes are also phosphorylated. DNA ligase I was shown to be phosphorylated by casein kinase II (CK-II) [Prigent, 1992 #3065]. Subsequent experiments revealed that dephosphorylation or inhibition of CK-II

dependent phosphorylation of mammalian DNA ligase I results in an inactive protein. Therefore, phosphorylation of DNA ligase I by CK-II is required for functional activity. In addition, APE1 was recently shown to be phosphorylated *in vitro* by protein kinase-C (PK-C) and CK-II [Hsieh, 2001 #3066]. The *in vitro* phosphorylation of APE1 by CK-II inhibited APE1 endonuclease activity. However, when mammalian cells were exposed to agents known to increase expression of CK-II there was no effect on APE1 activity in these cells. PK-C was shown to phosphorylate APE1 during *in vitro* and *in vivo* experiments. The result of phosphorylation by PK-C causes a decrease in the endonuclease activity of APE1 with a concomitant increase in redox activity that is associated with APE1 [Hsieh, 2001 #3066]. The redox activity of APE1 is separate from the associated AP endonuclease activity and each reside in different domains of the protein. The redox activity of APE1 has been shown to enhance the activity of several transcription factors. When human cells are exposed to the oxidizing agent hypochlorite or the alkylating agent methyl methanesulfonate (MMS) there is an increase in redox activity of APE1 that is involved with an increase in PK-C activity and a corresponding increase in phosphorylated APE1 [Hsieh, 2001 #3066]. Both of these agents are known to cause damage to DNA. These new phosphorylation experiments suggest that even though the domains of APE1 appear to be catalytically unrelated, they may both be involved in protecting the genome from DNA damage.

Casein kinase II is one of the most unspecific eukaryotic protein kinases [Niefind, 2001 #3067]. CK-II can use either ATP or GTP as phosphoryl donors and CK-II has been shown to phosphorylate serine, tyrosine, and threonine residues. There have been more than 160 *in vitro* protein substrates of CK-II [Pinna, 1997 #3068]. In addition, CK-

II, like other protein kinases, requires Mg^{2+} as a metal cofactor, but unlike other kinases CK-II is equally active in the presence of Mn^{2+} and Co^{2+} [Gatica, 1993 #3069]. CK-II is a ubiquitous protein kinase found in eukaryotic cells and the holoenzyme consists of an $\alpha\alpha'\beta_2$ tetramer. Phosphorylation by CK-II *in vitro* has been demonstrated to alter the DNA binding or catalytic activity of c-Myc, c-Jun, DNA ligase I, topoisomerase II, APE1, p53, Rb, and RNA polymerases I and II [Niefind, 2001 #3067]. The most common consensus pattern for substrate recognition by CK-II is STXXDE, where X represents any amino acid and S or T is the site of phosphorylation.

Protein kinase C exhibits a preference for phosphorylation of serine or threonine residues found close to a C-terminal basic residue. PK-C requires Mg^{2+} as a cofactor and uses ATP as a phosphoryl donor. In addition, the kinase activity of PK-C is enhanced *in vitro* by the addition of phosphatidyl serine. However, the addition of phosphatidyl serine has not been reported to change the substrate specificity of PK-C. Phosphorylation by PK-C is known to stimulate and inhibit the activity of some proteins.

The possibility exists that DNA glycosylases might also be regulated in some manner by phosphorylation. There are several putative CK-II and PK-C phosphorylation sites in hAAG (Figure 6-1). To begin to investigate these possibilities, we have designed and performed *in vitro* phosphorylation assays with full-length hAAG and hAAG Δ 79. These initial assays serve as a starting point for understanding some of the post-translational modifications that may occur *in vivo* to hAAG and other human DNA glycosylases.

hAAG Protein Sequence

MVTPALQMKKPKQFCRRMGQKKQRPARGQPHSSDAAQPAEQPHSSDAAQAPCPRER
 CLGPPTTPGPYRSIYF**SPK**GHILTRLGLEFFDQPAVPLARAFLGQVLVRRLPNGTELGR
 IVETEA YLGPEDEA AHSRGGGRQ**TPR**NRGMFMKPGTLYVYIYGMYFCMNISSQGDGACVL
 LRALEPLEGLE**TMR**QLR**STLR**KGTA SRVLKDRELCSGPSKLCQALAINKSFDQRDLAQDE
 AVWLERGPLE PSEPA VVAARVGVGHAGEWARKPLRFYVRGSPWVSVVDRVAEQDTQA

Figure 6-1. hAAG protein sequence. Representation of the full-length hAAG protein sequence showing the putative CK-II (underlined) and PK-C (bold, larger font) phosphorylation sites.

Results

Phosphorylation of hAAG by Casein Kinase-II (CK-II) and Protein Kinase-C (PK-C) *in vitro*

Purified full-length hAAG and hAAG Δ 79 proteins were used as substrates for CK-II and PK-C phosphorylation assays. Each protein contains putative CK-II and PK-C phosphorylation sites. CK-II and PK-C were both purchased from Promega Corporation and labeling reactions (20 μ L) were carried out as instructed in the experimental procedures chapter. In addition, CK-II and PK-C peptide substrates were purchased from Sigma to serve as controls during the phosphorylation assays. After labeling 50 μ L of 2X SDS-loading buffer was added to each labeling reaction and the samples were boiled for 5 minutes in a water bath. A 10 μ L aliquot of each sample was loaded onto a 12% SDS-polyacrylamide gel and electrophoresis was performed at 110 volts for 2 hours. After electrophoresis the gel was dried as previously described and exposed to a Kodak phosphoimaging screen. The results of the phosphorylation assay are shown in Figure 6-2. Briefly, under these *in vitro* conditions PK-C phosphorylates full-length hAAG and hAAG Δ 79. In contrast, CK-II is unable to phosphorylate either of the hAAG substrates. Lastly, both CK-II and PK-C are able to phosphorylate their respective peptide substrates under these conditions.

Discussion

It is well established that phosphorylation is one of many post-translational modifications that occur to regulate protein activity. Several DNA repair proteins are known to be phosphorylated in response to various cellular assaults. The effect of phosphorylation results in some proteins being activated, while in other proteins phosphorylation results in an inactive state. The exact nature that phosphorylation has

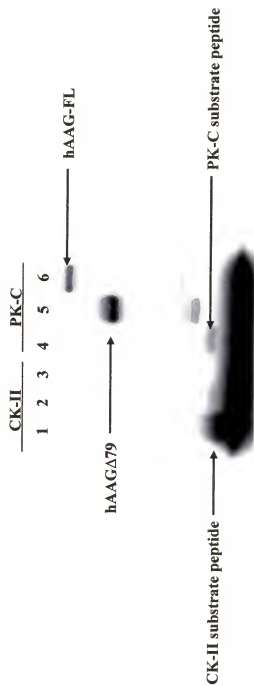


Figure 6-2. CK-II and PK-C phosphorylation of hAAG. An *in vitro* phosphorylation assay examining phosphorylation of hAAGΔ79 and hAAG-FL protein by CK-II and PK-C. CK-II did not phosphorylate either of the proteins, whereas PK-C did phosphorylate both hAAGΔ79 and hAAG-FL protein. Both CK-II and PK-C phosphorylated known peptide substrates demonstrating that both kinases are capable of phosphorylating proteins under these assay conditions.

upon the BER process is not understood. Actually, there have been only a few experiments examining the role of phosphorylation of BER components. There are not any reports of phosphorylation on any of the human DNA glycosylases or any experiments examining what effects phosphorylation has upon DNA glycosylase activity. These experiments demonstrate that PK-C is capable of phosphorylating hAAG *in vitro*, whereas CK-II does not.

Admittedly so, these simple assays do not address a biological role for phosphorylation of hAAG. However, these assays serve as a starting point to begin to examine the role of post-translational modifications of hAAG and other DNA glycosylases. Post-translational modifications are a common theme in human cells for regulating the activity of proteins known to be involved in cell-cycle regulation, DNA replication, transcription, and DNA repair. In light of the fact that BER components, such as APE1, are phosphorylated *in vivo* in response to agents known to damage DNA and PK-C activity is enhanced in response to these same agents, may suggest that phosphorylation of other BER components occur as well. Only by combining *in vitro* experiments with detailed *in vivo* experiments can we fully understand the nature of DNA repair pathways.

CHAPTER 7 CONCLUSIONS AND FUTURE STUDIES

Conclusions

It's a startling realization that approximately 20,000 endogenous base damages occur to DNA every day in human cells (55, 58). Combined with exogenous DNA base damages, single- and double-stranded DNA breaks, misincorporation of nucleotides during replication, chemical instability of the primary structure of DNA, and the spontaneous loss of DNA bases it is miraculous that human life exists. Elegant DNA repair pathways, which are constantly working to preserve human life, lessen the toxic and mutagenic consequences of DNA damage. There are over 130 known human DNA repair proteins (122) and the majority of these proteins have prokaryotic counterparts. However, DNA repair is not always 100% efficient and genome instability and human disease are hallmarks of faulty DNA repair.

Base excision repair (BER) is one of several DNA repair processes that are required by all cells to help maintain genome stability. BER primarily removes damaged bases from DNA that have been alkylated, deaminated, or oxidized. DNA glycosylases are thought to be the enzymes responsible for initiating BER. DNA glycosylases recognize the damaged base in DNA and hydrolyze the glycosidic bond connecting the base to the deoxyribose moiety. Other BER enzymes are sequestered to the resulting abasic site to hopefully restore the original genetic code. Because DNA glycosylases recognize DNA base damage, they are key to the overall effectiveness of the pathway. In

addition, DNA glycosylases must be able to locate the damaged DNA bases amid a huge excess of normal DNA bases. The nature of how DNA glycosylases locate their respective substrates is not known.

The purposes of our experiments were aimed at understanding some of the biochemical properties of human alkyladenine DNA glycosylase (hAAG). The work presented in Chapter 3 focused on understanding the *in vitro* substrate specificity of hAAG. hAAG has been reported to excise several structurally unrelated DNA damaged bases from DNA such as, *IN*⁶-ethenoadenine, hypoxanthine, 7,8-dihydro-8-oxoguanine, 7-methylguanine, 3-methyladenine, and undamaged purines (1, 8, 9, 124). Our study examines the structural and mechanistic principles for recognition and excision of damaged DNA bases by hAAG in the same DNA sequence context. Our approach was aimed at understanding which structural features of damaged bases were important for binding and excision by hAAG.

The experiments in Chapter 3 examined hAAG excision of four damaged DNA bases, *IN*⁶-ethenoadenine, hypoxanthine, 7,8-dihydro-oxoguanine, O⁶-methylguanine, as well as undamaged purines. 3-methyladenine and 7-methylguanine were excluded from this study because 3-methyladenine cannot be site-specifically incorporated into DNA and 7-methylguanine is relatively labile. Under our assay conditions we show that hAAG is only capable of excising *IN*⁶-ethenoadenine and hypoxanthine from DNA. The other substrates tested in this study may be excised at higher enzyme concentrations or after longer incubation times, but under our conditions excision of these substrates was very inefficient. We also examined the affect of the opposing pyrimidine base on excision of *IN*⁶-ethenoadenine and hypoxanthine. Our studies demonstrate that *IN*⁶-ethenoadenine

excision is relatively insensitive to the opposing pyrimidine bases, whereas excision of hypoxanthine is greatly affected. We conclude that these differences may be due to differences in hydrogen-bonding interactions between the damaged bases and the opposing pyrimidine partners. *IN*⁶-ethenoadenine is prevented from hydrogen bonding with any base because the etheno group bridges *N*¹ and the exocyclic amino group of adenine. This lack of hydrogen bonding interactions may make *IN*⁶-ethenoadenine easier to be detected by hAAG.

The work described in Chapter 4 was an attempt to see if APE1 has an affect on hAAG activity. Although, strong conclusions can not be drawn from this work, we were able to obtain some interesting results. The fact that APE1 stimulates hAAG-FL turnover and not hAAG Δ 79 may suggest that the N-terminal domain of hAAG is important for coordinating downstream BER events. We also showed that APE1 did not affect hAAG-FL activity under single enzyme turnover conditions. This result suggests that APE1 is not enhancing hAAG-FL flipping or excision, however more detailed and sensitive kinetic experiments are needed before anything can be ruled out.

We used yeast two-hybrid analysis to screen a human liver cDNA library for possible hAAG interacting proteins. We chose a liver cDNA library because hAAG is abundant in the liver compared with other tissues. Using this assay we found several proteins that bound to hAAG, however none of these proteins are currently known to participate in a DNA repair pathway, but one protein that we detected was quite interesting. We detected an interaction between hAAG and human MT-2A. MT-2A is a small metal binding protein whose primary function is still unclear. Interestingly, MT-2A mRNA and protein levels increase dramatically in response to several DNA

alkylating agents (62, 63, 76, 93). These studies show that there is a protective role, although unknown, provided by overexpressing MT-2A in CHO cells exposed to alkylating agents. We performed *in vitro* hAAG excision and binding assays in the presence of MT-2A and under our conditions there was no effect on hAAG activity. These limited assays were done just to see if there was an affect on hAAG activity. In our results we show that MT-2A interacts with the C-terminal portion of hAAG. Lastly, we also detected an interaction between APE1 and MT-2A. We are still unclear as to the role, if any, that MT-2A might have on base excision repair.

Future Studies

In order to obtain a more detailed insight into hAAG substrate recognition and base excision, site-directed mutants have already been constructed. Mutations have been made to residues that are thought to be important in substrate binding, nucleotide flipping, and base excision (catalysis). These mutants, when combined with wild-type data, should aid in defining a more detailed kinetic mechanism regarding hAAG substrate recognition and excision.

More thought provoking experiments are needed to determine the exact nature of hAAG-FL protein stimulation by APE1. Fluorescence anisotropy is a very sensitive approach to measure protein-protein interactions in real-time and in solution. This type of sensitive assay might yield clues into the nature of APE1 stimulation. Also other BER proteins besides APE1 might influence hAAG excision of damaged bases. Therefore other *in vitro* excision assays should be carried out in the presence of these enzymes in order to determine if they effect hAAG excision. In addition hAAG might affect downstream BER events and because all of the BER enzymes are commercially available

this hypothesis would be easy to test. Lastly these enzymes could be used with the hAAG-E125Q mutant to determine if other BER enzymes affected the binding of hAAG to damaged DNA bases.

LIST OF REFERENCES

1. **Abner, C. W., Lau, A.Y., Ellenberger, T., Bloom, L.B.** 2001. Base excision and DNA binding activities of human alkyladenine DNA glycosylase are sensitive to the base paired with a lesion. *J Biol Chem* **276**:13379-13387.
2. **Allen, J. B., Walberg, M.W., Edwards, M.C., Elledge, S.J.** 1995. Finding prospective partners in the library: the two-hybrid system and phage display find a match. *Trends Biochem Sci* **20**:511-516.
3. **Ames, B. N., Shigenaga, M.K., Hagen, T.M.** 1993. Oxidants, antioxidants, and the degenerative diseases of aging. *Proc Natl Acad Sci* **90**:7915-7922.
4. **Asaeda, A., Ide, H., Asagoshi, K., Matsuyama, S., Tano, K., Murakami, Y., Takamori, Y., Kubo, K.** 2000. Substrate specificity of human methylpurine DNA N-glycosylase. *Biochemistry* **39**:1959-1965.
5. **Barnes, D. E., Tomkinson, A.E., Lehmann, A.R., Webster, A.D.B., Lindahl, T.** 1992. Mutations in the DNA ligase I gene of an individual with immunodeficiencies and cellular hypersensitivity to DNA-damaging agents. *Cell* **69**:495-503.
6. **Beard, W. A., Osheroff, W.P., Prasad, R., Sawaya, M.R., Jaju, M., Wood, T.G., Kraut, J., Kunkel, T.A., Wilson, S.H.** 1996. Enzyme-DNA interactions required for efficient nucleotide incorporation and discrimination in human DNA polymerase beta. *J Biol Chem* **271**:12141-12144.
7. **Bennett, R. O., Wilson, D.W. III, Wong, D., Demple, B.** 1997. Interaction of human apurinic endonuclease and DNA polymerase B in the base excision repair pathway. *Proc Natl Acad Sci* **94**:7166-7169.
8. **Berdal, K. G., Johansen, R.F., Seeberg, E.** 1998. Release of Normal Bases from Intact DNA by a Native DNA Repair Enzyme. *EMBO J* **17**:363-367.
9. **Bessho, T., Roy, R., Yamamoto, K., Kasai, S., Nishimura, K., Tano, K., Mitra, S.** 1993. Repair of 8-hydroxyguanine in DNA by mammalian N-methylpurine DNA glycosylase. *Proc Natl Acad Sci* **90**:8901-8904.
10. **Boer, J., Hoeijmakers, J.H.J.** 2000. Nucleotide excision repair and human syndromes. *Carcinogenesis* **21**:453-460.
11. **Brash, D. E., Haseltine, W.A.** 1982. UV-induced mutation hotspots occur at DNA damage hotspots. *Nature (London)* **298**:189-192.

12. **Chakravarti, D., Ibanu, G.C., Tano, K., Mitra, S.** 1991. Cloning and expression in *Escherichia coli* of a human cDNA encoding the DNA repair protein N-methylpurine-DNA glycosylase. *J Biol Chem* **266**:15,710-15,715.
13. **Chen, J., Derfler, B., Maskati, A., Samson, L.** 1989. Cloning a eukaryotic DNA glycosylase repair gene by the suppression of a DNA repair defect in *Escherichia coli*. *Proc Natl Acad Sci* **86**:7961-7965.
14. **Chien, C. T., Bartel, P.L., Sternglanz, R., Fields, S.** 1991. The two-hybrid system: A method to identify and clone genes for proteins that interact with a protein of interest. *Proc Natl Acad Sci* **88**:9578-9582.
15. **Chubatsu, K. J., Admon, A., Stahl, J., Fellous, R., Linn, S.** 1995. Implication of mammalian ribosomal protein S3 in the process of DNA damage. *J Biol Chem* **270**:13620-13629.
16. **Cordeiro-Stone, M., Zaritskaya, L.S., Price, L.K., Kaufman, W.K.** 1997. Replication fork bypass of a pyrimidine dimer blocking leading strand DNA synthesis. *Journal of Biological Chemistry* **272**:13945-13954.
17. **Dianov, G., Lindahl, T.** 1994. Reconstitution of the DNA base excision-repair pathway. *Curr. Biol.* **4**:1069-1076.
18. **Dodson, M. L., Michaels, M.L., Lloyd, R.S.** 1994. Unified catalytic mechanism for DNA glycosylases. *J Biol Chem* **269**:32709-32712.
19. **Dosanjh, M. K., Chenna, A., Kim, E., Fraenkel-Conrat, H., Samson, L., Singer, B.** 1994. All four known cyclic adducts formed in DNA by the vinyl chloride metabolite chloroacetaldehyde are released by a human DNA glycosylase. *Proc Natl Acad Sci* **91**:1024-1028.
20. **Dosanjh, M. K., Roy, R., Mitra, S., Singer, B.** 1994. 1,N⁶-Ethenoadenine is preferred over 3-methyladenine as substrate by a cloned human N-methylpurine DNA glycosylase (3-methyladenine DNA glycosylase). *Biochemistry* **33**:1624-1628.
21. **Dudley, B., Hammond, A., Deutsch, W.A.** 1992. The presence of uracil-DNA glycosylase in insects is dependent upon developmental complexity. *J Biol Chem* **267**:11964-11967.
22. **Engelward, B. P., M. Boosalis, B. J. Chen, Z. Deng, M. J. Siciliano, Samson, L.** 1993. Cloning and characterization of a mouse 3-methyladenine/7-methylguanine/3-methylguanine DNA glycosylase cDNA whose gene maps to chromosome 11. *Carcinogenesis* **14**:175-181.

23. **Engelward, B. P., Weeda, G., Wyatt, M.D., Broekhof, J.L., de Wit, J., Donker, I., Allan, J.M., Gold, B., Hoeijmakers, J.H., Samson, L.D.** 1997. Base excision repair deficient mice lacking the AAG alkyladenine DNA glycosylase. *Proc Natl Acad Sci* **94**:13087-13092.
24. **Erzberger, J. P., Wilson, D.M. III.** 1999. The role of Mg²⁺ and specific amino acid residues in the catalytic reaction of the major human abasic endonuclease: New insights from EDTA-resistant incision of acyclic abasic sites analogs and site directed mutagenesis. *J Mol Biol* **290**:447-457.
25. **Estojak, J., Brent, R., Golemis, E.A.** 1995. Correlation of two-hybrid affinity data with in vitro measurements. *Mol Cell Biol* **15**:5820-5829.
26. **Evans, E., Moggs, J.G., Hwang, J.R., Egly, J.M., Wood, R.D.** 1997. Mechanism of open complex and dual incision formation by human nucleotide excision repair factors. *EMBO J* **16**:6559-6573.
27. **Fasman, G.** 1975. *Handbook of Biochemistry: Nucleic acids*, vol. 1. CRC Press, Inc., Boca Raton, FL.
28. **Fields, S., Song, O.** 1989. A novel genetic system to detect protein-protein interactions. *Nature* **340**:245-246.
29. **Frederico, L. A., Kunkel, T.A., Shaw, B.R.** 1993. Cytosine deamination in mismatched base pairs. *Biochemistry* **32**:6523-6530.
30. **Frederico, L. A., Kunkel, T.A., Shaw, B.R.** 1990. A sensitive genetic assay for the detection of cytosine deamination: determination of rate constants and the activation energy. *Biochemistry* **29**:2532-2537.
31. **Friedberg, E. C., Meira, L.B.** 2000. Database of mouse strains carrying targeted mutations in genes affecting cellular responses to DNA damage: version 4. *Mutation Res* **459**:243-274.
32. **Friedberg, E. C., Walker, G. C., Siede, W.** 1995. *DNA Repair and Mutagenesis*. ASM, Washington, DC.
33. **Gordon, L. K., Haseltine, W.A.** 1982. Quantitation of cyclobutane pyrimidine dimer formation in double and single-stranded DNA fragments of defined sequence. *Radiat Res* **89**:99-112.
34. **Gorman, M. A., Morera, S., Rothwell, D.G., de La Fortelle, E., Mol, C.D., Tainer, J.A., Hickson, I.D., Freemont, P.S.** 1997. The crystal structure of the human DNA repair endonuclease HAP1 suggests the recognition of extra-helical deoxyribose at DNA abasic sites. *EMBO J* **16**:6548-6558.
35. **Guarente, L.** 1993. Strategies for the identification of interacting proteins. *Proc Natl Acad Sci* **90**:1639-1641.

36. **Guibourt, N., Castaing, B., van der Kamp, P.A., Boiteux, S.** 2000. Catalytic and DNA binding properties of the OGG1 protein of *Saccharomyces cerevisiae*: comparison between the wild-type and the K241R and K241Q active-site mutant proteins. *Biochemistry* **39**:1716-1724.
37. **Hainaut, P., Pfeifer, G.P.** 2000. Patterns of p53 G>T transversions in lung cancers reflect the primary mutagenic signature of DNA-damage by tobacco smoke. *Carcinogenesis* **22**:367-374.
38. **Hill, J. W., Hazra, T.K., Izumi, T., Mitra, S.** 2001. Stimulation of human 8-oxoguanine-DNA glycosylase by AP-endonuclease: potential coordination of the initial steps in base excision repair. *Nucleic Acids Res* **29**:430-438.
39. **Hoffman, D., Hecht, S.S.** 1990. Advances in tobacco carcinogenesis, p. 63-102. *In* C. S. Cooper and P. L. Grover (ed.), *Chemical carcinogenesis and mutagenesis*, vol. I. Springer-Verlag, Berlin.
40. **Hollis, T., Lau, A., Ellenberger, T.** 2000. Structural studies of human alkyladenine glycosylase and *E. coli* 3-methyladenine glycosylase. *Mutation Res* **460**:201-210.
41. **Hollstein, M., Shomer, B., Greenblatt, M., Soussi, T., Hovig, E., Montesano, R., Harris, C.C.** 1996. Somatic point mutations in the p53 gene of human tumors and cell lines: updated compilation. *Nucleic Acids Res* **24**:141-146.
42. **Karran, P., Lindahl, T.** 1980. Hypoxanthine in deoxyribonucleic acid: generation by heat-induced hydrolysis of adenine residues and release in free form by deoxyribonucleic acid glycosylase from calf thymus. *Biochemistry* **19**:6005-6011.
43. **Kartalou, M., Samson, L.D., Essigmann, J.M.** 2000. Cisplatin adducts inhibit 1,N(6)-ethenoadenine repair by interacting with the human 3-methyladenine DNA glycosylase. *Biochemistry* **39**:8032-8038.
44. **Kingma, P. S., Osherooff, N.** 1997. Spontaneous DNA damage stimulates topoisomerase II-mediated DNA cleavage. *J Biol Chem* **272**:7488-7493.
45. **Klimasauskas, S., Kumar, S., Roberts, R.J., Cheng, X.** 1994. HhaI methyltransferase flips its target base out of the DNA helix. *Cell* **76**:357-369.
46. **Kouchakdjian, M., Bodepudi, V., Shibutani, S., Eisenberg, M., Johnson, F., Grollman, A., Patel, D.J.** 1991. NMR structural studies of the ionizing radiation adduct 7-hydro-8-oxodeoxyguanosine (8-oxo-7H-dG) opposite deoxyadenosine in a DNA duplex. 8-Oxo-7H-dG(syn)•dA(anti) alignment at lesion site. *Biochemistry* **30**:1403-1412.

47. **Kouchakdjian, M., Eisenberg, M., Yarema, K., Basu, A., Essigmann, J., Patel, D.J.** 1991. NMR studies of the exocyclic 1,N⁶-ethenodeoxyadenosine adduct (edA) opposite thymidine in a DNA duplex. Nonplanar alignment of edA (anti) and dT(anti) at the lesion site. *Biochemistry* **30**:1820-1828.
48. **Kubota, Y., Nash, R.A., Klungland, A., Schar, P., Barnes, D.E., Lindahl, T.** 1996. Reconstitution of DNA base excision-repair with purified human proteins: interaction between DNA polymerase beta and the XRCC1 protein. *EMBO J* **15**:6662-6670.
49. **Labahn, J., Schärer, O.D., Long, A., Ezaz-Nikpay, K., Verdine, G.L., Ellenberger, T.E.** 1996. Structural basis for the excision repair of alkylation-damaged DNA. *Cell* **86**:321-329.
50. **Lau, A. Y., Schärer, O.D., Samson, L., Verdine, G.L., Ellenberger, T.** 1998. Crystal structure of the human alkylbase-DNA repair enzyme complexed to DNA: Mechanisms for nucleotide flipping and base excision. *Cell* **95**:249-258.
51. **Lau, A. Y., Wyatt, M.D., Glassner, B.J., Samson, L.D., Ellenberger, T.** 2000. Molecular basis for discriminating between normal and damaged bases by the human alkyladenine glycosylase, AAG. *Proc Natl Acad Sci* **97**:13573-13578.
52. **Lemaire, D. G. E., Ruzsicska, B.P.** 1993. Kinetic analysis of the deamination reactions of cyclobutane dimers of thymidyl-3',5'-2'-deoxycytidine and 2'-deoxycytidyl-3',5'-thymine. *Biochemistry* **32**:2525-2533.
53. **Li, L., Elledge, S.J., Peterson, C.A., Bales, E.S., Legerski, R.J.** 1994. Specific association between the human DNA repair proteins XPA and ERCC1. *Proc Natl Acad Sci* **91**:5012-5016.
54. **Lindahl, T.** 1979. DNA Glycosylases, Endonucleases for Apurinic/Apyrimidinic Sites, and Base Excision Repair. *Prog Nucleic Acids Res Mol Biol* **22**:135-192.
55. **Lindahl, T.** 1993. Instability and decay of the primary structure of DNA. *Nature* **362**:709-715.
56. **Lindahl, T.** 1976. New class of enzymes acting on damaged DNA. *Nature* **259**:64-66.
57. **Lindahl, T.** 1974. An N-glycosylase from *Escherichia coli* that releases free uracil from DNA containing deaminated cytosine residues. *Proc Natl Acad Sci* **71**:3649-3653.
58. **Lindahl, T.** 2000. Suppression of spontaneous mutagenesis in human cells by DNA base excision-repair. *Mutation Res* **462**:129-135.
59. **Lindahl, T., Nyberg, B.** 1972. Rate of depurination of native DNA. *Biochemistry* **11**:3610-3618.

60. **Lober, G., Kittler, L.** 1977. Selected topics in photochemistry of nucleic acids. Recent results and perspectives. *Photochem Photobiol* **25**:215-233.
61. **Loeb, L. A., Preston, B.D.** 1986. Mutagenesis by apurinic/apyrimidinic sites. *Annual Review of Genetics* **20**:201-230.
62. **Lohrer, H., Robson, T.** 1989. Overexpression of metallothionein in CHO cells and its effect on cell killing by ionizing radiation and alkylating agents. *Carcinogenesis* **10**:2279-2284.
63. **Lohrer, H., Robson, T., Gridley, H., Foster, S., Hall, A.** 1990. Differential effects on cell killing in metallothionein overexpressing CHO mutant cell lines. *Carcinogenesis* **11**:1937-1941.
64. **Masuda, Y., Bennett, R.A.O., Demple, B.** 1998. Dynamics of the interaction of human apurinic endonuclease (APE1) with its substrate and product. *J Biol Chem* **273**:30352-30359.
65. **McAuley-Hecht, K. E., Leonard, G.A., Gibson, N.J., Thomson, J.B., Watson, W.P., Hunter, W.N., Brown, T.** 1994. Crystal structure of a DNA duplex containing 8-hydroxydeoxyguanine-adenine base pairs. *Biochemistry* **33**:10266-10270.
66. **McCullough, A. K., Dodson, M.L., Lloyd, R.S.** 1999. Initiation of base excision repair: Glycosylase mechanisms and structures. *Annu Rev Biochem* **68**:255-285.
67. **Mellon, I., Spivak, G., Hanawalt, P.C.** 1987. Selective removal of transcription-blocking DNA damage from the transcribed strand of the mammalian DHFR gene. *Cell* **51**:241-249.
68. **Miao, F., Bouziane, M., Dammann, R., Masutani, C., Hanaoka, F., Pfeifer, G., O'Connor, T.R.** 2000. 3-methyladenine-DNA glycosylase (MPG protein) interacts with human RAD23 proteins. *J Biol Chem* **275**:28433-28438.
69. **Miao, F., Bouziane, M., O'Connor, T.R.** 1998. Interaction of the recombinant human methylpurine-DNA glycosylase (MPG protein) with oligodeoxyribonucleotides containing either hypoxanthine or abasic sites. *Nucleic Acids Research* **26**:4034-4041.
70. **Minowa, O., Arai, T., Hirano, M., Monden, Y., Nakai, S., Fukuda, M., Itoh, M., Takano, H., Hippou, Y., Aburatani, H., Masumura, K., Nishimura, S., Noda, T.** 2000. Mmh/Ogg1 gene inactivation results in accumulation of 8-hydroxyguanine in mice. *Proc Natl Acad Sci* **97**:4151-4161.
71. **Mitchell, D. L., Jen, J., Cleaver, J.E.** 1992. Sequence specificity of cyclobutane pyrimidine dimers in DNA treated with solar (ultraviolet B) radiation. *Nucleic Acids Res* **20**:225-229.

72. **Mol, C. D., Izumi, T., Mitra, S., Tainer, J.A.** 2000. DNA-bound structures and mutants reveal abasic DNA binding by APE1: DNA repair and coordination. *Nature* **403**:451-456.
73. **Mol, C. D., Parikh, S.S., Putnam, C.D., Lo, T.P., Tainer, J.A.** 1999. DNA repair mechanisms for the recognition and removal of damaged DNA bases. *Annu Rev Biophys Biomol Struct* **28**:101-128.
74. **Moyer, R., Briley, D., Johnsen, A., Stewart, U., Shaw, B.R.** 1993. Echinomycin, a bis-intercalating agent, induces C>T mutations via cytosine deamination. *Mutation Res* **288**:291-300.
75. **Mu, D., Sancar, A.** 1997. Model for XPC-independent transcription-coupled repair of pyrimidine dimers in humans. *J Biol Chem* **272**:7570-7573.
76. **Nartey, N., Cerian, G.M., Banerjee, D.** 1987. Immunohistochemical localization of metallothionein in human thyroid cancers. *Am J Pathol* **129**:177-182.
77. **Nicholl, I. D., Nealon, K., Kenny, M.K.** 1997. Reconstitution of human base excision repair with purified proteins. *Biochemistry* **36**:7557-7566.
78. **Nilsen, H., Krokan, H.E.** 2001. Base excision repair in a network of defense and tolerance. *Carcinogenesis* **22**:987-998.
79. **Nilsen, H., Rosewell, I., Robins, P., Skjelbred, C.F., Andersen, S., Slupphaug, G., Daly, G., Krokan, H.E., Lindahl, T.** 2000. Uracil-DNA glycosylase (UNG)-deficient mice reveal a primary role of the enzyme during DNA replication. *Molecular Cell* **5**:1059-1065.
80. **O'Connor, T. R.** 1993. Purification and characterization of human 3-methyladenine DNA glycosylase. *Nucleic Acids Research* **21**:5561-5569.
81. **O'Connor, T. R., Laval, J.** 1990. Isolation and structure of a cDNA expressing a mammalian 3-methyladenine DNA glycosylase. *EMBO J* **9**:3337-3342.
82. **Parikh, S. S., Mol, C.D., Slupphaug, G., Bharati, S., Krokan, H.E., Tainer, J.A.** 1998. Base excision repair initiation revealed by crystal structures and binding kinetics of human uracil-DNA glycosylase with DNA. *EMBO J* **17**:5214-5226.
83. **Parikh, S. S., Walcher, G., Jones, G.D., Slupphaug, G., Krokan, H.E., Blackburn, G.M., Tainer, J.A.** 2000. Uracil-DNA glycosylase-DNA substrate and product structures: conformational strain promotes catalytic efficiency by coupled stereoelectric effects. *Proc Natl Acad Sci* **97**:5083-5088.
84. **Park, C. H., Mu, D., Reardon, J.T., Sancar, A.** 1995. The general transcription-repair factor TFIIH is recruited to the excision repair complex by the XPA protein independent of the TFIIIE transcription factor. *J Biol Chem* **270**:4896-4902.

85. **Petronzelli, F., Riccio, A., Markham, G.D., Seeholzer, S.H., Stoerker, J., Genuardi, M., Yeung, A.T., Matsumoto, Y., Bellacosa, A.** 2000. Biphasic kinetics of the human DNA repair protein MED1 (MBD4), a mismatch-specific DNA N-glycosylase. *J Biol Chem* **275**:32422-32429.
86. **Podlutzky, A. J., Dianova, I.I., Wilson, S.H., Bohr, V.A., Dianov, G.L.** 2001. DNA synthesis and dRPase activities of polymerase β are both essential for single-nucleotide patch base excision repair in mammalian cell extracts. *Biochemistry* **40**:809-813.
87. **Porello, S. L., Leyes, A.E., David, S.S.** 1998. Single-turnover and pre-steady-state kinetics of the reaction of the adenine glycosylase MutY with mismatch-containing DNA substrates. *Biochemistry* **37**:14756-14764.
88. **Pourquier, P., Ueng, L.M., Kohlhaagen, G., Mazumder, A., Gupta, M., Kohn, K.W., Pommier, Y.** 1997. Effects of uracil incorporation, DNA mismatches and abasic sites on cleavage and religation activities of mammalian topoisomerase I. *J Biol Chem* **272**:7792-7796.
89. **Prasad, R., Singhal, R.K., Srivastava, D.K., Molina, J.T., Tomkinson, A.E., Wilson, S.H.** 1996. Specific interaction of DNA polymerase β and DNA ligase I in a multiprotein base excision repair complex from bovine testis. *J Biol Chem* **271**:16000-16007.
90. **Privezentzev, C. V., Sapparbaev, M., Laval, J.** 2001. The HAP1 protein stimulates the turnover of human mismatch-specific thymine-DNA-glycosylase to process 3,N(4)-ethenocytosine residues. *Mutation Res* **480-481**:277-284.
91. **Reinisch, K. M., Chen, L., Verdine, G.L., Lipscomb, W.N.** 1995. The crystal structure of HaeIII methyltransferase covalently complexed to DNA: An extrahelical cytosine and rearranged base pairing. *Cell* **82**:143-153.
92. **Richardson, F. C., Richardson, K.K.** 1990. Sequence -dependent formation of alkyl DNA adducts: a review of methods, results, and biological correlates. *Mutation Res* **233**:127-138.
93. **Robson, T., Hall, A., Lohrer, H.** 1992. Increased sensitivity of a Chinese hamster ovary cell line to alkylating agents after overexpression of the human metallothionein II-A gene. *Mutation Res* **274**:177-185.
94. **Roy, R., Biswas, T., Hazra, T.K., Roy, G., Grabowski, D.T., Izumi, T., Srinivasan, G., Mitra, S.** 1998. Specific interaction of wild-type and truncated mouse N-methylpurine-DNA glycosylase with ethenoadenine-containing DNA. *Biochemistry* **37**:580-589.
95. **Roy, R., Brooks, C., Mitra, S.** 1994. Purification and biochemical characterization of recombinant N-Methylpurine-DNA glycosylase of the mouse. *Biochemistry* **33**:15131-15140.

96. **Roy, R., Kennel, S.J., Mitra, S.** 1996. Distinct substrate preference of human and mouse *N*-methylpurine DNA glycosylase. *Carcinogenesis* **17**:2177-2182.
97. **Rupp, W. D., Howard-Flanders, P.** 1968. Discontinuities in the DNA synthesized in an excision-defective strain of *Escherichia coli* following ultraviolet irradiation. *J Mol Biol* **31**:291-304.
98. **Rydberg, B., Lindahl, T.** 1982. Nonenzymatic methylation of DNA by the intracellular methyl group donor S-adenosyl-L-methionine is a potentially mutagenic. *EMBO J* **1**:211-216.
99. **Samson, L., Derfler, B., Boosalis, M., Call, K.** 1991. Cloning and characterization of a 3-methyladenine DNA glycosylase cDNA from human cells whose gene maps to chromosome 16. *Proc Natl Acad Sci* **88**:9127-9131.
100. **Santerre, A., Britt, A.B.** 1994. Cloning of a 3-methyladenine DNA glycosylase from *Arabidopsis thaliana*. *Proc Natl Acad Sci* **91**:2240-2244.
101. **Saparbaev, M., Kleibl, K., Laval, J.** 1995. *Escherichia coli*, *Saccharomyces cerevisiae*, rat and human 3-methyladenine DNA glycosylases repair 1,N⁶-ethenoadenine when present in DNA. *Nucleic Acids Research* **23**:3750-3755.
102. **Saparbaev, M., Laval, J.** 1994. Excision of hypoxanthine from DNA containing dIMP residues by the *Escherichia coli*, yeast, rat, and human alkylpurine DNA glycosylases. *Proc Natl Acad Sci* **91**:5873-5877.
103. **Savva, R., McAuley-Hecht, K., Brown, T., Pearl, L.** 1995. The structural basis of specific base-excision repair by uracil-DNA glycosylase. *Nature* **373**:487-493.
104. **Sawaya, M. R., Prasad, R., Wilson, S.H., Kraut, J., Pelletier, H.** 1997. Crystal structures of human DNA polymerase β complexed with gapped and nicked DNA: Evidence for an induced fit mechanism. *Biochemistry* **36**:11205-11215.
105. **Schar, P.** 2001. Spontaneous DNA damage, genome instability, and cancer-when DNA replication escapes control. *Cell* **104**:329-332.
106. **Scharer, O. D., Nash, H.M., Jiricny, J., Laval, J., Verdine, G.L.** 1998. Specific binding of a designed pyrrolidine abasic site analog to multiple DNA glycosylases. *Journal of Biological Chemistry* **273**:8592-8597.
107. **Seeberg, E., Eide, L., Bjoras, M.** 1995. The base excision repair pathway. *Trends Biochem Sci* **20**:391-397.
108. **Shimada, K., Ogawa, H., Tomizawa, J.** 1968. Studies on radiation-sensitive mutants of *E. coli*. II. Breakage and repair of ultraviolet irradiated intracellular DNA of phage lambda. *Mol Gen Genet* **101**:245-256.

109. **Sobol, R. W., Horton, J.K., Kuhn, R., Gu, H., Singhal, R.K., Prasad, R., Rajewsky, K., Wilson, S.H.** 1998. Mammalian abasic site base excision repair: Identification of the reaction sequence and rate-determining steps. *J Biol Chem* **273**:21203-21209.
110. **Srivastava, D. K., Vande Berg, B.J., Prasad, R., Molina, J.T., Beard, W.A., Tomkinson, A.E., Wilson, S.H.** 1998. Mammalian abasic site base excision repair: Identification of the reaction sequence and rate-determining steps. *J Biol Chem* **273**:21203-21209.
111. **Stivers, J. T., Pankiewicz, K.W., Watanabe, K.A.** 1999. Kinetic Mechanism of Damage Site Recognition and Uracil Flipping by *Escherichia coli* Uracil DNA Glycosylase. *Biochemistry* **38**:952-63.
112. **Taylor, J. S., O' Day, C. L.** 1990. *cis-syn* thymine dimers are not absolute blocks to replication by DNA polymerase I of *Escherichia coli* in vitro. *Biochemistry* **29**:1624-32.
113. **Teoule, R.** 1987. Radiation-induced DNA damage and its repair. *Int J Radiat Biol* **51**:573-589.
114. **Tessman, I., Kennedy, M.A.** 1991. The two-step model of UV mutagenesis reassessed: deamination of cytosine as the likely source of the mutations associated with deamination. *Mol Gen Genet* **227**:144-148.
115. **Tornaletti, S., Rozek, D., Pfeifer, G.P.** 1993. The distribution of UV photoproducts along the human p53 gene and its relation to mutations in skin cancer. *Oncogene* **8**:2051-2057.
116. **Varghese, A. J.** 1972. Photochemistry of nucleic acids and their constituents. *Photophysiology* **7**:207-274.
117. **Vidal, A. E., Hickson, I.D., Boiteux, S., Radicella, J.P.** 2001. Mechanism of stimulation of the DNA glycosylase activity of hOGG1 by the major human AP endonuclease: bypass of the AP lyase activity step. *Nucleic Acids Res* **29**:1285-1292.
118. **Waters, T. R., Gallinari, P., Jiricny, J., Swann, P.F.** 1999. Human thymine DNA glycosylase binds to apurinic sites in DNA but is displaced by human apurinic endonuclease 1. *J Biol Chem* **274**:67-74.
119. **Wilson, D. M. I., Takeshita, M., Demple, B.** 1997. Abasic site binding by the human apurinic endonuclease, APE, and determination of the DNA contact sites. *Nucleic Acids Res.* **25**:933-939.
120. **Wilson, S. H., Kunkel, T.A.** 2000. Passing the baton in base excision repair. *Nature Structural Biology* **7**:176-178.

121. **Wood, R. D.** 1996. DNA repair in eukaryotes. *Annu Rev Biochem* **65**:135-167.
122. **Wood, R. D., Mitchell, M., Sgouros, J., Lindahl, T.** 2001. Human DNA repair genes. *Science* **291**:1284-1289.
123. **Woodgate, R.** 1999. A plethora of lesion-replicating DNA polymerases. *Genes and Development* **13**:2191-2195.
124. **Wyatt, M. D., Allan, J.M., Lau, A.Y., Ellenberger, T.E., Samson, L.D.** 1999. 3-Methyladenine DNA glycosylases: Structure, function, and biological importance. *BioEssays* **21**:668-676.
125. **Wyatt, M. D., Samson, L.D.** 2000. Influence of DNA structure on hypoxanthine and 1,N(6)-ethenoadenine removal by murine 3-methyladenine DNA glycosylase. *Carcinogenesis* **21**:901-908.
126. **Yacoub, A., Augeri, L., Kelley, M.R., Doetsch, P.W., Deutsch, W.A.** 1996. A *Drosophila* ribosomal protein contains 8-oxoguanine and abasic site DNA repair activities. *EMBO J* **15**:2306-2312.
127. **Yamagata, Y., Kato, M., Odawara, K., Tokuno, Y., Nakashima, Y., Matsushima, M., Yasumura, K., Tomita, K., Ihara, K., Fujii, Y., Nakabeppu, Y., Sekiguchi, M., Fujii, S.** 1996. Three-dimensional structure of a DNA repair enzyme, 3-methyladenine DNA glycosylase II, from *Escherichia coli*. *Cell* **86**:311-319.
128. **Yang, M., Wu, Z., Fields, S.** 1995. Protein-peptide interactions analyzed with the yeast two-hybrid system. *Nucleic Acids Res* **23**:1152-1156.

BIOGRAPHICAL SKETCH

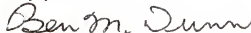
Clint William Abner was born on February 17, 1971, in West Memphis Arkansas. He is the youngest of six children. Clint grew up in Wilson, Arkansas, a small town in the northeastern part of the state, with a population of approximately 1,000. Clint realized his strong interest in science at an early age. At the age of seven Clint began injecting his mother's household plants with various substances in order to see how long they could survive post-treatment. This type of behavior continued up until he began high school. In high school Clint took every single science class that was offered and excelled in everyone. He graduated from Rivercrest High School in 1989 with honors. In the summer of 1997 he received a Bachelor of Science degree from the University of Arkansas and began graduate school three weeks later. After finishing the requirements for his Ph.D. degree, Clint will continue with his research endeavors in the laboratory of Dr. Peter McKinnon at St. Jude Children's Research Hospital in Memphis, Tennessee.

I certify that I have read this study and that in my opinion it conforms to acceptable standards of scholarly presentation and is fully adequate, in scope and quality, as a dissertation for the degree of Doctor of Philosophy.



Linda B. Bloom, Chair
Assistant Professor of Biochemistry and
Molecular Biology

I certify that I have read this study and that in my opinion it conforms to acceptable standards of scholarly presentation and is fully adequate, in scope and quality, as a dissertation for the degree of Doctor of Philosophy.



Ben M. Dunn
Distinguished Professor of Biochemistry and
Molecular Biology

I certify that I have read this study and that in my opinion it conforms to acceptable standards of scholarly presentation and is fully adequate, in scope and quality, as a dissertation for the degree of Doctor of Philosophy.



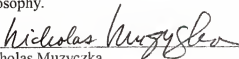
Susan C. Frost
Professor of Biochemistry and Molecular
Biology

I certify that I have read this study and that in my opinion it conforms to acceptable standards of scholarly presentation and is fully adequate, in scope and quality, as a dissertation for the degree of Doctor of Philosophy.



Arthur S. Edison
Assistant Professor of Biochemistry and
Molecular Biology

I certify that I have read this study and that in my opinion it conforms to acceptable standards of scholarly presentation and is fully adequate, in scope and quality, as a dissertation for the degree of Doctor of Philosophy.



Nicholas Muzyczka
Eminent Scholar of Molecular Genetics and
Microbiology

This dissertation was submitted to the Graduate Faculty of the College of Medicine and to the Graduate School and was accepted as partial fulfillment of the requirements for the degree of Doctor of Philosophy.

May 2002

Wayne J. McCormack

Dean, College of Medicine

Harold M. Phillips

Dean, Graduate School